INSTITUTO POLITÉCNICO DE LISBOA

Instituto Superior de Engenharia de Lisboa

Escola Superior de Tecnologia da Saúde de Lisboa

Development of Tissue-Engineered Temporomandibular Discs based on Xenogeneic Extracellular Matrices

Daniela Alexandra Pinheiro Trindade

Trabalho Final de Mestrado para obtenção do grau de
Mestre em Engenharia Biomédica

Orientadores
Carla Sofia Monteiro de Moura (CDRSP-PLeiria)
Cecília Ribeiro da Cruz Calado (ISEL)

maio de 2021

INSTITUTO POLITÉCNICO DE LISBOA

Instituto Superior de Engenharia de Lisboa

Escola Superior de Tecnologia da Saúde de Lisboa

Development of Tissue-Engineered Temporomandibular Discs based on Xenogeneic Extracellular Matrices

Daniela Alexandra Pinheiro Trindade

Trabalho Final de Mestrado para obtenção do grau de
Mestre em Engenharia Biomédica

Orientadores

Carla Sofia Monteiro de Moura (CDRSP-PLeiria)

Cecília Ribeiro da Cruz Calado (ISEL)

Júri

Presidente: Manuel Matos (ISEL)

Vogais: Nuno Manuel Fernandes Alves (CDRSP-PLeiria)

Carla Sofia Monteiro de Moura (CDRSP-PLeiria)

maio de 2021

“Não sabendo que era impossível, ele foi lá e fez”

Jean Cocteau

Acknowledgement

I would like to thank some people, in which with their contribution, it was possible the execution and conclusion of this thesis:

- First, I would like to express my deep gratitude to my supervisor, Professor Carla Moura, for giving me the opportunity and trust to carry out this thesis. She was the pillar of this work, not only helping me academically but also personally, through her guidance, support and motivation.
- A special thanks to my co-supervisor, Professor Cecília Calado, for accepting to embrace this project and always showing availability and providing valuable advice and guidance throughout the work.
- To Centre for Rapid and Sustainable Product Development of Polytechnic of Leiria for allowing me to carry out this work in its facilities.
- To Margarida Franco with the help of micro-computed tomography analysis and for her kindness and sympathy whenever necessary.
- To João Pinheiro for the help with the scanning electron microscopy images.
- To my colleague and friend Rachel Cordeiro for her help, friendship and words of encouragement.
- Last but not least, to my boyfriend, Fábio Costa, to my parents, João Trindade and Maria Trindade, to my brother, Sérgio Trindade, and to all my friends and family for believing in me and giving me the support that was essential for the conclusion of this work.

Resumo

O disco da articulação temporomandibular (ATM) é um tecido fibrocartilaginoso que suporta e lubrifica a articulação. Devido a esta importante característica e ao facto de apresentar uma baixa capacidade de regeneração intrínseca, está altamente predisposta a sofrer lesões traumáticas ou degeneração, incluindo nas estruturas ósseas da articulação. Em casos mais avançados de disfunção discal, a sua remoção total é essencial para diminuir a dor e aumentar a função oral. No entanto, é necessário um substituto para a estabilização da articulação, para a correção da oclusão dentária e para prevenir a degeneração nas estruturas ósseas.

Existem algumas tentativas no campo da engenharia de tecidos para encontrar um substituto adequado, mas a investigação persiste. O interesse em tecidos xenogénicos descelularizados tem vindo a aumentar, pelo que o presente estudo se centrou no desenvolvimento de um potencial disco de ATM baseado na descelularização de discos de borrego. Para este fim, diferentes protocolos de descelularização foram avaliados testando diferentes agentes/concentrações, tais como solventes (etanol/acetona), detergentes (sulfato de sódio dodecilo e Triton X-100) e enzimas (accutase). Um método físico (um ciclo de congelamento e descongelamento) foi também combinado com os dois detergentes. Uma análise completa da morfologia (peso, espessura e dimensões mediolateral e anteroposterior) e testes de compressão dos discos nativos e acelulares foram realizados para avaliar se havia alterações nas propriedades do disco. Foram aplicadas análises univariadas e multivariadas por espectroscopia de infravermelhos da transformada de Fourier para avaliar o impacto dos agentes de descelularização nos componentes da matriz extracelular (MEC), tais como colagénio e glicosaminoglicanos (GAGs). Além disso, o microscópio electrónico de varrimento e a microtomografia computorizada permitiram a visualização da morfologia do disco, permitindo a avaliação do MEC e a remoção do conteúdo celular.

Através desta tese foi possível realizar um estudo preliminar no qual foram avaliados diferentes métodos de descelularização, onde as experiências mostraram que a combinação de congelamento e descongelamento seguida de 0,1% de Triton X-100 leva à remoção completa das células, preservação da morfologia e do comportamento mecânico, enquanto que o colagénio e os GAGs são minimamente afetados. São propostos estudos futuros para a otimização deste protocolo, tais como a implementação de mais ciclos de congelamento e descongelamento e a combinação com a enzima accutase.

Palavras-chave: disco da articulação temporomandibular, distúrbios discais, engenharia de tecidos, descelularização, matriz extracelular

Abstract

The temporomandibular joint (TMJ) disc is a fibrocartilaginous tissue that supports and lubricates the joint. Due to this important feature and the fact that presents low intrinsic regeneration capacity, is highly predisposed to suffering traumatic injuries or degeneration, including all structures of the joint. In more advanced cases of disc dysfunction, its total removal is essential to decrease pain and increase oral function. However, a substitute is needed for joint stabilization, correct dental occlusion and to prevent degeneration in the remaining bone structures.

Some attempts in the field of tissue engineering to find a suitable substitute have been done, but the research persists. Interest in decellularized xenogeneic tissues has been increasing, so the present study has focused on developing a potential TMJ disc based on the decellularization of lamb discs. To this end, different decellularization protocols were evaluated by testing different agents/concentrations, such as solvents (ethanol/acetone), detergents (sodium dodecyl sulfate and Triton X-100) and enzymes (accutase). A physical method (one cycle of freeze and thaw) was also combined with the two detergents. A complete analysis of the morphology (weight, thickness and mediolateral and anteroposterior dimensions) and compression tests of the native and acellular discs were performed to evaluate if there were changes in the properties of the disc. Univariate and multivariate analyses by Fourier transform infrared spectroscopy were applied to assess the impact of the decellularization agents on the extracellular matrix (ECM) components, such as collagen and glycosaminoglycans (GAGs). Moreover, scanning electron microscope and micro-computed tomography allowed the visualization of the morphology of the disc, enabling the evaluation of the ECM and the removal of complete cell content.

Through this thesis it was possible to carry out a preliminary study in which different methods of decellularization were evaluated, where experiments showed that the combination of freezing and thawing followed by 0.1% Triton X-100 leads to the complete cell removal, preservation of morphology and mechanical behaviour, while collagen and GAGs are minimally affected. Future studies are proposed for the optimization of this protocol such as the implementation of more freeze and thaw cycles and the combination with accutase enzyme.

Keywords: temporomandibular joint disc, disc disorders, tissue engineering, decellularization, extracellular matrix

Index

List of Figures

List of Tables

Abbreviations

3D- Three Dimensional

AT- Anterior

CT- Central

DD- Disc displacement

DDwoR- Disc displacement without reduction

DDwR- Disc displacement with reduction

dECM- decellularized Extracellular Matrix

ECM- Extracellular Matrix

EDTA- Ethylenediaminetetraacetic acid

FDA- Food and Drug Administration

FTIR- Fourier-Transform Infrared

GAGs- Glycosaminoglycans

HA- Hyaluronic acid

HMDS- Hexamethyldisilazane

ID- Internal derangement

LT- Lateral

MD- Medial

Micro-CT- Micro-Computed Tomography

PBS- Phosphate buffered saline

PG- Proteoglycan

PGs- Proteoglycans

PT- Posterior

RT- Room temperature

SDS- Sodium Dodecyl Sulfate

SEM- Scanning electron microscopy

TE- Tissue Engineering

TMD- Temporomandibular Joint Disorders

TMJ- Temporomandibular Joint

UV- Ultraviolet radiation

Chapter 1: Introduction

1.1 Background

Cartilage is a connective tissue that functions as load-bearing and is divided into three types: articular cartilage, elastic cartilage, and fibrocartilage. They are present in different zones of the skeleton but predominantly in joints and where flexible support is needed. All of them differ in their matrix composition. Because cartilage is an avascular tissue with a low metabolic rate, it presents low regeneration and repair capacity after trauma or injury (Mescher et al., 2018). Nowadays, hearing about damage or degeneration in our body's articulations, such as the knee, hip, shoulders and ankle, regardless of their cause, is something common and several clinical options are available. However, the temporomandibular joint (TMJ) is one of the least understood joints of our body that allows performing activities such as communicating, eating and smiling (MacBarb et al., 2011). When these functions are compromised, strongly affecting the quality of life, we are faced with temporomandibular disorders (TMD).

The peak age for TMD is between 20 and 40 years, with a decreased prevalence in younger and older people. There are distinct onset ages for specific diseases: 30 years for the appearance of disc dislocations (DD) and 50 years for the onset of inflammatory/degenerative dysfunctions (Manfredini et al., 2011). The articular disc is crucial for the correct movement of the TMJ and, in severe cases of DD, can lead to thinning or perforation of it. Osteoarthritis is also a common dysfunction, but its relationship with DD is still debatable (Donahue et al., 2019).

Food and Drug Administration (FDA) has approved products for articular cartilage repair (Sutherland et al., 2015).However, for fibrocartilage and especially the TMJ disc, this does not exist yet. Although the avascular structure of the cartilage is considered a challenge for its repair, it is also due to its dense extracellular matrix (ECM) that it can be considered almost nonimmunogenic since it physically protects the cells present in the ECM in case of graft rejection, opening a wide option for the use of allogeneic or xenogeneic tissues (Benders et al., 2013).

Decellularized xenogeneic tissues are ideal for load-bearing or high ECM content tissues, resembling the characteristics and properties of the native one (Chan et al., 2008). Different commercial products are available from xenogeneic tissues, e.g. porcine dermis or porcine urinary bladder for soft tissues (Crapo et al., 2011). Tissue Engineered (TE) decellularized extracellular matrix (dECM) approaches could help in search of an engineered-disc construct. However, its application for the TMJ disc is still in the early stages.

1.2 Thesis Scope

Decellularized tissues are a well-known matter in the biomedical field. Through research in PubMed.org, it is possible to observe that this area is being increasingly explored and evolving over the years (Figure 1).

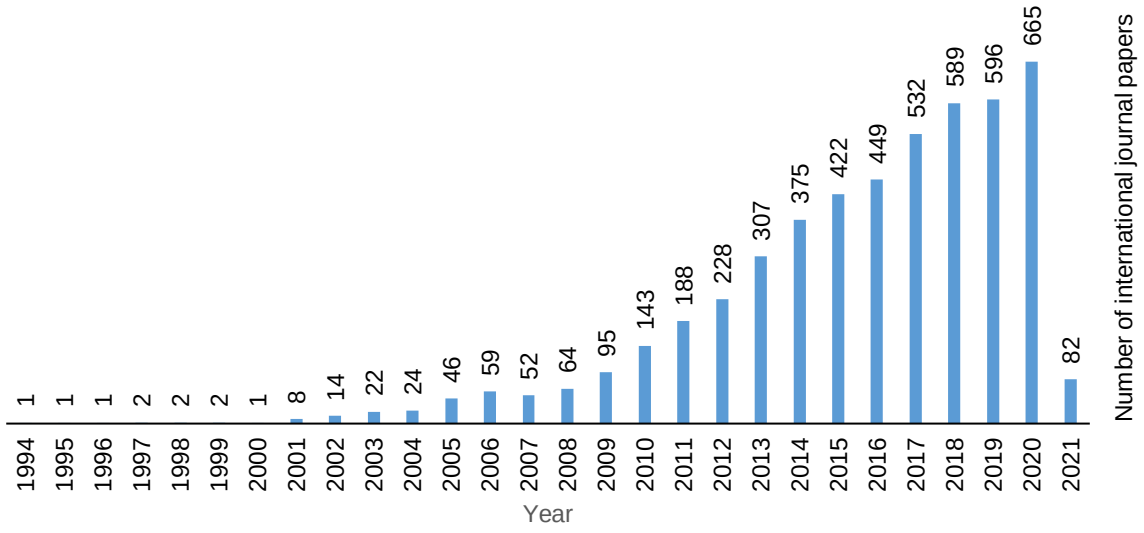

Figure 1 - Evolution of the decellularization area over the years. Retrieved from PubMed.org (30th of January of 2021) with the research designation "decellularization", where 4222 results were found.

Despite this, a TMJ disc based on decellularized xenogeneic tissues that mimic the native properties and functions has not been fully explored. The production of a material that has the characteristics required for implantation is highly dependent on the type of tissue under study and the decellularization agent used, which is also depend on the concentration, exposure time, temperature and post-processing.

The first use of dECM for TE of the TMJ disc was powdered porcine urinary bladder ECM encapsulated within sheets of the same material, and although an *in vivo* implantation in dogs led to proper tissue formation, it is necessary to perform an analysis of the remaining bone structures (Brown et al., 2011, 2012). Regarding the studies that evaluate methods of TMJ disc decellularization, five papers are found in the literature. A full description of these articles will be given in section 3.1, but briefly, the first investigation was performed on porcine discs, where three different reagents were tested (sodium dodecyl sulfate (SDS), Triton X-100 and ethanol/acetone) (Lumpkins et al., 2008). Since then, different authors have tried to improve the decellularization process by including the retrodiscal tissue (Matuska et al., 2018), as well as to implement artificial microporosities for cell diffusion (Juran et al., 2015; Matuska et al., 2018), but by always evaluating a chemical decellularization procedure. More recently, an

injectable hydrogel based on dECM porcine discs was developed based on the combination of physical, chemical and enzymatic decellularization methods, but a decrease in the glycosaminoglycans (GAGs) content was found (Liang et al., 2020). A sixth paper can also be considered in this topic. Despite a decellularization process was carried out based on the results of the above-mentioned articles, it did not study the results of decellularization, but rather studied different methods of sterilization (Matuska et al., 2015).

Although there is already some research on disc decellularization, its investigations are limited to a few decellularization agents, such as chemical agents, or if a more complete protocol is applied the biochemical content is affected. Thus, the main objective of this work was to develop a potential TMJ disc subtitute based on the decellularization of lamb discs. For this purpose, different decellularizing agents were tested, including physical, enzymatic and chemical. The evaluation of these included analysing whether the cellular content was removed, as well as, the effects on the ECM both in terms of biochemical content and biomechanical behaviour.

Chapter 2: State-of-Art

2.1 The Temporomandibular Joint

The masticatory system is composed of a set of anatomical structures that are responsible for complex biopsychosocial functions. These functions provide distinctive and selective daily functions including chewing, swallowing, eating and yawning, as well as emotional expressions, such as smiling, laughing and screaming. The TMJ is a complex articulation that is formed by bones, joints, ligaments, teeth, and muscles. Its organisation allows proper masticatory performance, bite force, and mandibular mobility (Asadi et al., 2018; Riera-Punet et al., 2018).

The TMJ (Figure 2) is positioned on both sides of the skull and it is the most commonly used joints in the body. It moves from 1500-2000 times a day. It is a bicondylar joint that articulates the condyle of the mandible against the glenoid fossa and the articular eminence of the temporal bone, allowing crucial normal mouth functions (Bae et al., 2013).

There is an articular disc between the mandible and the maxilla that divides the TMJ into two compartments: lower and upper. The lower compartment, which is formed from the association of the mandible with the articular disc, is considered a ginglymoid joint because it provides a hinging movement in one plane. The upper compartment that is formed by the association of the articular disc with the glenoid fossa is considered an arthrodial joint because it provides a gliding movement. These two types of movements classify the TMJ as a ginglymoarthrodial joint, one of the most complex in the human body. Besides this classification, the TMJ can also be characterised as a compound joint since the articular disc acts as an unossified bone to allow complex movements (Demerjian et al., 2018; Okeson et al., 2019).

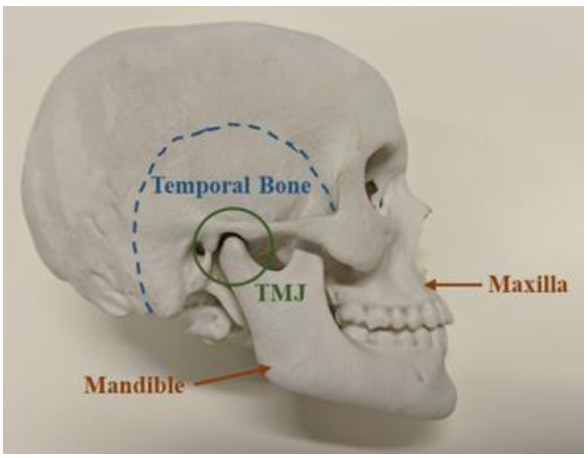

Figure 2 - Skull with different anatomical structures.

2.1.1 Glenoid Fossa and Articular Eminence

The glenoid or mandibular fossa and the articular tubercle or eminence are bony structures of the TMJ that belong to the temporal bone (Figure 3) (Norton et al., 2016). The temporal bone also contains the postglenoid process, which is located anterior to the external acoustic meatus canal. The glenoid fossa has a concave shape that is larger than the mandibular condyle and ideal for the interaction of these articular surfaces. The top of the fossa presents a thin thickness (1.0 - 1.2 mm), so it is functionally impossible to support the necessary stresses (Ramdhan et al., 2019; Sakul et al., 2019).

The articular eminence appears in the lower edge of the zygomatic arc, anterior to the mandibular fossa (Sakul et al., 2019) and medial to the posterior margin of the zygomatic process (de Pontes et al., 2019). The path and type of movement performed by the disc condyle complex, as well the rotation of the disc, is determined by the morphology of the joint eminence, as they slide back and forth along the mandibular movement (de Pontes et al., 2019; Rabelo et al., 2017).

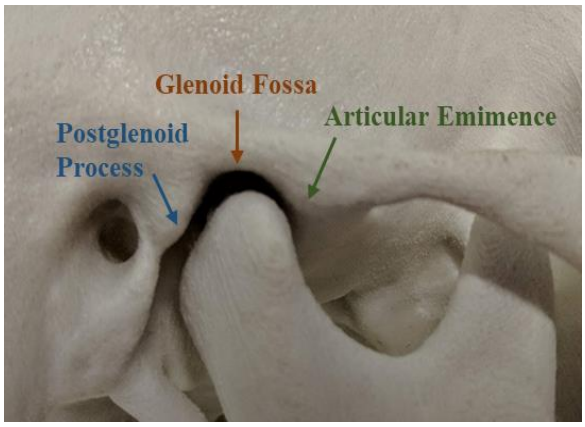

Figure 3 - Temporal bone structures.

2.1.2 Mandibular Condyle

The mandible, which forms the lower jaw, is divided into five regions (Figure 4): body, ramus, coronoid process, condylar process and alveolar process (Norton 2016b). The mandibular condyle has a convex configuration, that leans forward on the neck, with an angle of approximately 30º. It articulates indirectly with the glenoid fossa, on its anterior and superior surfaces, and directly with the TMJ disc (Kurup et al., 2017; Tamimi et al., 2016).

Both the glenoid fossa and the mandibular condyle are covered by fibroelastic tissue called fibrocartilage (Hargitai et al., 2018). It is a thick tissue where the transmission of vector forces occur throughout the disc (Sakul et al., 2019). Similar to the disc, which will be explained in the

following topic, the condylar cartilage functions as a load-bearing cushion that protects the underlying bone (Stocum et al., 2018).

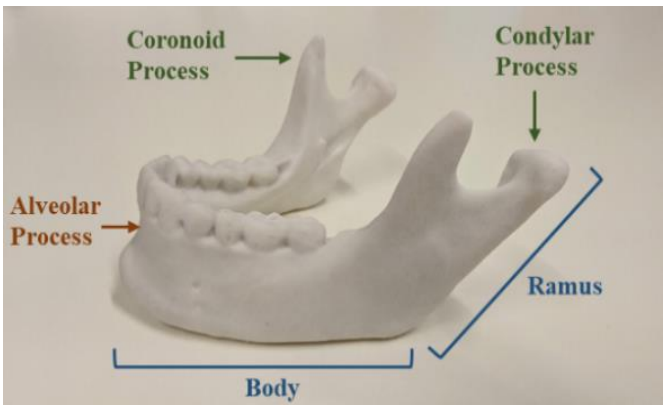

Figure 4 - Mandibular structures.

2.1.3 Articular Disc

2.1.3.1 Morphology

The TMJ disc is composed of dense fibrous connective tissue that is free of vessels and nerve fibres. It is only minimally innervated in the periphery of the disc (Okeson et al., 2019). It is located between the condyle and the glenoid fossa. It is in contact with these articulated surfaces and attached to the joint, and thus it is able to move freely (Willard et al., 2011).

The disc has multiple morphological classifications due to its differences in thickness. As seen in Figure 5, it is divided into three regions in the anteroposterior zone: the anterior, intermediate and posterior bands. The intermediate band can be divided into medial, central and lateral regions, exhibiting mediolateral variation. In the sagittal plane, the intermediate zone is the thinnest and gives the disc its biconcave shape. The disc is thicker in the posterior zone compared to in the anterior zone. It is also thicker medially than laterally from an anterior view. In the mediolateral dimension, the anterior and posterior zones are longer than the anteroposterior dimension. Moreover, due to the varying properties of the surfaces of the TMJ disc, it can be classified into superior and inferior regions (Morales et al., 2016; Okeson et al., 2019; Willard et al., 2011).

Since the TMJ is a structure involved in several important roles, the articular disc serves numerous purposes as it disseminates the complex loads to which it is subjected. It aids in joint lubrication, increases congruence between the articulating surfaces, absorbs shocks and smooths the movement by acting as a load-bearing (Vapniarsky et al., 2018; Willard et al., 2011). When performing daily functions, there are several mechanical forces, including shear, tensile, compression and rotation, indicating that the disc has a high resilience potential (Juran et al., 2015).

The disc is located between the condylar and mandibular fossa complex, depending on whether the mouth is closed or open. The morphology of this complex defines the form of the disc (Donahue et al., 2019; Okeson et al., 2019), and its exceptional properties and architecture are what provide the proper lubrication and stress-bearing functions for the TMJ (Willard et al., 2011).

The disc can adapt to its functional demands due to its flexibility and versatility. However, these properties may lead to irreversible morphological changes. Destructive forces or structural variations may occur in the joint and, consequently, modify the biomechanical properties of the original disc (Okeson et al., 2019).

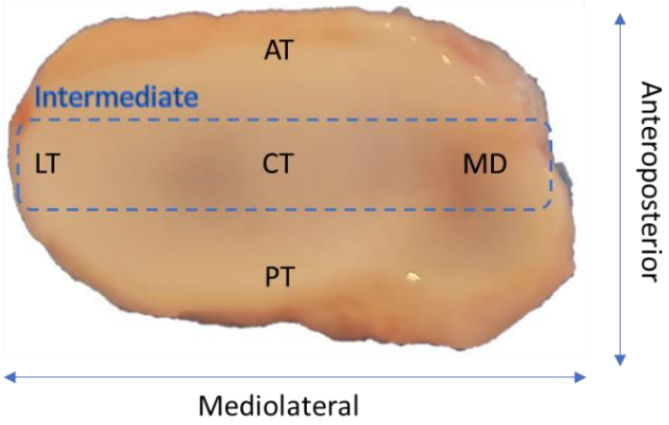

Figure 5 - Lamb articular disc and different morphological views. Abbreviations: PT - posterior; AT - anterior; MD - medial; LT – lateral and CT - central.

2.1.3.2 Cells and Biochemical Composition

Fibrocartilage is the tissue that constitutes the disc. It is composed of cells and an ECM. This comprises GAGs, aggrecans, water and elastin fibres (Shu et al. 2015). It contains a heterogeneous family of cells composed of fibroblasts (70%) and chondrocytes (30%), hence called fibrochondrocytes. The global cellularity per gram of tissue is reportedly between 20 and 50 million cells, but this number may differ among species. Regardless of the actual number, fibrochondrocytes are found in all species. A comparative study discovered that the anterior and posterior band presented higher cell density values in rat, porcine and goat disc, whereas for the human the same result was found but the differences with the remaining regions was not that pronounced compared to the other animal species (Kalpakci et al., 2011).

The ECM is composed of macromolecules and fluids. The principal macromolecules present in the disc are collagen and proteoglycans (PGs) (David et al., 2016; Willard et al., 2011). Water content ranges from 66% to 80% and decreases slightly with age (Detamore et al., 2003).

Collagen, in total, comprises 37% of the wet weight, 50% of the wet volume or 69–85% of the dry weight, where collagen I is the most abundant biochemical component. Elastin and GAGs comprise 3-7% and 1-10% of the dry weight, respectively (Acri et al., 2019).

Collagen fibre alignment is anisotropic, but there is a common orientation (Figure 6). There is a ring structure on the periphery of the disc. The fibres in the intermediate zone align in the anteroposterior direction. It is possible to observe a transitional region in the centre of the disc due to the fact that the fibres of the intermediate zone meet the fibres of the anterior and posterior bands that in turn are aligned in the mediolateral direction (Stocum et al., 2018; Willard et al., 2011).

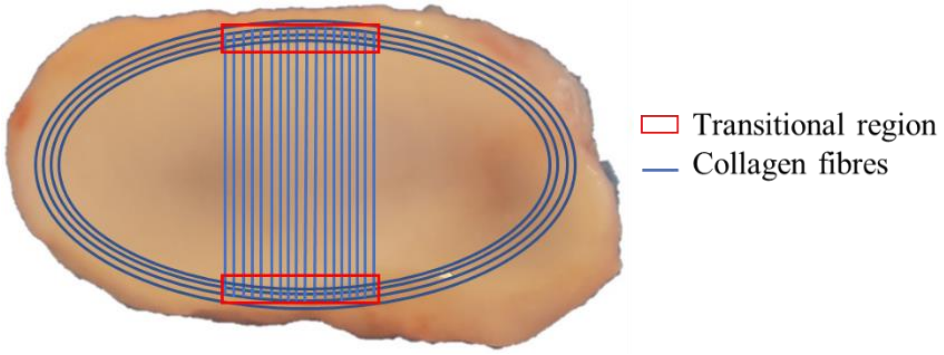

Figure 6 - Collagen fibre alignment.

2.1.3.3 Biomechanical Properties

Although the disc has exceptional characteristics, when the condyle moves there is deformation of the ECM solid component and pressurisation of the fluid changes causing disc fatigue. This phenomenon occurs due to the tangential tensile forces that are created (Wu et al., 2017). During dynamic loading there is a difference of fluid flow into and out of the disc, which causes the disc to behave in a less rigid manner than under static loads (David et al., 2016).

The biochemical composition and orientation define the mechanical properties of the disc, so its regeneration remains a challenge (Legemate et al., 2016). Regarding collagen, the elastic properties of the articular disc are associated with the anisotropic fibre orientation. The direction of the fibre alignment as well as the degree of these alignments changes from region to region. Thus, the disc presents heterogeneous mechanical properties (Gutman et al., 2018). The tensile modulus of the posterior band is half of the intermediate zone, due to the anteroposterior alignment of the fibres in the intermediate zone, which are perpendicular to the applied load. There is a substantial difference in the tensile variation in the anteroposterior direction, where the medial and lateral disc sections are less rigid compared to the central disc region (Willard et al., 2011). The disc has an elasticity that is derived more from collagen fibres

and less from PGs, and thus the compressive elastic modulus is lower than its tensile modulus (David et al., 2016).

In general, collagen fibres play a key role in disc stabilisation, so a simple break in this complex network can alter its mechanical properties. The disc plays an important role in mandibular kinematics and defines the anteroposterior path of the joint. Thus, a simple deviation of the disc can lead to internal disruption and, consequently, alter its biomechanical properties (Fazaeli et al., 2016)

Due to trauma, pathology or even ageing, the biomechanical properties of the disc may change. Until adulthood, the amount of collagen increases and the amount of water remains constant, phenomena that increase disc elasticity (Nakano et al., 1996). When there is damage due to increased friction and a consequent increase in shear stress, GAGs recomposition occurs and changes the mechanical properties of the disc (Stanković et al., 2013).

2.1.4 Articular Disc Attachments and Bilaminar Zone

The articular disc is bound by peripheral attachments (lateral, medial, posterior and anterior directions) that maintain its position and stability (Donahue et al., 2019; Matuska et al., 2018). It is attached inferiorly to the anterior condyle and superiorly to the eminence, in the anterior direction. Moreover, the disc is fixed to the bilaminar zone, which is also fixed superiorly to the temporal bone and inferiorly to the posterior condyle, in the posterior direction. The disc attachment merges into the joint capsule laterally and medially. Due to this multifaceted arrangement, it is possible to have a wide opening of the mouth because the disc and the condyle function as a single element. This complex also allows the condyle to rotate relatively to the disc (Willard et al., 2011).

In the bilaminar zone, the posterior part of the disc has the most significant attachment, termed retrodiscal tissue, that is located posterior to the disc and connected to the temporal bone. It is vascularised, innervated and comprises connective tissue (Matuska et al., 2018; Sakul et al., 2019; Talmaceanu et al., 2018). This tissue is attached to the disc superiorly and inferiorly through two laminas called the superior retrodiscal lamina and inferior retrodiscal lamina, respectively. Both superior and inferior laminas have defined functions. They prevent disc slippage when opening the mouth and prevent excessive rotation of the disc, respectively (Sakul et al., 2019).

As mentioned above, the disc acts as a trampoline by distributing the load and absorbing shock. The disc is connected by the attachments and, thus it is easier to dissipate applied loads. The attachments present less GAGs and collagen II content and higher cellularity compared to the articular disc (Murphy et al., 2013; Willard et al., 2012). This disc and the

attachments can suffer from pathological remodelling or deterioration in the case of damage or illness. These issues interfere with the regular joint role. Eventually, this dysfunction may lead to the removal of the disc and alter the performance of the remaining structures (Matuska et al., 2018).

2.1.5 Capsule and Synovial Membrane

The TMJ is surrounded by an articular capsule that is coated by a synovial lining, a dense connective tissue composed in endothelial cells that produce synovial fluid. This tissue surrounds the internal surfaces of the joint capsule, except the disc and surrounding cartilage, and forms a fibroelastic, highly vascular synovial membrane (David et al., 2016; Okeson et al., 2019). It contains an intimal and subintimal layer, both composed mainly of fibroblasts and macrophage-like cells (David et al., 2016). In a healthy TMJ, the key component of the synovial fluid that determines the viscosity and, consequently, reduces friction is hyaluronic acid (HA) (Stanković et al., 2013).

In terms of size, the capsule is wider than the articular surfaces to allow the condyle to move forward in a smooth way during protraction (Sakul et al., 2019). The capsule is connected to the neck of the mandible and the articular surfaces of the temporal bone (Ramdhan et al., 2019).

As mentioned above, the joint is divided into the superior and inferior compartments, and synovial fluid fills both cavities. The volumes present in the superior and inferior joint compartments are 1.2 ml and 0.9 ml, respectively (David et al., 2016). The synovial fluid has many purposes in order to provide normal TMJ function. Its composition includes a proteoglycan (PG), lubricin, that it is synthesized by the chondrocytes present in the cartilage and the fibroblastoid synovial lining cells. This PG minimises friction and allows lubrication during condylar movements due to a surface tension that spreads the fluid to the cartilage (Balatgek et al., 2018; David et al., 2016). Furthermore, because the articular surfaces are avascular, the synovial fluid serves as a medium for nutrients providing the required metabolites to the fibrocartilages and also serves to eliminate waste products (Okeson et al., 2019; Willard et al., 2011). A study demonstrated that there is more space in the superior joint for males. Additionally, in patients with disorders, this same cavity is smaller (de Pontes et al., 2019).

2.2 Temporomandibular Joint Disorders

Throughout this chapter, TMJ has been described as a complex load-receiving structure. Therefore, it is predisposed to extreme or unbalanced loading that can produce dysfunctional remodelling that is often asymptomatic and may affect joint function (Urtane et al., 2016). The

ability of TMJ components to adapt to normal or abnormal behaviours defines joint health (Schilling et al., 2013).

TMD are a heterogeneous group of conditions related to the anatomy, functionality, dysfunctions and pathologies of the TMJ and associated structures (Aryaei et al., 2016). They are the second most common musculoskeletal condition and affect approximately 5 to 12% of the population. The major problem that results from these conditions is orofacial pain, which affects the health and quality of life of the individual (Riera-Punet et al., 2018; Shoukri et al., 2019).

Approximately 50 to 75% of adults and 60 to 70% of the general population have shown at least one sign of TMD, but only 1 to 3% of the population seeks treatment (Armijo-Olivo et al., 2016; Chisnoiu et al., 2015). Symptoms include bruxism, muscle soreness, reduced range of jaw motion, joint sounds and chronic pain that can affect the ears, eyes, neck and face or produce headache. The pain is usually experienced in the chewing muscles and the preauricular region (Aryaei et al., 2016; Bitiniene et al., 2018; Gil-Martínez et al., 2018). Symptoms have a three to five times higher incidence in women compared to men (Gil-Martínez et al., 2018), but this difference may be related to the fact that women seek treatment, whereas men do not (Bitiniene et al., 2018).

Although TMJ is able to adapt to changes in functional load within physiological limits (Roberts et al., 2018) there are some factors that can increase a person´s predisposition to develop TMD, including poor posture, trauma, parafunctional habits, changes in occlusion and physical and emotional problems including stress, anxiety or depression (Figure 7) (Armijo-Olivo et al., 2016; Bartley et al., 2018; Bitiniene et al., 2018; Nascimento Falcão et al., 2017). Stress affects the appearance of the disorder and its evolution (Urbani et al., 2019). A study demonstrated that the association between poor sleep quality and the onset of a TMD is mediated by stress. The authors concluded that improving sleep and reducing stress may help reduce the risk of developing a disorder (Sanders et al., 2017). There is also a relationship between TMD and long-term back pain (Wiesinger et al., 2007).

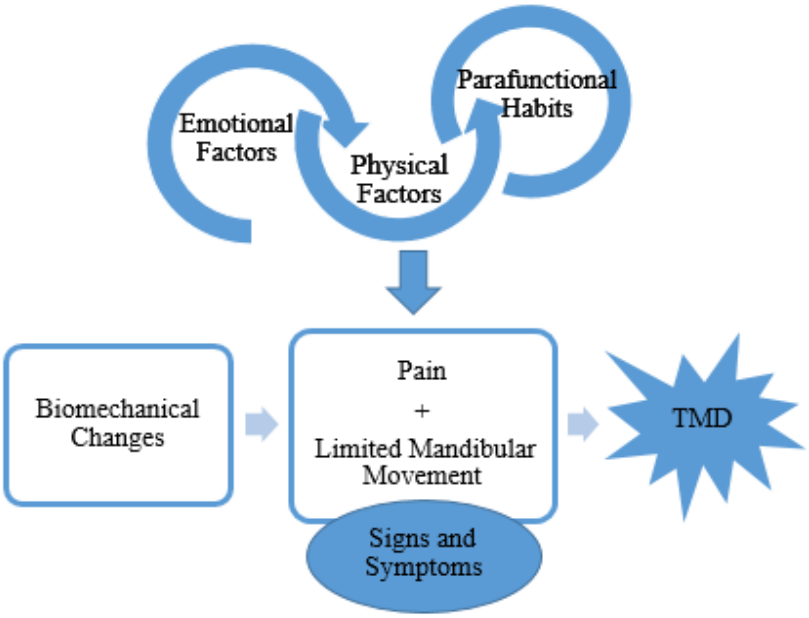

Figure 7 - Schematic diagram of temporomandibular disorders (TMD) development.

2.2.1 Articular Disc Dysfunctions

A subset of disc-related TMD involves internal derangement (ID) or DD, disc thinning and disc perforation. As it will be explained in the following topic, disc thinning and perforation could be related to ID, where these events represent 5-15% of ID patients. However, it may not only be related to this problem (Donahue et al., 2019; Vapniarsky et al., 2018). Biomechanical unbalance or extreme loading can also lead to damage in the articular disc (Tanaka et al., 2000).

2.2.1.1 Disc Displacement

The relationship between the disc and the other articulating joint structures has been recognized as a TMD. An abnormal position or malfunction of the disc alters the condylar position relatively to the glenoid fossa. This malfunction leads to DD or internal derangement of the TMJ (Rabelo et al., 2017). Up to 70% of TMD patients suffer from DD (Aryaei et al. 2016). Most of the times DD is asymptomatic, but brief pain and dysfunctions may occur (Sperry et al., 2019). With age and trauma, the disc may decrease in thickness, more specifically in its central region, and compromise its normal function (Balatgek et al., 2018).

DD is associated with any disorder that affects the anatomical features of the TMJ and, consequently, its function (Warmling et al., 2015). With DD, there is displacement and excessive extension of retrodiscal tissue and associated ligaments, a phenomenon that enhances tissue deformation and underlies a loss of elasticity (Machon et al., 2017). However, it can also alter the morphological features of the osseous structures (Rabelo et al., 2017).

The disc can adopt eight abnormal positions, but the most common are the anterior and anterior-lateral displacements, and the rarest is the posterior. The dislocation can either be partial or complete (Lalue-Sanches et al., 2015). As seen in Figure 8, when the disc is not in its normal position, and if a click is heard when opening the mouth, the disc has repositioned itself. This condition is referred to as DD with reduction (DDwR). If the sound is not heard when opening the mouth, the disc has not returned to its original position, and the condition is called DD without reduction (DDwoR) (Michelotti et al., 2019; Okeson et al., 2017; Slater et al., 2019).

There are two further possible classifications: *i)* DD with limited opening and *ii)* DD without limited opening. Both cases occur without reduction. In the first former, there is a limited mandibular opening with a maximum of 40 mm. In the latter, there is no limited opening and the mandibular opening is a minimum of 40 mm (de Leeuw et al., 2018).

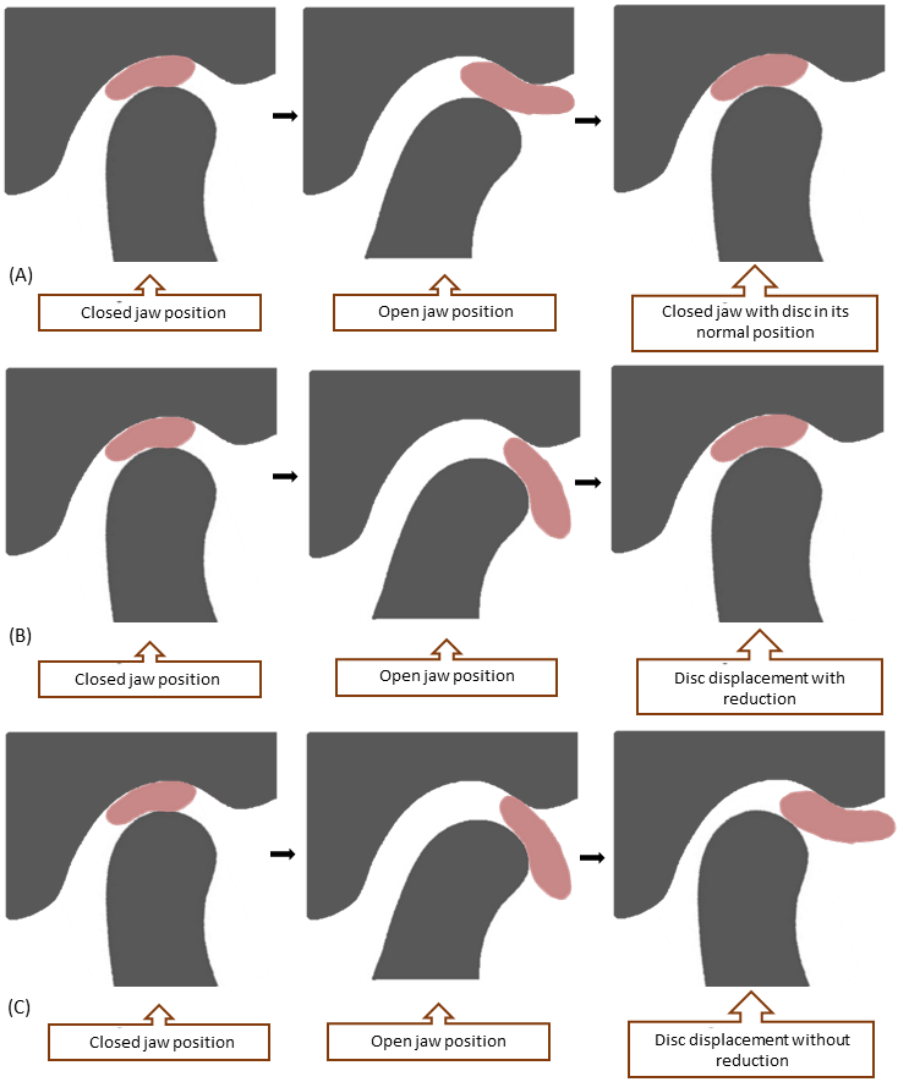

Figure 8 - Normal jaw function (A). Disc displacement (B) with reduction and (C) without reduction.

2.2.1.2 Disc Structural Changes

The articular disc presents a biconcave shape. However, some morphological deformations may be found. These deformations may be classified as lengthened, biconvex, thickening, folded and rounded (Incesu et al., 2004; Katzberg et al., 2005; Orhan et al., 2006; Taşkaya-Yılmaz et al., 2001).

DD is the main problem that leads to disc deformation. This deformation is mostly found on joints with DDwoR and begins with the thickening and enlargement of the posterior band of the articular disc (Incesu et al., 2004; Katzberg et al., 2005; Orhan et al., 2006). Hasan & Abdelrahman (2014) supported these facts by proving that the risk of degenerative changes increased with the prevalence of an anterior DDwoR, being the anterior displacement the most frequent type of occurrence. It was also found a relationship between the articular structures and the anterior DD, where deterioration may occur to the disc and its ligaments if there is a posterior condylar position.

Disc degeneration leads to the formation of fibrous tissue and loss of normal TMJ disc morphology, such as thinning and perforation (Bae et al., 2014; Incesu et al., 2004).

In conditions of closed-mouth position and teeth contact, if there is an extreme and long load, it could cause the thinning of the disc in the central band (Ivkovic et al., 2018). Moreover, cases of displacement could also lead to thinning of the posterior band (Figure 9) (Vladimir Machon et al., 2012).

Disc perforation could be related to osteoarthritis, rheumatic/inflammatory disease, or ID (Embree et al., 2015), normally with anterior DDwoR (Muñoz-Guerra et al., 2013). It usually ruptures in the bilaminar zone and the lateral part of the disc, but depending on the type of DD it can perforate in different places (Liu et al., 2010). The major problems related to perforation is the fact that the disc loses its functionality of lubrication due to interference with the synovial fluid, leading to increased friction between the articular structures of the TMJ and, consequently, resulting in hypertrophy (Kim et al., 2018; Muñoz-Guerra et al., 2013).

A more recent study classified the deformities based on closed-mouth images and categorized them into folded, flattened, eyeglass and amorphous. The authors concluded that disc perforation increases with the eyeglass and amorphous shapes, age, abnormal joint space, and 2 or more structural changes in the condyle and fossa bones (Kim et al., 2018).

Figure 9 - Temporomandibular disc thinning and perforation in an anterior view.

2.2.2 Management for Temporomandibular Disc Disorders

The comprehension of the pathogenesis and evolution of TMD are still unknown. TMD are marked by *(i)* displacement, thickening, and/or perforation of the articular disc, *(ii)* reduction to complete loss of the articular fibrocartilage, *(iii)* sclerosis and remodelling of supporting bone, and *(iv)* periarticular osteophyte formation (Aryaei et al., 2016). Therefore, a viable way to manage these disorders will be through the application of medical therapies that will allow the reduction of the symptoms and hypertonic muscles, consequently improving the mobility of the joint and surrounding structures. Conventional TMJ treatments can be divided into non-invasive, minimally invasive and invasive (Dashnyam et al., 2018; Khan et al., 2013). In an early stage of the disease, non-invasive treatments are ideal, while in the final stage the best option is an invasive method. However, there is no fully effective treatment and repeating therapy is still a possibility (Aryaei et al., 2016). Though, the effectiveness of conservative treatments varies from 70 to 95% (Lalue-Sanches et al., 2015). In terms of the surgical procedure, there is still some debate regarding its ability to manage pain and dysfunction, even though only 5% of TMD patients undergo this practice. For non-surgical, the success rate is 60%, although the possibility of an unresponsive treatment could happen (Chandrashekhar et al., 2015).

2.2.2.1 Non-Invasive

A large part of TMD patients does not benefit from surgical procedures, especially if referring to muscle disorders (Dolwick et al., 2019). Noninvasive treatments include physical therapy, occlusal splints, pharmacological methods, or acupuncture (Dashnyam et al., 2018). Physical therapy is used to relieve the symptoms of TMD, such as pain, to help lubricate and maintain jaw normal function. It includes neuromuscular stabilization, electrostimulation, low-intensity ultrasound, low-level laser therapy, and exercises (Cobo et al., 2019; Ingawalé et al., 2009; Khan et al., 2013). For anterior DDwoR, joint mobilization exercises were shown to be more effective than splints in improving mouth range and reducing pain after 8 weeks of treatment (Haketa et al., 2010), whereas joint mobilization exercises and massages alone did not show significant improvement after 6 weeks of treatment (Craane et al., 2012).

Occlusal splints are removable plastic devices that fit into the dentition, that can be used to repositioning the teeth or to prevent contact between them and, consequently, the clenching or grinding effect (bruxism) or myofascial pain. However, there is still some controversy in whether it is an appropriate treatment or not (Deshpande et al., 2010; Ingawalé et al., 2009). A systematic review showed no evidence of occlusal splint efficacy for TMD (List et al., 2010). However, some authors demonstrated temporary satisfactory results of anterior repositioning splints for treating DDwR (Liu et al., 2017; Pihut et al., 2018).

Pharmacological therapy is the primary intervention to be performed in the case of TMD and the main goal is to manage pain and discomfort, rather than being a curative therapy (Mujakperuo et al., 2010). It can be used drugs, as analgesics, anti-depressants, muscle relaxants, or non-steroidal anti-inflammatory drugs (Dashnyam et al., 2018). At last, acupuncture or laser acupuncture, where specific points of the body are stimulated, have also been shown to be effective in reducing signs of TMD, such as myofascial pain (Fernandes et al., 2017).h

Disadvantages of this type of treatments include the possibility of cardiovascular problems, gastrointestinal poisonousness and anaphylaxis and the fact that it is limited to restore severe or chronic disorders (Dashnyam et al., 2018). For all the treatments the long-term solutions effectiveness still needs confirmation (Cobo et al., 2019)

2.2.2.2 Minimally invasive

Minimally invasive treatments include arthrocentesis, arthroscopy or injections. Arthrocentesis is a safe, repeatable and clinically easy to execute procedure, where a needle is inserted inside the affected joint and aspirated, followed by injection of a therapeutic fluid. It can be done under local anaesthesia and it helps to normalise jaw opening and disc abnormal positions (Chandrashekhar et al., 2015; Ingawalé et al., 2009; Nitzan et al., 2018).

Arthroscopy is performed by making a small incision near to the patient´s ear and inserting an instrument that allows joint visualization. It can be used as a diagnostic tool or to perform surgical procedures, such as lavage of the TMJ, lysis of adhesions or inflamed tissue, reposition of the articular disc or medicaments injection. It is a low-cost and well-tolerated procedure (Connor et al., 2017; Ingawalé et al., 2009; Israel et al., 2016).

Several authors investigate the effectiveness of these procedures to manage ID. Arthroscopy lavage and lysis were shown to have an 86.7% efficacy when assessing pain and jaw opening (Smolka et al., 2008) and in a 5-year study, a success rate of 67% when assessing joint loading sign, TMJ noise, TMJ pain, and muscle pain (Hossameldin et al., 2018). Arthrocentesis was effective in repositioning the dislocated disc, along with decreased pain in DDwoR patients (Grossmann et al., 2019) and effective in improving jaw opening and pain decrease for patients

with ID with closed lock (Malik et al., 2014). TMJ closed lock may be caused by the anchored disc phenomenon. A study compared these two minimally procedures and concluded that both of them could treat this condition, whereas non-invasive treatments failed (Sanromán et al., 2004). Furthermore, a combination of arthrocentesis and occlusal splints is effective in managing discomfort in anterior DDwoR patients (Lee et al., 2013).

Via intra-articular injections, diverse medications can be administered directly to the target site within the joint space. Medications include corticosteroids, platelet-rich plasma from blood, HA, analgesics, and anti-depressants (Aryaei et al., 2016; Dashnyam et al., 2018). Due to the large presence of the HA in the synovial fluid and, consequently, its role in lubrication, HA injection has been widely studied for the management of ID. HA proved effective (Basterzi et al., 2009; Bonotto et al., 2014) and after arthrocentesis (Alpaslan et al., 2001; Ungor et al., 2015). In short-term treatments, HA presents similar outcomes to corticosteroids, but in long-term treatments HA presents better results (Machado et al., 2013). HA combined with corticosteroids or arthrocentesis alone are effective for ID, but considering the simplicity of the injection, this one is preferred (Marzook et al., 2020). Platelet-rich plasma did not show improvement after 2 years of the procedure (Fernández Sanromán et al., 2016), but compared with arthrocentesis showed better results (Hancı et al., 2015).

Side effects include dizziness, dry mouth, and probably drug dependence (Aryaei et al., 2016; Dashnyam et al., 2018). In the early stages of the disease, they help to relieve pain, but in a chronic situation, they are not effective (Cobo et al., 2019). The delivery of nano- or micro-biomaterials, drugs, and stem cells for therapeutic proposes have also been investigated, but further *in vitro* and *in vivo* studies need to be performed (Dashnyam et al., 2018).

2.2.2.3 Invasive

In TMD, especially for disc disorders or ID, surgical procedures are the last line of treatment. However, when nonsurgical clinical options fail, an open joint surgical (arthrotomy) option is taken into account. (Han et al., 2019). In this option, there can be adjustments to the TMJ components or the replacement of the entire or parts of the joint (Aryaei et al., 2016).

Regarding the joint disc, it can be repaired/reshaped and/or repositioned (discopexy or discoplasty) or completely removed (discectomy) (Frederick Liu et al., 2013; Renapurkar et al., 2018). Disc repositioning should be performed in healthy joint discs that can be placed in their native position without tension (Dolwick et al., 2001). This procedure was effectively achieved during arthroscopic procedures for TMJ ID (McCain et al., 2015; Zhang et al., 2010). However, a meta-analysis assessing the management of ID, concluded that open surgery is more effective than arthroscopic surgery in reducing pain, but it has similar results concerning maximum inter-incisal opening and maxillary function (Al-Moraissi et al., 2015). Kondoh et al.

(2003) investigated a new open surgery, with a 5-year follow-up, for reshaping the inferior surface of the articular disc without repositioning the disc, with a success rate of 91%. Despite these results, there is still some controversy regarding long-term successful outcomes of these procedures, as disc tend to return to their displaced position, and repair tends to fail due to the disc avascular structure (Dimitroulis et al., 2011b; Dolwick et al., 2001; Miloro et al., 2010).

Discectomy is the most common conducted intracapsular surgery (Ângelo et al., 2018) for unsalvaged deformed, displaced ou perforated discs. It can be performed with or without a replacement. Although discectomy without replacement results in reduction of pain and range of motion, crepitation and degenerative changes to the remaining articular surfaces tend to appear (Han et al., 2019; Liu et al., 2013; Renapurkar et al., 2018). The first synthetic replacements that emerged were Teflon-Proplast and silicone rubber that led to foreign-bodies reactions (Kaplan et al., 1988; Westesson et al., 1987). Also, autogenous grafts such as temporalis muscle flat (Smith et al., 1999), auricular cartilage (Matukas et al., 1990), full-thickness skin (Dimitroulis et al., 2006), dermal grafts (Meyer et al., 1988) and dermal-fat grafts (Dimitroulis et al., 2004) were developed, but a critical review states that none of them satisfies the necessities for a successful replacement of the disc after discectomy (Dimitroulis et al., 2011a). Moreover, there are no different success rates between discectomy alone compared with autogenous replacement, neither between the autogenous options (Kramer et al., 2005).

Joint replacement with prosthetics is the last stage of TMD management and it should only be applied when nonsurgical strategies fail. It consists of removing and replacing the TMJ structures that are highly injured with a prosthesis. There are three FDA approved prostheses for total joint replacement: Christensen prosthesis; TMJ Concepts device; and Biomet Microfixation system. Although they present good outcomes (Gerbino et al., 2017; Ingawalé et al., 2009) the disadvantages of prostheses are the possibility of wear and tear residues and, consequently, occurrence of inflammatory responses, metal fatigue and loose screws leading to mechanical failure, the cost of the device and the potential for secondary surgery (Quinn et al., 2016).

2.3 Tissue Engineering of the Temporomandibular Disc

As described above, existing clinical options are appropriate for early or more advanced stages of dysfunction and there is no intermediate treatment option. Also, there is no consistently fully effective treatment and consensus in what treatment to choose, being highly dependent on the doctor’s experience. Thus, the search for a solution for the complex regeneration of the disc and improvement of the patient's dysfunction has been investigated in the area of TE. With TE it is possible to produce implants capable of renewal, performing an adequate mechanical and

biological performance and, at the same time, integrating with the host structures for a successful repair of a failing tissue or organ (Patnaik et al., 2014).

To develop an optimized strategy for TMJ disc TE, the selection of the proper biomaterials, approaches, and consequent characterisation is essential. It is then, with the selected biomaterials, that cells are incorporated and exposed to stimuli to build the desired ECM microenvironment (Allen et al., 2006).

2.3.1 Biomaterials and Current Status in Research

For a successful TE of the TMJ disc, the first big challenge passes through the selection of the appropriate biomaterial for an optimal mechanical response. Biomaterials can be characterized as materials for use in medical devices or for repairing biological tissues or organs. They can be divided into natural (animal or human origin), or synthetic materials (Chan et al., 2008; Chen et al., 2016). They must meet several requirements to be applied in TE: biocompatibility with the host, to avoid an inflammatory response; biodegradability, to allow the material to be replaced by a suitable tissue; appropriate mechanical properties relative to the tissue function; and adequate permeability and architecture, such as porosity, to allow the transport and exchange of oxygen, nutrients, and waste (Armiento et al., 2018; Nasution et al., 2016). This mechanism is important due to the avascular structure of the disc and the fact that it is through mechanical stimuli of the synovial fluid that cells receive glucose and oxygen (Juran et al., 2015).

The current aim of biomaterials is to serve the necessary medical or surgical purposes to be safely implanted in the human body (Ramdan et al., 2016). Upon implantation, they can be used to provide a biodegradable support structure, with desirable shape and integrity for an intended period of time, effectively providing functionality, support and attachment to the cells and give rise to the creation and maturation of new tissue (Chen et al., 2016).

2.3.1.1 Natural Biomaterials

Natural biomaterials are derived from natural forms. They have a wide variety of applications in the biomedical field in the repair or replacement of biological tissues and organs. They present great biological requirements, such as biocompatibility, biodegradability, bioactivity, promote cell adhesion, proliferation and/or differentiation, which are essential for tissue construction. Moreover, they present similar behaviour to the biological macromolecules present in human tissues, which is an advantage. Despite these benefits, in certain situations, they present immunological reactions and some degree of variability, and there is the possibility of disease transmission. Another important fact is that natural materials can degrade at temperatures below their melting point (Manoukian et al., 2019; Nasution et al., 2016;

Ramdan et al., 2016). This property can be a problem regarding material processability, which result in low mechanical properties and unstable degradation rates (Cao et al., 2014).

Within the natural materials used for TMJ disc TE it is possible to find alginate alone (Almarza et al., 2004) or in combination with chitosan (Bousnaki et al., 2018), collagen (Kobayashi et al., 2015), and a combination of fibrin and chitosan (Wu et al., 2014).

2.3.1.2 Synthetic Biomaterials

Compared to natural biomaterials, synthetic ones present several advantages, such as their availability and reproducibility as they are controllable and easy to process. For TE purposes, they can be modified according to the characteristics of the implant site to present adequate mechanical (stiffness, porosity and elasticity), physical and biochemical properties and degradation rate. The major issue with these materials is the structural difference comparatively to native tissues, which may lead to a negative effect on biocompatibility (Grigore et al., 2017; Manoukian et al., 2019; Qian et al., 2019). One of the major issues associated with them is limited cell adhesion sites and homogeneous cell proliferation, which compromises tissue synthesis. Still, some biomaterials have high biocompatibility and incorporate well into the human body (Manoukian et al., 2019).

Several studies have shown the potential of synthetic biomaterials in the regeneration of the TMJ disc and the materials used were polylactide acid (Mäenpää et al., 2010), polyamide monofilaments and expanded polytetrafluoroethylene (Springer et al., 2001), polyglycolic acid and poly-L-lactic acid (Allen et al., 2008), poly (glycerol sebacate) (Hagandora et al., 2013) and poly(ε)-caprolactone alone (Legemate et al., 2016) or in combination with polyethylene glycol diacrylate hydrogel (Moura et al., 2020).

2.4 Decellularization of xenogeneic tissues

Cartilage has a low regeneration capacity and therefore, different substitutes have been focus of research to repair cartilage defects. Cartilage matrix can be collected from different sources, but access to allogeneic or autologous donor tissue is restricted, so the interest in using xenogeneic tissues for cartilage constructions has been increasing, where the TE field can offer a positive alternative. Regardless, for these tissue types, decellularization and sterilization methods are required with the aim of removing the immunogenic components that lead to the infection and disease transmission (Benders et al., 2013; Lumpkins et al., 2008; Schwarz et al., 2012).

Decellularization aims to preserve the organic, biological activity and three-dimensional (3D) architecture, as the immunogenic and inflammatory components, such as cells and antigens, are removed. The ECM is composed of proteins (collagen and elastin), cell adhesion proteins

(fibronectin and laminin), GAGs and PGs, and growth factors (Gupta et al., 2017; Keane et al., 2016).

The dECM has immense potential to serve as a beneficial material for tissue damage repair as it preserves the native environment by providing cells with the necessary elements, such as support and biochemical components, that are needed to provide their proliferation and/or differentiation. ECM organization and compounds differ from tissue to tissue (Kim et al., 2019; Sutherland et al., 2015), but in terms of cartilage, the two major components are collagen and PGs, that include bioactive factors, such as growth factors (e.g. transforming growth factor-beta, fibroblast growth factor and insulin-like growth factor), integrins, and functional peptides (Benders et al., 2013).

The benefits and disadvantages of using a dECM are referred to in Table 1 (Benders et al., 2013; Chan et al., 2008; Garreta et al., 2017; Hoshiba et al., 2010).

Table 1 - Advantages and disadvantages of decellularized tissues and organs.

Advantages	Disadvantages
(i) preservation of the ECM structure and its composition that induces tissue organization and remodelling	*(i)* ECM architecture variation from different species or donors
(ii) modulates cell performance: seeding, migration and/or differentiation	*(ii)* possibility of remaining cell content, eliciting negative reactions
(iii) ECM components are conserved across species, so it does not elicit rejection	*(iii)* the difficulty of obtaining an intact ECM
(iv) exhibits mechanical properties and environment similar to the native tissue	*(iv)* heterogeneous cell distribution after recellularization
(v) dECM organ guarantees the upkeep of the necessary cell and phenotypes functions	
(vi) unlimited access to obtain ECM	
(vii) the positive relationship between cost and effectiveness	

It is possible to decellularize a tissue or whole organ and after obtaining the acellular scaffold there can be various ways of application (Figure 10): *(i)* recellularization, where the cells repopulate the matrix; *(ii)* direct implantation; *(iii)* use as a cell culture substrate; and *(iv)* transform to create *(iv-1)* ECM sheets where is used as a mesh or patch graft or, *(iv-2)* ECM tubular grafts, e.g vascular tissue or process to *(iv-3)* ECM powder or particles, that can be suspended in a solution or used as it is; alternatively, it can be solubilized to form an injectable

hydrogel (e.g. for minimally invasive treatments). These applications can be used in combination with other biomaterials (Chen et al., 2016; Edgar et al., 2018; Hussey et al., 2018).

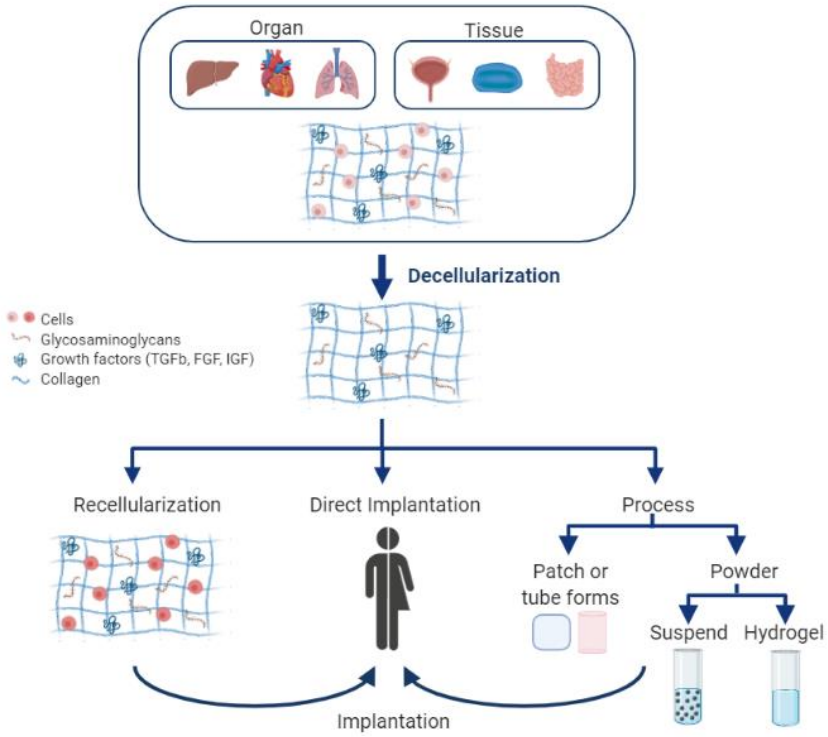

Figure 10 - Decellularization possible applications.

2.4.1 Effects on Extracellular Structure

The biomechanical properties, ECM composition, and structure and architecture of the tissue may be disturbed after decellularization and its negative effects are highly dependent on the applied agent. Also, the process of tissue collection and sterilization may lead to changes in the biomechanical behaviour, since it is related to the hydration and the 3D arrangement of the tissue. These characteristics are important for tissue regeneration. With respect to cartilage, more decellularization protocols are needed as their cells are incorporated along with the dense ECM. Because of this, GAGs may be depleted leading to a loss of water, consequently, the collagen network is affected, altering its biomechanical viscoelastic properties (Benders et al., 2013; Chen et al., 2016; Gilpin et al., 2017).

Therefore, to minimize these consequences the search and selection for the adequate decellularization agent to a specific tissue or organ is essential.

2.4.2 Assessment of Decellularized ECM

After decellularization, the evaluation of the acellular scaffold is important to prove its quality and that the necessary features are present. For this, it needs to be in consideration and confirm that *(i)* all cellular and genetic material was removed; *(ii)* the ECM components and its

architecture are preserved; *(iii)* there are no residual chemical agents; and (iv) that the mechanical behaviour is maintained (Garreta et al., 2017; Gilpin et al., 2017). All to prevent toxic and inflammatory reactions and prevent negative cell and host outcomes. Regarding EMC components and their structural organisation as well as their mechanical behaviour, there should be similar conservation to the native tissue (Crapo et al., 2011; Garreta et al., 2017).

These characteristics can be evaluated from different methods, such as histological or immunohistochemistry analyses, gel electrophoresis, biochemical assays, Scanning Electron Microscopy (SEM) and Micro-Computed Tomography (Micro-CT) (Hrebikova et al., 2015).

2.4.3 Decellularization Agents and Methods

Choosing the right animal species for a specific tissue is a critical step, and the decellularization method depends on the tissue choice, as cells and structure density, lipid content, and tissue thickness and shape vary. Decellularization includes physical, chemical, and biological agents or methods and all of them can eliminate cellular components. However, they also adversely affects the ECM. A combination of these methods could enhance the decellularization approach (Hoshiba et al., 2010; Keane et al., 2015; Lumpkins et al., 2008).

Tissues that undergo physical treatment are consider devitalized, more than decellularized since it only lyses cells and the debris are maintained in the tissue. It preserves more the ECM constituents and arrangement. Still, since it presents some part of cellular content, it will lead to immunological responses. This way, this type of treatment is usually applied in combination with chemical or biological ones. The success of a chemical treatment depends on the agent concentration, exposure time and tissue type. Enzymes, included in the biological category, are mostly applied after chemical treatment (Kim et al., 2019; Sutherland et al., 2015).

A complete description of the different reagents and techniques are described in Table 2 (Crapo et al., 2011; Gupta et al., 2017; Hrebikova et al., 2015; Keane et al., 2015, 2016).

Table 2 - Decellularization agents and methods commonly used.

	Method/Agent	Mechanism of action	Results on ECM
Physical	Freeze and thaw	Temperature ranging from freezing (ex: -80ºC) with ice crystals formation leading to cell lysis by breaking the cell membrane, and thawing (ex: 25ºC)	Ice crystals may disrupt the ECM; cellular material remnants
	Pressure or force	Their application burst cells and the act of removing tissue eliminates cells	Damage or disrupt the ECM
	Electroporation	Pulsed electric field leads to cell lysis by breaking the cell membrane	Causes oscillation disrupting the ECM
Chemical	Acids and Bases	Hydrolysis cytoplasmatic constituents; degrades nucleic acids	Collagen, GAGs and growth factors are damaged
	Hypotonic and Hypertonic Solutions	Induces osmotic shocks causing cell lysis; DNA-protein interactions are disrupted	Cellular material is lysed but not effectively removed. Hypo and hypertonic agents' alternation may decrease GAGs
	Solvents (e.g. alcohols and acetone)	Dehydration causes cell lysis and removes lipids	Proteins precipitate and tissue may become stiff
	Organic solvents (e.g. Tributyl phosphate)	Protein-protein interactions are disrupted	Collagens, GAGs and biomechanical behaviour may be affected; residual cytoskeletal proteins may remain
	Ionic detergents		
	(SDS)	Dissolute cell and nuclear membranes, lipids and DNA	Effective in removing cellular material and cytoplasmatic proteins; disruption of the spatial arrangement; GAGs and growth factors may be removed; damages collagen
	Sodium deoxycholate (SD)		Effectiveness in removing cellular material dependent on tissue thickness; disruption of the spatial arrangement; GAGs removal
	Triton X-200		Higher effectiveness in removing cellular material from thin tissues; greater spatial arrangement disruption than other detergents
	Non-ionic detergents		

	Triton X-100	Disrupt more DNA-protein, lipid-lipid, lipid-protein interactions, rather than protein-protein interactions	Higher effectiveness in removing cellular material from thin tissues; disruption of the spatial arrangement and decrease in GAGs content.
	Zwitterionic detergents		
	CHAPS	Presents ionic and non-ionic characteristics	Effective in removing cellular material; minor disruption of the spacial arrangement; cytoplasmatic proteins remnants
Biological	Chelating agent (e.g. Ethylenediamine tetraacetic acid (EDTA))	Cell adhesion is destroyed by binding metallic ions	Usually used with trypsin. Alone it is ineffective
	Enzymes		
	Endo/Exo nucleases	Catalyze the hydrolysis of the interior or terminal bonds of ribonucleotide and deoxyribonucleotide chains	Hard to eliminate from the tissue
	Trypsin	Cleaves peptide bonds on the carboxyl side of the amino acids arginine and lysine	Spatial arrangement disruption after long time exposure; ECM components are removed
	Dispase	Cleaves fibronectin and collagen IV peptides	Spatial arrangement disruption after long time exposure; fibronectin and collagen IV may be removed
	Esterases	Cell phospholipid content is hydrolysed	GAGs decrease; spatial arrangement is preserved
Techniques	Perfusion	Usually applied in whole organs; Enables agent exposure and helps in cell removing	Causes pressure that can damage ECM and decreases growth factors
	Agitation and immersion	Enables agent exposure and helps in cell removing	Agent choice, degree of agitation or sonication, and time of exposure are all parameters than can affect ECM
	Pressure gradient	Enables agent exposure and helps in cell removing	Pressure damages ECM
	Supercritical Fluid	Uses pressure to burst cells; enables agent exposure and helps in cell removing	Pressure damages ECM

Chapter 3: Materials and Methods

3.1 Tissue preparation

Lamb's heads (6 to 8 months) were obtained from butchers and the TMJ discs were dissected from their joints. They were carefully removed and the remaining retrodiscal tissue and ligaments were cut. All samples used for the proposed work were not perforated, cut or injured (Figure 11). All samples were morphologically evaluated in weight, thickness with a digital calliper and the mediolateral and anteroposterior dimensions with software Image J. Discs were stored in 0.1 M phosphate buffered saline (PBS) (pH= 7.4) at 4°C until use.

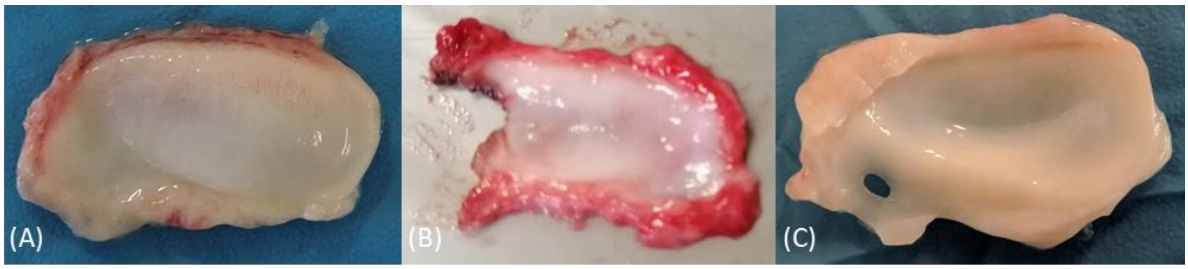

Figure 11 - Intact (A) and injured (B, C) lamb native discs

3.2 Decellularization procedures

Lamb discs were divided into 15 sets, including the native control, to test different decellularization protocols. The agents and/or methods used were: *i)* freeze and thaw; *ii)* SDS; *iii)* Triton X-100; *iv)* Accutase; *v)* ethanol/acetone; and *vi)* a combination of them. Different agent concentrations were tested and in Table 3 and Table 4 there is a full description of the protocols.

Decellularization procedures were performed in an orbital agitator at room temperature (RT) for 24 hours at 150 rpm, except for the Accutase in which it was used for 2 hours at 37ºC at 100 rpm. A cycle of freeze and thaw was performed by freezing the samples in -20ºC for 24h, followed by a thaw in a water bath at 37ºC.

Afterwards, extensive washing was performed with PBS, 2×45min and 2×60min at 150 rpm. After decellularization, discs were morphologically analysed as performed after dissection. Discs were stored in 0.1 M PBS (pH= 7.4) at 4°C until use.

Table 3 - Different chemical agents used and their decellularization conditions

Group	Chemical Treatment	Rpm/Time/Temperature
Control	-	-
1	1:1 solution of ethanol (96%) and acetone (99.5%)	150/24h/RT
2	0.1% SDS	
3	0.5% SDS	
4	1% SDS	
5	0.1% Triton X-100	
6	0.5% Triton X-100	
7	1% Triton X-100	
8	Accutase	100/2h/37°C

Table 4 - Combination of the physical and chemical agents used for decellularization

Group	Physical Treatment	Chemical Treatment
9	1 cycle of freeze and thaw (-20°C followed by 37°C)	0.1% SDS
10		0.5% SDS
11		1% SDS
12		0.1% Triton X-100
13		0.5% Triton X-100
14		1% Triton X-100

3.3 Micro-Computed Tomography

To evaluate the internal structure of the native and acellular tissues, images were obtained with Micro-CT equipment (SkyScan 1174^{TM}, Bruker, Kontich, Belgium). Before visualisation, the discs were immersed in 2.5% (w/v) glutaraldehyde with 0.1%M of PBS for 30 minutes to cell fixation. Then, they were subjected to ethanol dehydration cycles of 30%, 70%, and 96% for 30 minutes each. The staining was performed with hexamethyldisilazane (HMDS) by immersing the samples for 2h and left to air-dry for at least 2h.

3.4 Scanning Electron Microscope

To analyse the effects of the decellularizing agents on the ECM structure of the scaffolds, as well as the removal of the cellular content, SEM (Tescan, Vega 3) was performed, with an electron beam of 10 kV, on portions of the disc. For visualisation, the discs were prepared as for Micro-CT and then sputter-coated with gold/palladium. A sterilization procedure was implemented in which samples were subjected to ultraviolet radiation (UV) light for 2h while submerged in 70% ethanol, followed by UV light overnight.

3.5 Fourier-Transform Infrared Spectroscopy Analysis

The whole molecular composition of the native disc and the discs subjected to the different decellularization protocols were analysed by Fourier-transform infrared (FTIR) spectroscopy with an attenuated total reflectance detection mode (Alpha FT-IR, Bruker) in the mid-infrared region (400 to 4000 cm^{-1}), with a resolution of 4 cm^{-1} and 64 scans per spectrum. All spectra were corrected in relation to an analysis conducted without a biological sample. Spectra were acquired with OPUS® software (version 6.5, Bruker) and triplicate spectra were acquired for each sample.

The 5 morphological regions of the disc (medial, lateral, central, posterior and anterior) were analysed. Three independent samples of the native disc and from each decellularization protocol were analysed. Both cellular and acellular ECM samples before their analysis were kept in 0.1 M PBS (pH= 7.4) at 4°C.

3.5.1 Univariate and Multivariate analysis

For univariate analysis, different ratios between adjacent spectral bands were determined. The second derivative spectra were also considered for collagen and GAGs quantitative analysis. The second derivative was calculated from each spectrum using a Savitzky-Golay filter with a second-order polynomial over a 15-point window followed by uni-vector normalization. Multivariate analysis was performed by principal component analysis (PCA). Pre-processing and processing were conducted on Matlab R2012b (Mathworks Natick, MA, USA).

3.6 Mechanical Assays

The native and decellularized discs were subjected to compression testing using a texture analyser with a 1.2 mm min^{-1} extension rate and a 50 kg load cell until a compression of at least 55% was achieved. (TA.XTplusC, Stable Micro Systems, UK). Three samples of the native disc and each decellularization protocol were tested. During the tests, the discs were removed from the refrigerator where they were stored at -4°C and tested at RT. Compression modulus was calculated from the linear region of the stress-strain curve.

3.7 Statistical Analysis

Statistical differences between samples were evaluated on GraphPad Prism 8 software. For morphological and FTIR analysis, a two-way ANOVA was performed except for the quantification of biochemical components of the native disc, where a one-way ANOVA was conducted. For the mechanical assays, a one-way ANOVA was also performed. All tests were calculated with Fisher's LSD *post-hoc* analysis, with a confidence interval of 95%.

Chapter 4: Results and Discussion

4.1 Selection of the Animal Model

The choice of animal to study is key to the translation of its application to clinical practice so that it can successfully replace the human TMJ disc. Different authors have been investigating different animal models and the pig is considered to be the gold standard as it resembles the human anatomy when compared to the rabbit, goat, and cow (Kalpakci et al., 2011). Recently a review of different physiological, anatomical and practical considerations on the different animals studied in the literature was conducted and it was concluded that sheep and goats should be the first choice for a TMJ TE approach as they present several advantages when compared to pig, such as they are easy to obtain, inexpensive and present an easily accessible surgical site (Almarza et al., 2018). Even more, the TMJ fibrocartilage of Black Merino sheep is histologically similar to that of humans (Ângelo et al., 2018). Since the obtaining of sheep discs was scarcer, it was chosen to perform this work with lamb discs.

4.2 Selection of the Decellularization Methods

Decellularization is a technique that allows the retention of the extracellular cartilaginous structure of the disc, while the cellular content is removed. However, it is necessary to investigate appropriate techniques and reagents, as a balance between cell removal and unwanted matrix degradation needs to be achieved. Moreover, it is dependent on the tissue under study. For this, the chosen decellularization techniques and reagents for the TMJ disc were based on a literature review of some established methods. The search began by finding articles about the decellularization of the TMJ disc and cartilage in general. These articles are described by the selected reagent.

Ionic detergents are characterized by the presence of a head group that could have a positive (cationic) or negative (anionic) charge. SDS is an anionic detergent that forms micelles and solubilizes membrane proteins (Seddon et al., 2004). The first study on TMJ disc decellularization was in a porcine animal model and reported that 1% (m/v) of SDS agitation for 24h at 25ºC followed by PBS washes is an appropriate reagent for this purpose since histological results demonstrated a complete cell removal, maintaining the mechanical properties, although collagen fibres became compressed (Lumpkins et al., 2008). Juran et al. (2015) also evaluated the use of 1% (m/v) SDS agitation for 24h followed by deoxyribonuclease solution and results demonstrated that the ECM also exhibits collagen fibre compaction, but with higher compressive modulus compared to porcine native disc. A lyophilization and rehydration approach was shown to be effective in recovering its collagen organization and mechanical behaviour.

When investigating the TMJ disc with its retrodiscal tissue, 0.1% (m/v) SDS agitation for 48h followed by PBS washes has been shown to be effective in removing cells while maintaining the anterior-posterior tensile behaviour. However, tissue swelling has been found. Although the retrodiscal tissue is not the topic of this work, authors propose a combination of 0.1% (m/v) SDS and 2:1 solution of chloroform (99.8%)/ methanol (99.8%) for the decellularization of the disc-retrodiscal tissue complex, as cells and lipidic content were removed, respectively (Matuska et al., 2018). Preliminary studies by Matuska et al. (2018) demonstrated that concentrations between 0.1% and 1% (m/v) SDS in culture media lead to cell solubilization. Also, it has been shown that lower concentration of SDS result in lower collagen degradation, as well as, there is a lower risk of detergent residues in the tissue which may lead to cytotoxic effects.

Triton X -100 is a nonionic detergent that is characterized by the presence of an uncharged hydrophilic head (Seddon et al., 2004). Regarding the TMJ disc, this detergent has only been used by Lumpkins et al. (2008), in a concentration of 1% for 24h at 25ºC, where, cells were removed, but energy dissipation ability decreased due to the existence of a softer disc. For SDS, as described, 0.1% and 1% concentrations have already been tested, and although it has been mentioned that both remove cells, a complete analysis of the biochemical components of the ECM has not been conducted. Thus, these two concentrations were tested in this work, adding a mid-term concentration of 0.5% to better understand its impact. For comparison, Triton X-100 was also used, using the same concentrations and conditions.

Alcohols, such as ethanol, and acetone have the capacity to lysate cells and remove lipid content (Crapo et al., 2011). A combination of 1:3 (vol.%) acetone/ethanol was used for 24h at 25ºC to decellularize a porcine TMJ disc and, although cells were removed, the disc turned stiffer, dehydrated and with an increased energy dissipation (Lumpkins et al., 2008). Also, a combination of 1:1 solution of acetone (99.5%)/ ethanol (96%) for decellularization of the porcine TMJ disc for 48h led to cell removal, maintaining disc tensile anterior-posterior behaviour, but it became thinner (Matuska et al., 2018). Considering these results, it was proposed to replicate the 1:1 solution of acetone (99.5%)/ ethanol (96%), but with the alteration to decellularize for only 24h to assess the impact on the compression behaviour of the disc.

Freezing and thawing cycles are characterized by the formation of ice crystals which, consequently, lead to cell bursts. Moreover, since it allows the opening of the ECM, if there are further decellularization treatments, there is a greater fluidity of reagents diffusion (Schneider et al., 2016). Regarding the stability of the maintenance of the mechanical properties with this physical treatment, Allen & Athanasiou (2005) investigated from one to five freezing and thawing cycles, at -20°C during 6-18h followed by RT thaw, and demonstrated that there was no change in the mechanical behaviour of the hogs TMJ discs. However, if it is

frozen for more than 30 days there are differences in the viscoelastic properties (Calvo-Gallego et al., 2017). Despite this, in both studies, only the intermediate/central zone was analysed. Also, osteochondral dowels obtained from the tibial plateaus when frozen at -20°C or -80°C for 24h followed by thawing at 37.5°C did not result in any alteration of its mechanical behaviour (Szarko et al., 2010). The effectiveness of cell removal in tendon horses has also been shown to be more effective when five cycles of freeze and thaw (liquid nitrogen followed by 37°C) are combined with a detergent (1% SDS or Triton X-100) compared to the detergent alone (Burk et al., 2014).

Considering these papers, for the present work it was chosen to test one freeze and thaw cycle of -20°C for 24h followed by thaw at 37°C. Despite articles in the literature that used this technique in the TMJ disc used thawing at RT, it was decided to use a higher thaw temperature, but not too high to lead to a greater diffusion of the reagent and remove more cells. In addition, this method was implemented following the different concentrations of SDS and Triton X-100 tested to assess the existence of any pattern.

Accutase solution contains proteolytic and collagenolytic enzymes for cell detachment. Although not often used in decellularization, this enzyme has been used to replace trypsin/EDTA, which in turn is widely used for this purpose. In cell digestion accutase has demonstrated higher cell viability, but also higher cell apoptosis. Although this later one is not preferable in cell dissociation, for decellularization this may be a positive outcome (Li et al., 2015).

Decellularization procedures were performed under continuous agitation. For the washing steps, and because SDS and Triton X-100 are detergents, PBS media was renewed until no more bubbles were formed. For comparison, for the remaining reagents the same procedure was conducted, two washing steps of 45min and two washing steps of 1h in PBS.

4.3 Morphological Evaluation

The preservation of the morphological characteristics is essential for the success of the engineered-disc. To analyse the effects of the decellularizing reagents in the disc morphology, thickness, weight and mediolateral and anteroposterior dimensions were analysed. Table 5 shows discs before and after treatments, where it is possible to see the changes. The ethanol/acetone discs became stiffer and darker in colour, while for SDS and Triton X-100, including the freeze-thaw treatment, the discs become whitened. For accutase, on the other hand, there seems to be no noticeable changes. Interestingly, comparing the native discs, it is possible to observe different morphologies, in which some discs are more elongated, others more rounded and some present a more prominent medial zone, demonstrating the morphological variability of lamb TMJ discs.

Table 5 – Gross morphology of the discs before and after decellularization treatments: Ethanol/Acetone; 0.1%, 0.5% and 1% SDS; freeze and thaw followed by 0.1%, 0.5% and 1% SDS; accutase; 0.1%, 0.5% and 1% Triton X-100; and freeze and thaw followed by 0.1%, 0.5% and 1% Triton X-100, where FT is freeze and thaw and Triton X-100 is Tri.

Sample	Native	Treated
Ethanol/Acetone		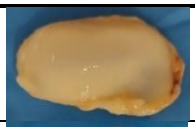
0.1% SDS	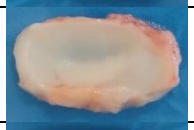	
0.5% SDS	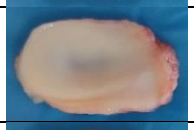	
1% SDS		
FT 0.1% SDS		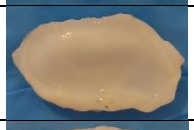
FT 0.5% SDS	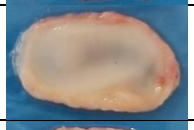	
FT 1% SDS	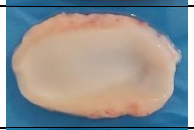	
Accutase	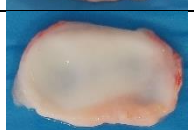	
0.1% Tri	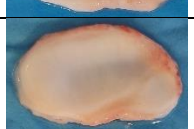	
0.5% Tri	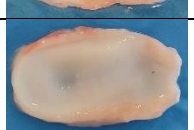	
1% Tri		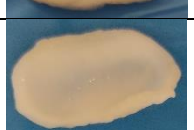
FT 0.1% Tri	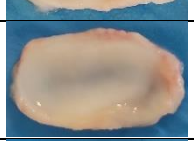	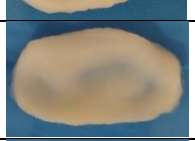
FT 0.5% Tri	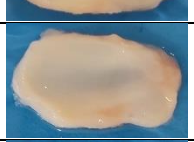	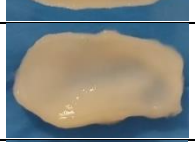
FT 1% Tri	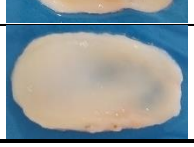	

The following morphological evaluation included all disc used for the FTIR spectroscopy (N=3) and mechanical testing (N=3). The native discs used for the proposed work presented a thickness of 1.62 ± 0.674 mm, an anteroposterior dimension of 13.44 ± 0.645 mm, a mediolateral dimension of 23.35 ± 1.109 mm and weighted 0.385 ± 0.029 g. Thickness variations of the discs upon the different treatments can be observed in Figure 12 – Ai, Aii. Measurements were taken in the posterior zone, since it is the thickest portion of the disc. Results revealed that all SDS treatments led to tissue swelling, where thickness increase was most pronounced for 0.5% SDS, with a 47.6% increase ($p<0.001$), and for freeze and thaw followed by 1% SDS with a 39.2% increase ($p<0.001$). 1% SDS led to an increase of 35.4% ($p<0.01$) and freeze and thaw followed by 0.5% SDS of 28.8% (* $p<0.05$). For treatments with 0.1% SDS (with and without freeze and thaw), ethanol/acetone, accutase and Triton X-100 no statistical differences were found.

SDS results are in agreement with the literature, where decellularization with 0.1% SDS only led to a 17% increase in thickness (Matuska et al., 2018) and that with higher SDS concentrations (1%), this increase is more pronounced (Matuska et al., 2018). Interestingly, in the present work, the addition of freeze and thaw was advantageous for 0.1% and 0.5% SDS where there was less swelling. However, for 1% SDS the opposite occurred, although the difference was of only 3.8%. For ethanol/acetone, Matuska & McFetridge (2018) also indicated tissue swelling (increase of around 6%). However, in the present study, compaction was found (decrease of 17.5%). Although the decellularization solution is the same, the differences found may be due to the decellularization time (24h vs 48h) and to the animal model used (lamb vs pig).

Regarding the tissue weight (Figure 12 – Bi, Bii), for accutase and higher concentrations of SDS, 0.5% and 1%, including freeze and thaw, there was a weight increase, in which for 1% SDS was statistically different at 5% significance (increase of 26.9%). For the remaining treatments, there was a weight decrease, more pronounced in the ethanol/acetone with 17.5%, but not statistically significant. In the porcine discs, opposite results were found for 0.1% SDS and ethanol/acetone, in which tissue increased 16% and 3%, respectively (Matuska et al., 2018). Once again, these differences may be due to decellularization time (24h vs 48h) and animal model used (lamb vs pig).

Anteroposterior (Figure 12 – Ci, Cii) and mediolateral (Figure 12 – Di, Dii) dimensions were also evaluated. In the anteroposterior dimension, all treatments led to a decrease in length, where differences of 5% significance are found in the ethanol/acetone treatment (decrease of 10.0%) and the 1% Triton X-100 (decrease of 12.5%). In the mediolateral dimension, all treatments also led to a decrease in length, except for freeze and thaw followed by either 0.1% or 0.5% SDS. Although there were no statistical differences for all methods, the ethanol

treatment was the one that led to the greatest change, in which there was a decrease of 8.90%. The difference by which the anteroposterior measurement presents major differences may be explained by the fact that collagen fibres in the intermediate zone are oriented anteroposteriorly, leading to a decrease in their length as a consequence of the decellularization methods.

Lumpkins et al. (2008) also found a decrease in both dimensions when porcine TMJ discs were decellularized with a solution of 1:3 (vol.%) acetone/ethanol, whereas for 1% SDS no change occurred. Contradictorily, for the same animal specie, Matuska et al. (2018) found an increase in both dimensions for 50% ethanol/ 50% acetone (the same solution as the present work but for 48h decellularization) and a decrease after 0.1% SDS.

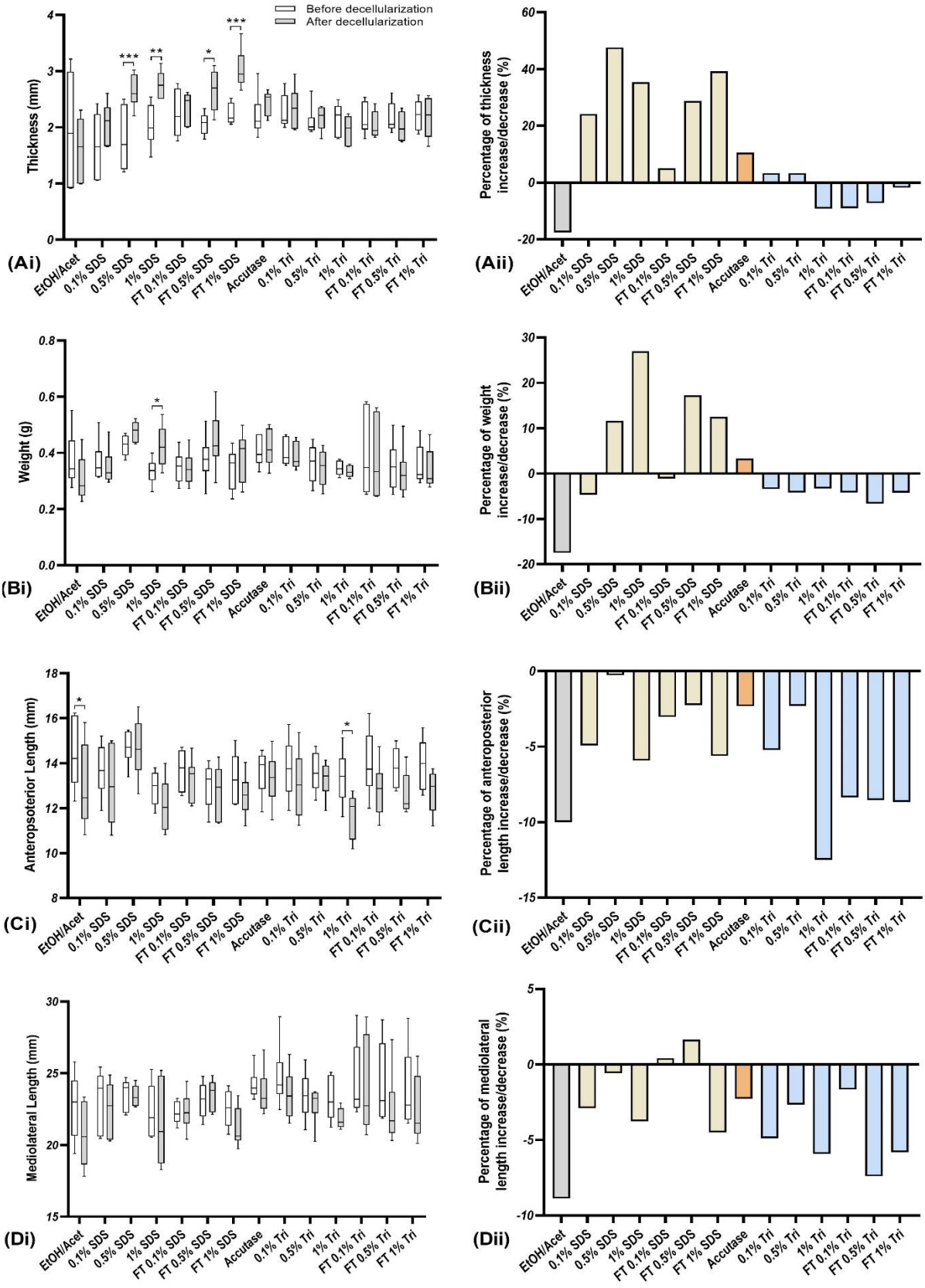

Figure 12 - Relative thickness (Ai), weight (Bi) and anteroposterior (Ci) and mediolateral lengths (Di) of the decellularized discs, before and after the treatments and its correspondent percentage of increase or decrease (Aii, Bii, Cii, Dii). EtOH/Acet is ethanol/acetone, FT is freeze and thaw and Triton X-100 is Tri. Statistically significant were calculated with a two-way ANOVA with Fisher's LSD *post-hoc* analysis and differences are represented by a bracket (* $p<0.05$, ** $p<0.01$ and *** $p<0.001$).

4.4 FTIR Spectroscopy Analysis

To evaluate the decellularization process of a cartilaginous tissue, usually diverse laborious and complex methods are conducted, based on histology and biochemical testing (Tint et al., 2019). FTIR spectroscopy may present complementary information concerning the molecular characterization of the sample, while enabling a simple, rapid (spectra is normally acquired in 1 min) and economic (expensive reagents are not required) analysis (Araújo et al., 2020; Baker et al., 2014).

FTIR spectroscopy is characterized by the absorption of infrared radiation by the sample, resulting in a spectrum that represents chemical vibrational modes. In biological tissues, the main chemical bonds represented in the spectra are proteins, lipids, nucleic acids and carbohydrates (Belbachir et al., 2009; Malek et al., 2014). Despite the advantages of this technique, it lacks specificity due to overlap bands and even due to common bonds present in different molecules (Rieppo et al., 2012). One approach to overcome this issue is the calculation of the second derivative, which improves the spectral band resolution (Saarakkala et al., 2010).

In Figure 13-A it is possible to visualize the spectra of the native lamb TMJ disc, with two strong absorptions representing amide I at 1630 cm^{-1} which is assigned to C=O stretch vibrations, and amide II at 1550 cm^{-1} which is assigned to N-H bending and C-N stretching vibrations. Since both collagen and PGs have these molecules in their constitution, both have contributions in the amides. However, since collagen is the main constituent of cartilage, it is believed to be dominant in these regions. Smaller absorptions are found between 2875 and 2963 cm^{-1} related to CH_3 symmetric and asymmetric vibrations, respectively, and in the 1749 cm^{-1} related to the C=O symmetric vibrations. The 1454 cm^{-1} band is assigned to CH_3 asymmetric bending vibrations, at 1402 cm^{-1} is present the COO^- symmetric vibration and at 1338 cm^{-1} the CH_2 side chains vibrations of collagen. In the raw spectra is possible to visualize a shoulder at 1376 cm^{-1} that in the second derivative is highlighted (Figure 13-B), and is related to CH_3 symmetric bending vibration of GAGs (sulfated and non-sulfated). The amide III region presents contributions from different bonds. The higher band, at 1240 cm^{-1}, is assigned to C-N stretching and N-H bending, as well as, SO_3^- asymmetric stretching vibrations of sulfated GAGs. At this band, the PO_2^- asymmetric stretch also from nucleic acids can also be assign. The two lower bands of the amide III region, at 1283 and 1203 cm^{-1}, are related to the collagen vibrations in this region with CH_2 wagging vibration from the glycine backbone and proline sidechain. The sugar bands are present between 1033 and 1160 cm^{-1} and represent the carbohydrates and nucleic acids. The 1160 cm^{-1} band is assigned to C-O stretching vibrations of the carbohydrate residues. The C-O stretching vibrations of the carbohydrate residues in collagen and PGs are found at 1033 and 1080 cm^{-1}, with the addition that this later band also presents an assignment

of PO_2^- asymmetric from nucleic acids. The band 1052 cm^{-1} is assigned to C-O stretching vibrations of the carbohydrate residues in PGs and SO_3^- asymmetric stretching vibrations of sulfated GAGs (Heise et al., 1997; Malek et al., 2014; Movasaghi et al., 2008; Saarakkala et al., 2010; Wood et al., 2016).

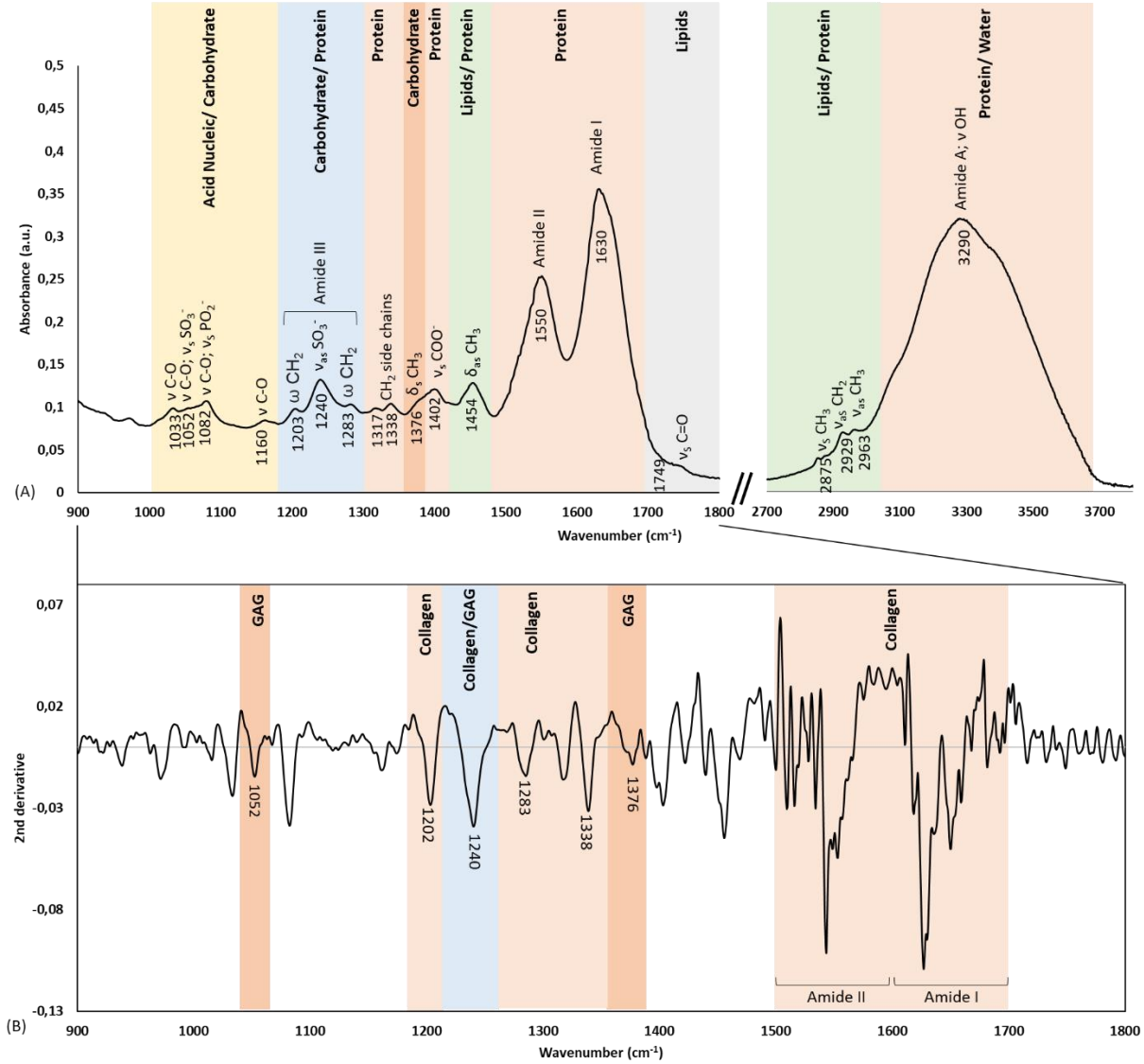

Figure 13 - Spectrum of the native TMJ disc (A) and its second derivative (B), where ν= stretching, δ= bending, ω= waggins, s= symmetric and as= asymmetric vibrations.

4.4.1 Spectral Band Ratios on the non-pre-processed FTIR spectra

The first evaluation was carried out on the spectra without processing and consisted of the ratio analysis between adjacent bands. Ratios between bands are less dependent on the optical path, i.e. from the sample quantity or thickness analysed, and baseline problems.

Some ratios found in the literature related to collagen degradation and orientation were evaluated. The ratio between the area under the band at 1338 cm^{-1} (1325-1355 cm^{-1}) and the amide II region (1588-1485 cm^{-1}), indicates collagen integrity, where its decrease results from

collagen degradation. For example, this ratio decreases with osteoarthritis increase (Bi et al., 2006; Boskey et al., 2007; Oinas et al., 2016; West et al., 2005). The ratio between amide III (1240 cm^{-1}) and 1450 cm^{-1} bands is an indicator of the triple helix conformation of collagen and must be equal to or greater than 1. In gelatine, which is composed of denatured collagen, the value is 0.59 (Gopinath et al., 2004; Guzzi Plepis et al., 1996). Regarding the orientation of the collagen network, the ratio between the amide I (1700-1588 cm^{-1}) and amide II (1588-1485 cm^{-1}) area bands have been used, where polarised infrared light can be used to determine its specific orientation, as perpendicular or parallel (Bi et al., 2005; Camacho et al., 2001). In the present work, this ratio was applied without the use of this equipment because, although the orientation of the collagen fibres in the disc is not assessed, it is possible to know if there was any alteration in them.

Table 6 presents the bands analysed in the present work. Although a specific designation to these ratios is difficult due to the spectral overlapping, some designations were defined according to the most common components in cartilage.

Table 6 - Spectral band ratios evaluated to assess differences between the native disc and decellularization procedures, and their corresponding assignments, where v= stretching, δ= bending, s= symmetric and as= asymmetric vibrations.

Ratios	Assignment
1033/1052	Sugar
1082/1052	Sugar
1082/1240	Sugar/Amide III
1160/1082	Sugar
1203/1240	Amide III
1283/1240	Amide III
1317/1338	Collagen CH_2 side chains
1376/1338	Sulfated GAGs/Collagen
1402/1454	v_s COO^-/ δ_{as} CH_3
1534/1550	Amide II
1610/1630	Amide I
1749/1630	Lipids/ Amide I
2875/2963	Lipids
Amide I/Amide II	Collagen orientation
1338/Amide II	Collagen integrity
1240/1454	Triple helix conformation of collagen

4.4.1.1 Native disc

First, the differences between the 5 morphological regions on the native disc were conducted. In Table 7 it is possible to observe that in the sugar region there are significant statistical differences between regions, except in the posterior-anterior and lateral-central region which is consistent in all calculated ratios. At 1082/1050 cm^{-1} ratio it is possible to observe that there are no differences between any region. However, when rationed to amide III, the statistical difference is $p<0.001$. Interestingly, in the amide III band ratios, there are no differences between regions.

Collagen CH_2 side chains present differences between lateral-anterior ($p<0.05$), medial-central ($p<0.01$), medial-lateral ($p<0.001$) and posterior-medial ($p=0.01$) regions. When the sulfated GAGs band is rationed to collagen, these regions lower their significance value by one point, lateral-anterior (ns), medial-central ($p<0.05$), medial-lateral ($p<0.01$) and posterior-medial ($p<0.05$).

The ratio 1402/1454 cm^{-1} shows a significant difference of 5% in the medial-lateral and posterior-medial region and the amide II band in the same way, except that in the lateral-medial region the significant difference is 0.1%. Due to the similarity of the results and the fact that they are attributed to the presence of proteins, the small difference that exists may be due to 1054 cm^{-1} band that also has influences from lipids. Amide I and lipids do not present significant statistical differences between regions.

Willard et al. (2011) refers that collagen fibres of the native disc are orientated in a ring conformation in the periphery and in the anteroposterior direction in the intermediary zone. This way, differences of amide I/amide II ratio is indicative of different conformations. Results showed a statistical difference at 5% significance between anterior/posterior regions and the medial region (mediolateral and anteroposterior orientation, respectively). Furthermore, the fibres in the central region are anteroposterior aligned, which resulted in a difference at 1% significance when compared to the anterior region (Figure 14). Despite these correlations, it was also expected the same results for the remaining zones, where the fibres are perpendicularly oriented. However, this ratio was used for a gross analysis of the collagen and, as referred, the use of polarised infrared light would be a complementary technique for a more detailed evaluation of the collagen orientation.

As a final observation, it is possible to conclude that the posterior-anterior and lateral-central regions are similar to each other because no statistical differences were found in any ratio. The medial-posterior is the one that presents statistical differences in almost all the ratios, being these two regions completely distinct from each other.

Table 7- Statistically significant differences at diverse spectral bands ratios between the 5 regions of the native disc, evaluated by Two way ANOVA with Fisher's LSD *post-hoc* analysis and represented by * p<0.05, ** p<0.01 and *** p<0.001.

	Anterior	**Central**	**Lateral**	**Medial**	**Posterior**
(1033/1052 || 1082/1052)					
Anterior (0.972 ± 0.032 || 1.09 ± 0.012)		ns	ns	ns	ns
Central (1.00 ± 0.024 || 1.09 ± 0.010)	**		ns	ns	ns
Lateral (1.00 ± 0.018 || 1.09 ± 0.018)	*	ns		ns	ns
Medial (0.941 ± 0.033 || 1.11 ± 0.016)	**	***	***		ns
Posterior (0.974 ± 0.032 || 1.10 ± 0.017)	ns	**	*	**	
(1082/1240 || 1160/1082)					
Anterior (0.841 ± 0.067 || 0.768 ± 0.030)		***	ns	**	ns
Central (0.788 ± 0.048 || 0.808 ± 0.016)	***		ns	***	**
Lateral (0.779 ± 0.033 || 0.790 ± 0.026)	***	ns		***	ns
Medial (0.879 ± 0.046 || 0.734 ± 0.038)	***	***	***		**
Posterior (0.828 ± 0.063 || 0.772 ± 0.041)	ns	***	***	***	
(1203/1240 || 1283/1240)					
Anterior (0.748 ± 0.024 || 0.789 ± 0.018)		ns	ns	ns	ns
Central (0.735 ± 0.015 || 0.784 ± 0.015)	ns		ns	ns	ns
Lateral (0.731 ± 0.008 || 0.772 ± 0.015)	ns	ns		ns	ns
Medial (0.752 ± 0.013 || 0.784 ± 0.018)	ns	ns	ns		ns
Posterior (0.749 ± 0.015 || 0.781 ± 0.022)	ns	ns	ns	ns	
(1317/1338 || 1376/1338)					
Anterior (0.966 ± 0.029 || 1.04 ± 0.019)		ns	ns	ns	ns
Central (0.952 ± 0.021 || 1.03 ± 0.012)	ns		ns	*	ns
Lateral (0.943 ± 0.018 || 1.02 ± 0.011)	*	ns		**	ns
Medial (0.986 ± 0.015 || 1.05 ± 0.010)	ns	**	***		*
Posterior (0.956 ± 0.027 || 1.03 ± 0.018)	ns	ns	ns	**	
(1402/1454 || 1534/1550)					
Anterior (0.956 ± 0.029 || 0.855 ± 0.043)		ns	ns	ns	ns
Central (0.944 ± 0.019 || 0.855 ± 0.021)	ns		ns	ns	ns
Lateral (0.934 ± 0.028 || 0.834 ± 0.025)	ns	ns		***	ns
Medial (0.963 ± 0.016 || 0.876 ± 0.20)	ns	ns	*		*
Posterior (0.938 ± 0.027 || 0.855 ± 0.029)	ns	ns	ns	*	
(1610/1630 || 1749/1630)					
Anterior (0.668 ± 0.007 || 0.075 ± 0.008)		ns	ns	ns	ns
Central (0.677 ± 0.007 || 0.075 ± 0.009)	ns		ns	ns	ns
Lateral (0.671 ± 0.007 || 0.072 ± 0.007)	ns	ns		ns	ns
Medial (0.658 ± 0.008 || 0.072 ± 0.005)	ns	ns	ns		ns
Posterior (0.671 ± 0.012 || 0.078 ± 0.005))	ns	ns	ns	ns	
(2875/2963 || Amide I/Amide)					
Anterior (0.570 ± 0.008 || 1.41 ± 0.060)		*	ns	**	ns
Central (0.574 ± 0.010 || 1.38 ± 0.030)	ns		ns	ns	ns
Lateral (0.571 ± 0.013 || 1.39 ± 0.018)	ns	ns		ns	ns
Medial (0.584 ± 0.012 || 1.38 ± 0.021)	ns	ns	ns		*
Posterior (0.581 ± 0.013 || 1.40 ± 0.023)	ns	ns	ns	ns	

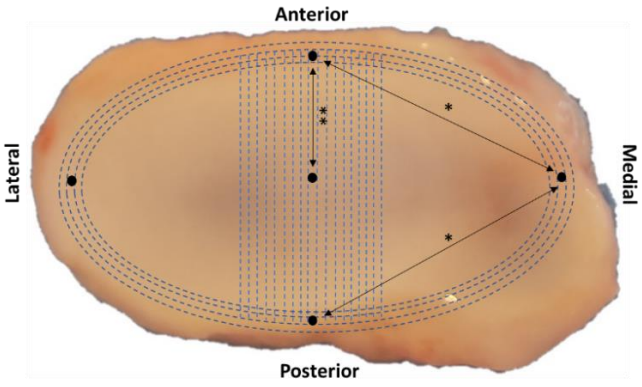

Figure 14 - Differences in collagen orientation calculated from amide I/amide II (table 7) in all the morphological regions of the disc. Statistically significant differences were evaluated by Two way ANOVA with Fisher's LSD *post-hoc* analysis and represented by * p<0.05, ** p<0.01 and *** p<0.001.

To evaluate the impact of the decellularization treatments in the ECM, a comparison among the different regions of native and treated discs was also conducted. FTIR spectra of the decellularized disc for all regions are presented in Figure 15 and statistically significant differences are presented in Table 8 for the anterior region, Table 9 for the central region, Table 10 for the lateral region, Table 11 for the medial region and Table 12 for the posterior region. A summarised conclusion of the results can be seen in the appendix 1. Furthermore, by analysing the spectra it is possible to see that there was no alteration or addition of bands, showing that there was no detergent residues present in the samples.

4.4.1.2 Ethanol/Acetone Decellularization

This treatment presents differences in the sugar bands in all regions, but mainly in the anterior and medial region, where there are differences at 0.1% significance in the 1082/1240 and 1160/1082 cm^{-1} band ratio. The 1082/1050 cm^{-1} band ratio is the only one that does not present differences when compared to the native disc in all regions. In the amide III band, no differences are found in the central and lateral region, and in the other zones, differences are only found in the 1203/1240 cm^{-1} band ratio. As this band is assigned to carbohydrate and proteins, this could mean that collagen and GAGs content may have changed. For collagen CH_2 side chains and sulfated GAGs/collagen ratios, only the central region exhibits significant differences of 5% significance and 1% significance, respectively. Amide II is only different in the posterior zone and amide I in the posterior and medial zone, being the latter more affected ($p<0.001$). Lipids values are maintained in the anterior zone, but the central, lateral, and posterior are different at a 5% significance, and the medial zone at a 0.1% significance. However, when ratio to the amide I, no differences are found between regions.

The orientation of the collagen has changed in the anterior and posterior zone with a significance of 5%, being oriented in a lower helical conformation, as this value has decreased. Concerning collagen degradation, there was a statistical difference for the 1338/amide II ratio,

with the reduction of the values in the anterior, lateral ($p<0.05$) and posterior ($p<0.001$) zone, indicating that there was degradation. However, for the ratio 1240/1454 cm^{-1}, there was a statistical difference only in the posterior zone ($p<0.05$). Despite these results, as mentioned above, the complete degradation of collagen is present when the ratio value is 0.5, so although the values decrease, they are not close to it. This indicates that a degradation process of collagen may have started, especially in the posterior region, and is likely to be more pronounced if decellularization treatment with ethanol/acetone is longer. This is in accordance with (Arun Gopinath et al., 2014) where the collagen maintains its triple helix conformation, but becomes thermodynamically unstable in the presence of ethanol.

4.4.1.3 SDS Decellularization

All SDS samples show large differences when compared to native discs. For SDS alone, the sugar band area for each ratio shows a difference of 0.1% significance, for 0.5% and 1% SDS. For 0.1% SDS the same situation occurs, except for the ratio 1082/1052 cm^{-1} that the difference is smaller for the lateral ($p<0.01$), medial ($p<0.05$) and posterior ($p<0.01$) region. Freeze and thaw samples were highly affected ($p<0.001$) at 1082/1240 cm^{-1} ratio band in all regions and 1160/1082 cm^{-1} ratio band in the anterior and posterior. The remaining ratios vary across the region and the concentration of SDS, where some do not even present statistical differences, specifically freeze and thaw followed by 0.1 and 0.5% SDS. The addition of a freeze and thaw cycle has not led to as many chemical changes when compared to SDS alone, consequently lower SDS concentrations are preferable.

In the amide III band, the 1283/1240 cm^{-1} ratio band is statistically different at 0.1% significance in all regions and all samples. For the 1203/1240 cm^{-1} ratio band a gradual increase in the statistical difference occurs between SDS alone and freeze and thaw followed by SDS. The 0.1% SDS and freeze and thaw followed by 0.1% SDS do not show statistical differences in all regions except the 0.1% SDS which shows a $p>0.05$ in the lateral zone. This indicates that this band, which is attributed to proteins and carbohydrates, has fewer changes with a lower SDS concentration.

For collagen CH_2 side chains and sulfated GAGs/collagen ratios, the medial region is statistically different at 0.1% significance in all regions and all samples. But, once again, freezing and thawing followed by 0.1% SDS is the one with lower statistically differences. In the anterior and posterior regions at 1376/1338 cm^{-1} ratio band, there is a difference at 1% significance and in the central region, there are no statistical differences. In the lateral zone in either the ratios, there are no differences.

The 1402/1454 cm^{-1} ratio is highly affected ($p<0.001$), except for the freeze and thaw followed by 0.1% SDS in the lateral (ns) and central ($p<0.01$) zones. Amide II band does not present

modifications in the lateral zone for all freeze and thaw samples and in the anterior zone for freeze and thaw followed by 1% SDS. Amide II band also presents some high changes in the central, medial and posterior zone ($p<0.001$). Interestingly, in the anterior zone, freeze and thaw followed by 1% SDS present a lower significant difference ($p<0.05$) and in the lateral zone, no significant changes are found in the freeze and thaw treatments. Amide I band does not show a consistent pattern between regions and samples, but it is possible to visualize that the freeze and thaw treatments are less affected. Lipids values also do not present a consistent pattern, but major changes are not found in all samples. Mainly, 0.1% and 0.5% SDS are unaltered in all regions and the lateral region is less affected. This is in accordance with Matuska et al. (2018), where it was shown that 0.1% SDS is ineffective in removing lipids from the retrodiscal tissue of the porcine disc.

The orientation of collagen only changed at higher SDS concentrations (alone or with freezing and thawing). Since SDS treatment lead to a ratio increase, that probably is due to an increase of collagen helical orientation compared to the native. This change can be explained by the fact that collagen fibre compaction was found in decellularization with 1% SDS (Juran et al., 2015; Lumpkins et al., 2008), possibly changing its conformation. Regarding collagen degradation, although values are almost all statistically different, except in freeze and thaw followed by 0.1% SDS in the central and lateral region and 0.1% SDS and freeze and thaw followed by 0.5% SDS in the lateral region, its increase indicates that the integrity of the collagen is favoured.

4.4.1.4 Accutase Decellularization

Accutase treatment led to significant changes in the sugar bands. The 1082/1052 cm^{-1} ratio is the one less affected, where differences are only found in the anterior zone ($p<0.05$) and the 1033/1052 cm^{-1} ratio is the one with major changes in all regions ($p<0.001$). Amide III band does not present significant differences, except in the central region in both ratios ($p<0.001$) and in the lateral region at 1282/1240 cm^{-1} ratio ($p<0.05$). Collagen CH_2 side chains, sulfated GAGs/collagen, COO^- symmetric stretch/ CH_3 asymmetric bend and amide II ratios are extremely altered in all regions ($p<0.001$).

Amide I band presents statistical differences at 0.1% significance in the anterior, lateral and posterior zone, and in the central region a 5% difference. Lipids 2875/2963 cm^{-1} ratio was highly altered ($p<0.001$) in all regions, but the 1749/1630 cm^{-1} ratio it is only different in the central ($p<0.001$) and medial ($p<0.01$) zones.

Collagen orientation presents higher values in all regions with statistical differences at 0.1% significance, which means that collagen is oriented with higher helical conformation compared to the native disc. No collagen degradation was found, as 1240/1454 cm^{-1} band ratio presents

no statistical differences in all regions and, although 1338/amide II is statistically different ($p<0.001$), their values increased, which is not indicative of degradation.

4.4.1.5 Triton X-100 Decellularization

The sugar ratios, 1033/1052 and 1082/1052 cm^{-1} in the anterior and posterior zones present similar results, where the first band is highly affected, and the later band only presents significative differences in freeze and thaw followed by 1% Triton X-100. The 1060/1082 cm^{-1} band ratio is also highly altered for all samples ($p<0.001$), except for freeze and thaw followed by 1% Triton X-100 that statistical differences are only found in the medial region ($p=0.01$). Amide III band presents mixed results between samples, wherein the anterior and posterior zones 1203/1240 cm^{-1} band ratio presents no statistically differences in any sample, in the lateral and medial zone only the freeze and thaw followed by 0.1% Triton X-100 presents no differences and the remaining samples of this zone and the central zone present statistical differences at 0.1% significance.

For collagen CH_2 side chains and sulfated GAGs/collagen ratios, in general, the anterior, medial and posterior region are extremely different ($p<0.001$), except for freeze and thaw followed by the higher concentrations of Triton X-100. Contradictorily for 1317/1338 cm^{-1} band ratio only freeze and thaw followed by 1% Triton X-100 is affected in the central ($p<0.05$) and lateral ($p<0.001$) region.

Amide II band presents no statistically significant differences in freeze and thaw followed by 1% Triton X-100 in any region, whereas the freeze and thaw followed by 0.5% Triton X-100 in the central zone is different at 5% significance, in the anterior and posterior at 1% significance, and the medial at 0.1% significance. The remaining samples are extremely affected in all regions ($p<0.001$), except in the lateral region for freeze and thaw followed by 0.1% Triton X-100 ($p<0.01$). For amide I band the anterior and lateral region present no statistically significant differences in any sample. For the remaining regions, a pattern was not found, but it seems that, for the medial and posterior region, samples with freeze and thaw are preferable, while for the central regions the Triton X-100 samples. Lipids in 2875/2963 cm^{-1} band ratio are different in all regions for all samples.

Collagen orientation was extremely affected in all samples and regions ($p<0.001$), except for freeze and thaw followed by 0.5% Triton X-100 in the anterior ($p<0.05$) and posterior zone (ns). Concerning the degradation of collagen, the values for the 1338/amide II cm^{-1} area ratio have increased, so no degradation has been found. Furthermore, the ratio of bands 1240/1454 cm^{-1} does not show significant differences, supporting the results obtained. However, this rise in values was more accentuated in the central and medial regions for all samples and for the remaining regions for samples of Triton X-100 only.

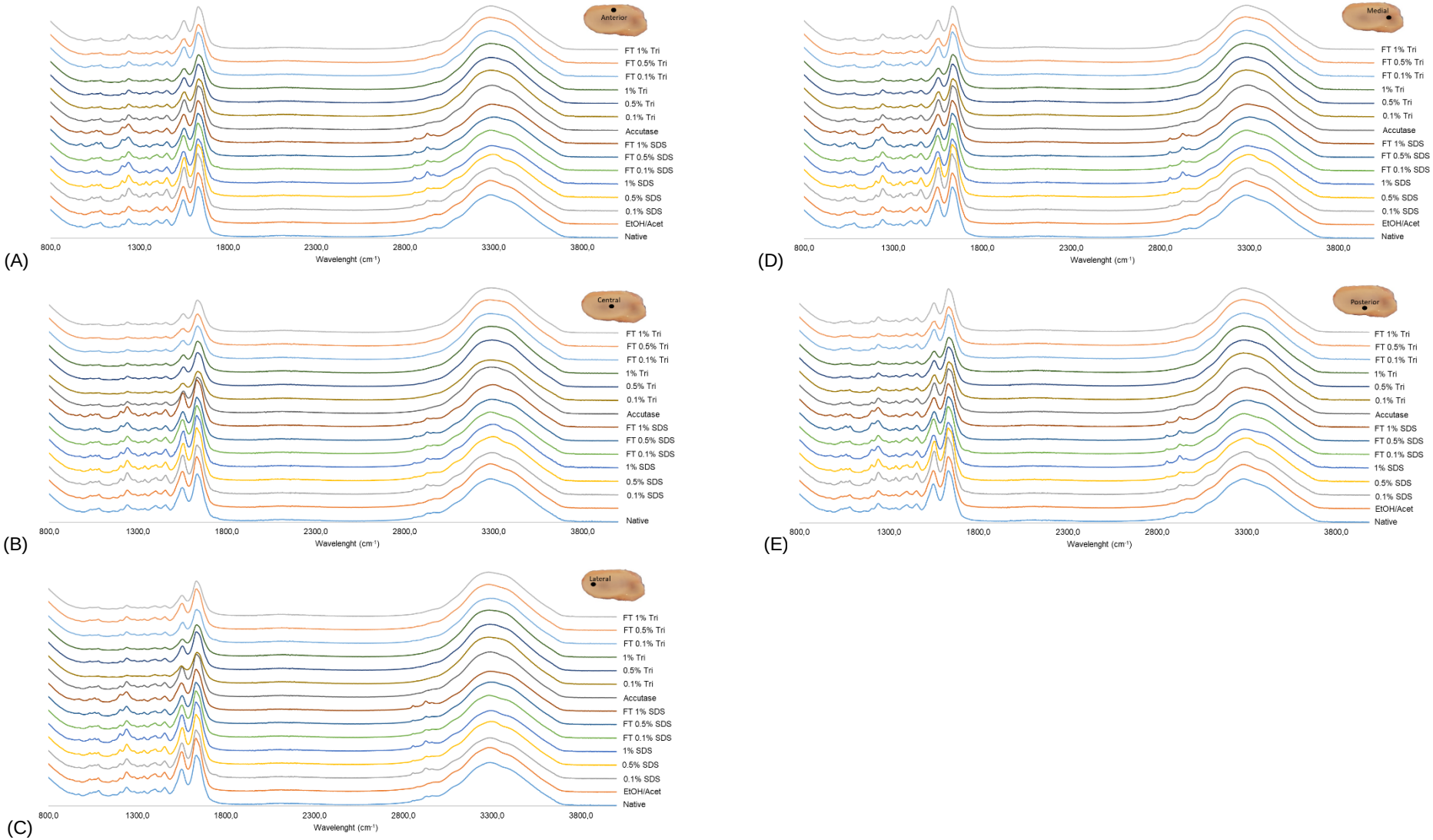

Figure 15 - FTIR spectra of the native and decellularized discs in the anterior (A), central (B), lateral (C), medial (D) and posterior (E) zones, where EtOH/Acet is ethanol/acetone, FT is freeze and thaw and Triton X-100 is Tri

Table 8 - Mean and standard deviation values of spectral bands ratios of the native disc and the different decellularization procedures, considering the anterior zone of the disc. EtOH/Acet is ethanol/acetone, FT is freeze and thaw and Triton X-100 is Tri. Statistical significant differences are presented and calculated against the native disc using a Two-way ANOVA with Fisher's LSD post-hoc analysis and represented by * p<0.05, ** p<0.01 and *** p<0.001.

Ratios	Native	EtOH/Acet	0.1% SDS	0.5% SDS	1% SDS	FT 0.1% SDS	FT 0.5% SDS	FT 1% SDS	Accutase	0.1% Tri	0.5% Tri	1% Tri	FT 0.1% Tri	FT 0.5% Tri	FT 1% Tri
1033/1052	0.972 ± 0.032	**1.00 ± 0.024****	**1.04 ± 0.020*****	**1.04 ± 0.012*****	**1.03 ± 0.037*****	**1.04 ± 0.019*****	0.968 ± 0.030	0.976 ± 0.014	**1.04 ± 0.010*****	**1.04 ± 0.012*****	**1.04 ± 0.012*****	**1.04 ± 0.012*****	**1.04 ± 0.015*****	**1.02 ± 0.018*****	**1.02 ± 0.025*****
1082/1052	1.09 ± 0.012	1.09 ± 0.014	1.07 ± 0.012	**1.04 ± 0.024*****	**0.922 ± 0.056*****	1.07 ± 0.039	**1.03 ± 0.051*****	**0.995 ± 0.016*****	**1.12 ± 0.010***	1.09 v 0.015	1.08 ± 0.014	1.08 ± 0.016	1.08 ± 0.020	1.08 ± 0.012	**1.06 ± 0.024***
1082/1240	0.841 ± 0.067	**0.773 ± 0.049*****	**0.646 ± 0.019*****	**0.592 ± 0.015*****	**0.590 ± 0.030*****	**0.699 ± 0.027*****	**0.677 ± 0.024*****	**0.646 ± 0.019*****	**0.745 ± 0.037*****	**0.799 ± 0.039***	0.819 ± 0.051	0.807 ± 0.041	**0.762 ± 0.054*****	**0.804 ± 0.040***	**0.798 ± 0.057***
1160/1082	0.768 ± 0.030	**0.809 ± 0.015*****	**0.833 ± 0.022*****	**0.867 ± 0.010*****	**0.877 ± 0.042*****	**0.829 ± 0.014*****	**0.817 ± 0.055*****	**0.841 ± 0.015*****	0.791 ± 0.015	**0.822 ± 0.023*****	**0.823 ± 0.023*****	**0.830 ± 0.017*****	**0.829 ± 0.012*****	**0.820 ± 0.014*****	0.791 ± 0.015
1203/1240	0.748 ± 0.024	**0.723 ± 0.012***	0.744 ± 0.013	0.770 ± 0.024	**0.798 ± 0.047*****	0.746 ± 0.021	**0.830 ± 0.036*****	**0.833 ± 0.022*****	0.731 ± 0.019	0.759 ± 0.013	0.766 ± 0.018	0.765 ± 0.022	0.733 ± 0.032	0.751 ± 0.016	0.754 ± 0.015
1283/1240	0.789 ± 0.018	0.795 ± 0.025	**0.709 ± 0.043*****	**0.664 ± 0.015*****	**0.640 ± 0.036*****	**0.726 ± 0.010*****	**0.651 ± 0.021*****	**0.640 ± 0.015*****	0.776 ± 0.023	**0.809 ± 0.010***	**0.823 ± 0.016*****	**0.820 ± 0.019****	0.797 ± 0.028	**0.812 ± 0.016***	**0.822 ± 0.017*****
1317/1338	0.966 ± 0.029	0.954 ± 0.026	**0.903 ± 0.009*****	**0.885 ± 0.016*****	**0.904 ± 0.027*****	**0.931 ± 0.030*****	**0.915 ± 0.024*****	**0.931 ± 0.013*****	**0.900 ± 0.015*****	**0.925 ± 0.008*****	**0.936 ± 0.007*****	**0.932 ± 0.018*****	**0.943 ± 0.012****	**0.941 ± 0.019****	0.962 ± 0.011
1376/1338	1.04 ± 0.019	1.03 ± 0.020	**0.955 ± 0.005*****	**0.970 ± 0.008*****	**0.982 ± 0.025*****	**1.02 ± 0.023****	**0.999 ± 0.017*****	**1.01 ± 0.010*****	**0.978 ± 0.011*****	**0.989 ± 0.006*****	**0.999 ± 0.006*****	**0.993 ± 0.009*****	**1.01 ± 0.011*****	**1.00 ± 0.013*****	**1.02 ± 0.007****
1402/1454	0.956 ± 0.029	0.950 ± 0.026	**0.885 ± 0.021*****	**0.846 ± 0.009*****	**0.861 ± 0.014*****	**0.908 ± 0.038*****	**0.860 ± 0.022*****	**0.876 ± 0.010*****	**0.833 ± 0.015*****	**0.921 ± 0.008*****	**0.931 ± 0.009****	**0.921 ± 0.018*****	0.943 ± 0.017	**0.928 ± 0.024****	0.960 ± 0.019
1534/1550	0.855 ± 0.043	0.870 ± 0.034	**0.751 ± 0.036*****	**0.756 ± 0.040*****	**0.780 ± 0.037*****	**0.800 ± 0.034*****	**0.806 ± 0.052*****	**0.828 ± 0.024***	**0.745 ± 0.012*****	**0.767 ± 0.010*****	**0.779 ± 0.009*****	**0.776 ± 0.025*****	**0.811 ± 0.022*****	**0.822 ± 0.031****	0.835 ± 0.023
1610/1630	0.668 ± 0.007	0.675 ± 0.006	**0.633 ± 0.029*****	**0.646 ± 0.015*****	0.660 ± 0.009	0.660 ± 0.007	0.665 ± 0.019	0.675 ± 0.012	**0.645 ± 0.008*****	0.663 ± 0.007	0.664 ± 0.006	0.665 ± 0.013	0.661 ± 0.014	0.669 ± 0.008	0.665 ± 0.009
1749/1630	0.075 ± 0.008	0.070 ± 0.005	0.071 ± 0.007	0.073 ± 0.006	0.073 ± 0.005	0.067 ± 0.011	**0.090 ± 0.026*****	0.081 ± 0.005	0.081 ± 0.004	**0.092 ± 0.006*****	**0.091 ± 0.010*****	**0.091 ± 0.008*****	0.074 ± 0.013	**0.085 ± 0.008***	0.075 ± 0.019
2875/2963	0.570 ± 0.008	0.564 ± 0.008	0.577 ± 0.018	0.576 ± 0.006	**0.593 ± 0.015*****	**0.583 ± 0.016***	**0.584 ± 0.021***	0.577 ± 0.007	**0.533 ± 0.010*****	**0.509 ± 0.007*****	**0.505 ± 0.009*****	**0.509 ± 0.010*****	**0.533 ± 0.020*****	**0.530 ± 0.015*****	**0.508 ± 0.033*****
Amide I/Amide II	1.41 ± 0.060	**1.36 ± 0.041***	1.42 ± 0.032	1.44 ± 0.031	1.44 ± 0.021	1.43 ± 0.036	**1.49 ± 0.057*****	**1.47 ± 0.024***	**1.52 ± 0.080*****	**1.61 ± 0.039*****	**1.61 ± 0.055*****	**1.63 ± 0.050*****	**1.47 ± 0.071***	**1.51 ± 0.057*****	**1.51 ± 0.023*****
1338/Amide II	0.159 ± 0.008	**0.155 ± 0.005***	**0.169 ± 0.004*****	**0.168 ± 0.003*****	**0.168 ± 0.002*****	**0.165 ± 0.005****	**0.169 ± 0.008*****	**0.165 ± 0.001****	**0.171 ± 0.04*****	**0.176 ± 0.003*****	**0.175 ± 0.005*****	**0.176 ± 0.003*****	0.163 ± 0.004	**0.166 ± 0.008****	0.161 ± 0.004
1240/1454	1.02 ± 0.020	0.991 ± 0.025	**1.11 ± 0.038*****	**1.15 ± 0.034*****	**1.22 ± 0.103*****	**1.08 ± 0.032*****	**1.21 ± 0.061*****	**1.24 ± 0.038*****	1.02 ± 0.014	1.03 ± 0.007	1.02 ± 0.021	1.02 ± 0.011	1.01 ± 0.021	0.995 ± 0.023	0.998 ± 0.021

Table 9 - Mean and standard deviation values of spectral bands ratios of the native disc and the different decellularization procedures, considering the central zone of the disc. EtOH/Acet is ethanol/acetone, FT is freeze and thaw and Triton X-100 is Tri. Statistical significant differences are presented and calculated against the native disc using a Two-way ANOVA with Fisher's LSD *post-hoc* analysis and represented by * p<0.05, ** p<0.01 and *** p<0.001.

Ratios	Native	EtOH/Acet	0.1% SDS	0.5% SDS	1% SDS	FT 0.1% SDS	FT 0.5% SDS	FT 1% SDS	Accutase	0.1% Tri	0.5% Tri	1% Tri	FT 0.1% Tri	FT 0.5% Tri	FT 1% Tri
1033/1052	1.00 ± 0.024	**1.04 ± 0.015****	**1.06 ± 0.004*****	**1.05 ± 0.013*****	**1.04 ± 0.018*****	**1.04 ± 0.029*****	1.00 ± 0.033	**1.02 ± 0.039***	**1.04 ± 0.008*****	**1.03 ± 0.006****	**1.04 ± 0.010*****	**1.03 ± 0.008****	**1.04 ± 0.015*****	**1.02 ± 0.009***	**1.03 ± 0.020****
1082/1052	1.09 ± 0.010	1.08 ± 0.008	1.08 ± 0.009	**1.05 ± 0.018*****	**1.02 ± 0.035*****	**1.07 ± 0.024***	**1.02 ± 0.033*****	**1.03 ± 0.037*****	1.08 ± 0.016	**1.05 ± 0.007*****	**1.05 ± 0.009*****	**1.04 ± 0.004*****	**1.05 ± 0.015*****	**1.04 ± 0.010*****	**1.02 ± 0.028*****
1082/1240	0.788 ± 0.048	**0.733 ± 0.028****	**0.639 ± 0.021*****	**0.607 ± 0.012*****	**0.611 ± 0.032*****	**0.703 ± 0.023*****	**0.658 ± 0.028*****	**0.620 ± 0.030*****	0.802 ± 0.028	**0.867 ± 0.018*****	**0.862 ± 0.033*****	**0.862 ± 0.030*****	0.822 ± 0.056	**0.881 ± 0.036*****	**0.847 ± 0.038*****
1160/1082	0.808 ± 0.016	0.829 ± 0.010	**0.848 ± 0.013****	**0.877 ± 0.014*****	**0.870 ± 0.044*****	0.832 ± 0.011	0.823 ± 0.028	**0.855 ± 0.014*****	0.829 ± 0.024	**0.863 ± 0.013*****	**0.859 ± 0.011*****	**0.862 ± 0.009*****	**0.854 ± 0.009*****	**0.864 ± 0.008*****	0.829 ± 0.024
1203/1240	0.735 ± 0.015	0.718 ± 0.010	0.745 ± 0.011	**0.772 ± 0.016*****	**0.773 ± 0.028*****	0.744 ± 0.019	**0.806 ± 0.025*****	**0.790 ± 0.039*****	**0.780 ± 0.020*****	**0.818 ± 0.007*****	**0.814 ± 0.014*****	**0.818 ± 0.014*****	**0.785 ± 0.034*****	**0.823 ± 0.017*****	**0.821 ± 0.018*****
1283/1240	0.784 ± 0.015	0.766 ± 0.014	**0.705 ± 0.014*****	**0.681 ± 0.015*****	**0.674 ± 0.036*****	**0.742 ± 0.012*****	**0.669 ± 0.020*****	**0.664 ± 0.017*****	**0.818 ± 0.020*****	**0.867 ± 0.015*****	**0.860 ± 0.007*****	**0.858 ± 0.010*****	**0.841 ± 0.024*****	**0.867 ± 0.016*****	**0.871 ± 0.024*****
1317/1338	0.952 ± 0.021	**0.932 ± 0.016***	**0.902 ± 0.007*****	**0.891 ± 0.013*****	**0.891 ± 0.016*****	**0.933 ± 0.021***	**0.910 ± 0.015*****	**0.903 ± 0.028*****	**0.917 ± 0.010*****	0.953 ± 0.011	0.951 ± 0.010	0.946 ± 0.012	0.945 ± 0.013	0.960 ± 0.011	**0.970 ± 0.017***
1376/1338	1.03 ± 0.012	**1.01 ± 0.011****	**0.991 ± 0.006*****	**0.971 ± 0.009*****	**0.973 ± 0.011*****	1.02 ± 0.017	**0.995 ± 0.009*****	**0.985 ± 0.018*****	**0.979 ± 0.004*****	**0.955 ± 0.006*****	**0.997 ± 0.007*****	**0.990 ± 0.008*****	**1.00 ± 0.007*****	**0.999 ± 0.007*****	**1.01 ± 0.007****
1402/1454	0.944 ± 0.019	0.931 ± 0.020	**0.881 ± 0.008*****	**0.861 ± 0.011*****	**0.856 ± 0.011*****	**0.918 ± 0.019****	**0.871 ± 0.010*****	**0.870 ± 0.016*****	**0.899 ± 0.014*****	0.948 ± 0.014	0.937 ± 0.011	0.932 ± 0.013	0.936 ± 0.010	0.944 ± 0.012	**0.964 ± 0.031***
1534/1550	0.855 ± 0.021	0.848 ± 0.014	**0.775 ± 0.010*****	**0.763 ± 0.021*****	**0.760 ± 0.036*****	**0.806 ± 0.038*****	**0.803 ± 0.039*****	**0.787 ± 0.036*****	**0.754 ± 0.008*****	**0.795 ± 0.015*****	**0.780 ± 0.016*****	**0.785 ± 0.021*****	**0.791 ± 0.034*****	**0.827 ± 0.026***	0.833 ± 0.37
1610/1630	0.677 ± 0.007	0.682 ± 0.006	**0.652 ± 0.007*****	**0.660 ± 0.009****	0.669 ± 0.012	**0.666 ± 0.004***	0.672 ± 0.008	0.668 ± 0.014	**0.665 ± 0.009***	**0.688 ± 0.006***	0.683 ± 0.008	**0.687 ± 0.010***	0.673 ± 0.020	**0.696 ± 0.10*****	**0.692 ± 0.009****
1749/1630	0.075 ± 0.009	0.073 ± 0.007	0.069 ± 0.006	0.069 ± 0.004	0.073 ± 0.010	**0.062 ± 0.013****	0.071 ± 0.015	0.073 ± 0.005	**0.100 ± 0.006*****	**0.109 ± 0.003*****	**0.108 ± 0.007*****	**0.111 ± 0.005*****	**0.093 ± 0.015*****	**0.11 ± 0.007*****	**0.094 ± 0.020*****
2875/2963	0.574 ± 0.010	**0.561 ± 0.005***	0.581 ± 0.012	0.570 ± 0.006	**0.600 ± 0.015*****	0.569 ± 0.010	0.576 ± 0.008	0.571 ± 0.009	**0.500 ± 0.014*****	**0.486 ± 0.006*****	**0.479 ± 0.007*****	**0.484 ± 0.007*****	**0.504 ± 0.014*****	**0.489 ± 0.008*****	**0.463 ± 0.039*****
Amide I/Amide II	1.38 ± 0.030	1.36 ± 0.026	1.40 ± 0.046	**1.46 ± 0.034****	**1.46 ± 0.040****	1.43 ± 0.013	**1.45 ± 0.047****	**1.44 ± 0.053***	**1.68 ± 0.073*****	**1.75 ± 0.043*****	**1.78 ± 0.035*****	**1.79 ± 0.024*****	**1.66 ± 0.060*****	**1.73 ± 0.055*****	**1.72 ± 0.032*****
1338/Amide II	0.161 ± 0.005	0.160 ± 0.004	**0.167 ± 0.003****	**0.171 ± 0.003*****	**0.173 ± 0.004*****	0.169 ± 0.006	**0.168 ± 0.005****	**0.169 ± 0.003*****	**0.181 ± 0.006*****	**0.182 ± 0.004*****	**0.184 ± 0.003*****	**0.186 ± 0.002*****	**0.177 ± 0.003*****	**0.180 ± 0.005*****	**0.177 ± 0.007*****
1240/1454	1.01 ± 0.015	1.00 ± 0.014	**1.09 ± 0.017*****	**1.13 ± 0.029*****	**1.15 ± 0.062*****	**1.06 ± 0.024*****	**1.16 ± 0.036*****	**1.18 ± 0.049*****	1.02 ± 0.013	1.01 ± 0.017	1.01 ± 0.012	1.02 ± 0.010	1.01 ± 0.019	0.993 ± 0.015	0.996 ± 0.025

Table 10 - Mean and standard deviation values of spectral bands ratios of the native disc and the different decellularization procedures, considering the lateral zone of the disc. EtOH/Acet is ethanol/acetone, FT is freeze and thaw and Triton X-100 is Tri. Statistical significant differences are presented and calculated against the native disc using a Two-way ANOVA with Fisher's LSD *post-hoc* analysis and represented by * p<0.05, ** p<0.01 and *** p<0.001.

Ratios	Native	EtOH/Acet	0.1% SDS	0.5% SDS	1% SDS	FT 0.1% SDS	FT 0.5% SDS	FT 1% SDS	Accutase	0.1% Tri	0.5% Tri	1% Tri	FT 0.1% Tri	FT 0.5% Tri	FT 1% Tri
1033/1052	1.00 ± 0.018	**1.03 ± 0.015****	**1.04 ± 0.019*****	**1.05 ± 0.013*****	**1.04 ± 0.023*****	**1.04 ± 0.021*****	0.984 ± 0.024	**0.981 ± 0.028***	**1.04 ± 0.015*****	**1.04 ± 0.014*****	**1.04 ± 0.011*****	**1.04 ± 0.014*****	**1.04 ± 0.010*****	**1.02 ± 0.009***	**1.03 ± 0.021****
1082/1052	1.09 ± 0.018	1.09 ± 0.015	**1.06 ± 0.021****	**1.05 ± 0.021*****	**1.02 ± 0.048*****	**1.06 ± 0.032***	**1.01 ± 0.032*****	**1.02 ± 0.039*****	1.10 ± 0.012	1.08 ± 0.019	**1.07 ± 0.010***	**1.06 ± 0.012****	**1.07 ± 0.008***	**1.06 ± 0.015****	**1.03 ± 0.020*****
1082/1240	0.779 ± 0.033	**0.739 ± 0.038***	**0.666 ± 0.031*****	**0.604 ± 0.020*****	**0.573 ± 0.013*****	**0.704 ± 0.028*****	**0.660 ± 0.027*****	**0.649 ± 0.032*****	0.760 ± 0.028	**0.814 ± 0.050***	**0.849 ± 0.53*****	**0.849 ± 0.041*****	0.792 ± 0.018	**0.830 ± 0.023****	**0.836 ± 0.053****
1160/1082	0.790 ± 0.026	**0.822 ± 0.009****	**0.843 ± 0.018*****	**0.874 ± 0.017*****	**0.877 ± 0.024*****	**0.831 ± 0.017*****	**0.822 ± 0.021****	**.831 ± 0.033*****	0.803 ± 0.019	**0.840 ± 0.031*****	**0.847 ± 0.021*****	**0.845 ± 0.018*****	**0.937 ± 0.024*****	**0.832 ± 0.017*****	0.803 ± 0.019
1203/1240	0.731 ± 0.008	0.715 ± 0.011	**0.756 ± 0.016***	**0.67 ± 0.019****	**0.776 ± 0.037*****	0.745 ± 0.016	**0.824 ± 0.026*****	**0.826 ± 0.034*****	0.743 ± 0.019	**0.779 ± 0.033*****	**0.796 ± 0.026*****	**0.794 ± 0.023*****	0.752 ± 0.018	**0.773 ± 0.019*****	**0.788 ± 0.017*****
1283/1240	0.772 ± 0.015	0.778 ± 0.017	**0.708 ± 0.010*****	**0.676 ± 0.019*****	**0.649 ± 0.023*****	**0.733 ± 0.013*****	**0.654 ± 0.018*****	**0.647 ± 0.016*****	**0.792 ± 0.015***	**0.832 ± 0.044*****	**0.848 ± 0.024*****	**0.848 ± 0.015*****	**0.817 ± 0.008*****	**0.832 ± 0.016*****	**0.853 ± 0.018*****
1317/1338	0.943 ± 0.018	0.941 ± 0.021	**0.924 ± 0.019***	**0.896 ± 0.013*****	**0.893 ± 0.020*****	0.936 ± 0.020	**0.920 ± 0.014****	**0.920 ± 0.024****	**0.912 ± 0.013*****	0.935 ± 0.035	0.951 ± 0.015	0.950 ± 0.011	0.948 ± 0.01	0.956 ± 0.010	**0.981 ± 0.009*****
1376/1338	1.02 ± 0.011	1.02 ± 0.011	**1.01 ± 0.015****	**0.972 ± 0.009*****	**0.975 ± 0.015*****	1.02 ± 0.016	**1.00 ± 0.010****	**1.01 ± 0.014****	**0.998 ± 0.006*****	**0.922 ± 0.015*****	**1.00 ± 0.007*****	**0.998 ± 0.005*****	1.01 ± 0.016	**1.01 ± 0.009***	1.03 ± 0.010
1402/1454	0.934 ± 0.028	0.943 ± 0.026	**0.900 ± 0.017*****	**0.868 ± 0.010*****	**0.856 ± 0.016*****	0.922 ± 0.023	**0.878 ± 0.015*****	**0.875 ± 0.019*****	**0.898 ± 0.013*****	0.933 ± 0.038	0.942 ± 0.014	0.938 ± 0.011	0.945 ± 0.024	0.947 ± 0.012	**0.980 ± 0.014*****
1534/1550	0.834 ± 0.025	0.848 ± 0.023	**0.791 ± 0.021*****	**0.763 ± 0.028*****	**0.786 ± 0.022*****	0.815 ± 0.019	0.817 ± 0.028	0.812 ± 0.041	**0.76 ± 0.012*****	**0.760 ± 0.040*****	**0.779 ± 0.020*****	**0.787 ± 0.015*****	**0.800 ± 0.023****	0.818 ± 0.017	0.854 ± 0.021
1610/1630	0.671 ± 0.007	0.678 ± 0.005	**0.658 ± 0.010***	0.666 ± 0.013	**0.656 ± 0.010****	0.668 ± 0.006	0.671 ± 0.007	0.675 ± 0.014	**0.647 ± 0.008*****	0.667 ± 0.015	0.675 ± 0.015	0.677 ± 0.013	0.662 ± 0.008	0.672 ± 0.009	0.681 ± 0.005
1749/1630	0.072 ± 0.007	0.064 ± 0.004	0.065 ± 0.006	0.065 ± 0.005	0.063 ± 0.03	0.063 ± 0.009	0.072 ± 0.009	0.071 ± 0.007	0.079 ± 0.007	**0.094 ± 0.008*****	**0.100 ± 0.014*****	**0.098 ± 0.010*****	0.078 ± 0.016	**0.088 ± 0.006*****	0.081 ± 0.016
2875/2963	0.571 ± 0.013	**0.558 ± 0.008***	0.578 ± 0.012	0.568 ± 0.007	**0.589 ± 0.012****	0.570 ± 0.013	0.578 ± 0.007	0.58 ± 0.010	**0.522 ± 0.010*****	**0.498 ± 0.010*****	**0.492 ± 0.008*****	**0.494 ± 0.011*****	**0.519 ± 0.013*****	**0.510 ± 0.010*****	**0.484 ± 0.033*****
Amide I/Amide II	1.39 ± 0.018	1.38 ± 0.037	1.42 ± 0.031	**1.45 ± 0.04***	1.42 ± 0.052	1.42 ± 0.031	**1.46 ± 0.035****	**1.47 ± 0.073****	**1.56 ± 0.056*****	**1.67 ± 0.064*****	**1.72 ± 0.064*****	**1.71 ± 0.061*****	**1.55 ± 0.069*****	**1.59 ± 0.062*****	**1.60 ± 0.054*****
1338/Amide II	0.162 ± 0.005	**0.158 ± 0.00***	0.165 ± 0.004	**0.170 ± 0.003*****	**0.169 ± 0.002****	0.163 ± 0.004	0.166 ± 0.004	**0.168 ± 0.003****	**0.174 ± 0.003*****	**0.179 ± 0.006*****	**0.181 ± 0.005*****	**0.180 ± 0.004*****	**0.169 ± 0.008****	**0.169 ± 0.004****	0.166 ± 0.006
1240/1454	1.02 ± 0.017	1.01 ± 0.018	**1.10 ± 0.012*****	**1.13 ± 0.032*****	**1.19 ± 0.055*****	**1.07 ± 0.024*****	**1.20 ± 0.039*****	**1.22 ± 0.046*****	1.03 ± 0.023	1.03 ± 0.027	1.02 ± 0.019	1.01 ± 0.012	1.01 ± 0.013	1.00 ± 0.013	1.00 ± 0.024

Table 11 - Mean and standard deviation values of spectral bands ratios of the native disc and the different decellularization procedures, considering the medial zone of the disc. EtOH/Acet is ethanol/acetone, FT is freeze and thaw and Triton X-100 is Tri. Statistical significant differences are presented and calculated against the native disc using a Two-way ANOVA with Fisher's LSD *post-hoc* analysis and represented by * p<0.05, ** p<0.01 and *** p<0.001.

Ratios	Native	EtOH/Acet	0.1% SDS	0.5% SDS	1% SDS	FT 0.1% SDS	FT 0.5% SDS	FT 1% SDS	Accutase	0.1% Tri	0.5% Tri	1% Tri	FT 0.1% Tri	FT 0.5% Tri	FT 1% Tri
1033/1052	0.941 ± 0.033	**0.998 ± 0.015*****	**1.05 ± 0.010*****	**1.04 ± 0.026*****	**1.03 ± 0.035*****	**1.04 ± 0.024*****	0.953 ± 0.025	0.958 ± 0.034	**1.01 ± 0.022*****	**1.04 ± 0.012*****	**1.03 ± 0.016*****	**1.03 ± 0.009*****	**1.04 ± 0.026*****	**1.00 ± 0.013*****	**0.994 ± 0.018*****
1082/1052	1.11 ± 0.016	1.09 ± 0.009	**1.09 ± 0.016***	**1.05 ± 0.027*****	**1.00 ± 0.066*****	**1.08 ± 0.031***	**1.05 ± 0.020*****	**1.06 ± 0.019*****	1.22 ± 0.016	**1.07 ± 0.014*****	**1.08 ± 0.014****	**1.06 ± 0.021*****	**1.09 ± 0.019***	**1.06 ± 0.019*****	**1.05 ± 0.014*****
1082/1240	0.879 ± 0.046	**0.787 ± 0.028*****	**0.647 ± 0.028*****	**0.597 ± 0.019*****	**0.585 ± 0.027*****	**0.697 ± 0.025*****	**0.714 ± 0.028*****	**0.694 ± 0.039*****	**0.825 ± 0.056****	0.852 ± 0.048	0.868 ± 0.059	0.875 ± 0.037	**0.797 ± 0.051*****	0.866 ± 0.030	0.909 ± 0.065
1160/1082	0.734 ± 0.038	**0.806 ± 0.010*****	**0.829 ± 0.010*****	**0.843 ± 0.006*****	**0.881 ± 0.038*****	**0.813 ± 0.017*****	0.746 ± 0.029	**0.765 ± 0.037***	**0.765 ± 0.038***	**0.837 ± 0.024*****	**0.838 ± 0.034*****	**0.833 ± 0.025*****	**0.825 ± 0.013*****	**0.828 ± 0.030*****	**0.765 ± 0.038***
1203/1240	0.752 ± 0.013	**0.720 ± 0.012****	0.740 ± 0.013	0.768 ± 0.028	**0.796 ± 0.051*****	0.742 ± 0.017	**0.826 ± 0.022*****	**0.818 ± 0.026*****	0.760 ± 0.018	**0.795 ± 0.027*****	**0.974 ± 0.030*****	**0.803 ± 0025*****	0.747 ± 0.029	**0.789 ± 0.020*****	**0.813 ± 0.041*****
1283/1240	0.784 ± 0.018	0.797 ± 0.016	**0.695 ± 0.015*****	**0.666 ± 0.018*****	**0.643 ± 0.039*****	**0.726 ± 0.018*****	**0.655 ± 0.017*****	**0.649 ± 0.016*****	0.786 ± 0.017	**0.842 ± 0.022*****	**0.844 ± 0.019*****	**0.848 ± 0.027*****	**0.812 ± 0.023****	**0.847 ± 0.025*****	**0.868 ± 0.033*****
1317/1338	0.986 ± 0.015	0.975 ± 0.013	**0.912 ± 0.015*****	**0.887 ± 0.015*****	**0.914 ± 0.025*****	**0.931 ± 0.021*****	**0.918 ± 0.015*****	**0.922 ± 0.016*****	**0.924 ± 0.015*****	**0.949 ± 0.012*****	**0.958 ± 0.016*****	**0.955 ± 0.017*****	**0.952 ± 0.017*****	0.972 ± 0.014	0.990 ± 0.014
1376/1338	1.05 ± 0.010	1.05 ± 0.011	**1.00 ± 0.011*****	**0.979 ± 0.012*****	**0.991 ± 0.020*****	**1.02 ± 0.019*****	**1.01 ± 0.014*****	**1.01 ± 0.013*****	**1.00 ± 0.011*****	**1.00 ± 0.006*****	**1.01 ± 0.011*****	**1.00 ± 0.009*****	**1.02 ± 0.015*****	**1.02 ± 0.006*****	**1.03 ± 0.005*****
1402/1454	0.963 ± 0.016	0.975 ± 0.011	**0.891 ± 0.012*****	**0.856 ± 0.008*****	**0.874 ± 0.008*****	**0.910 ± 0.021*****	**0.872 ± 0.013*****	**0.884 ± 0.013*****	**0.903 ± 0.015*****	0.948 ± 0.012	0.948 ± 0.015	0.950 ± 0.018	**0.946 ± 0.021***	0.964 ± 0.014	0.979 ± 0.010
1534/1550	0.876 ± 0.20	0.887 ± 0.027	**0.766 ± 0.013*****	**0.736 ± 0.023*****	**0.781 ± 0.044*****	**0.908 ± 0.026*****	**0.788 ± 0.033*****	**0.803 ± 0.030*****	**0.755 ± 0.014*****	**0.777 ± 0.017*****	**0.785 ± 0.021*****	**0.790 ± 0.017*****	**0.805 ± 0.027*****	**0.833 ± 0.021*****	0.857 ± 0.020
1610/1630	0.658 ± 0.008	**0.680 ± 0.009*****	**0.646 ± 0.010***	**0.640 ± 0.009*****	0.662 ± 0.008	0.663 ± 0.006	0.660 ± 0.014	**0.670 ± 0.011***	0.651 ± 0.009	**0.676 ± 0.016*****	**0.677 ± 0.016*****	**0.680 ± 0.011*****	0.657 ± 0.013	**0.675 ± 0.011****	**0.685 ± 0.014*****
1749/1630	0.072 ± 0.005	0.064 ± 0.003	0.069 ± 0.008	**0.061 ± 0.005***	0.064 ± 0.005	**0.061 ± 0.006***	0.068 ± 0.004	0.068 ± 0.004	**0.087 ± 0.008****	**0.098 ± 0.009*****	**0.104 ± 0.019*****	**0.102 ± 0.008*****	0.078 ± 0.016	**0.089 ± 0.008*****	**0.094 ± 0.012*****
2875/2963	0.584 ± 0.012	**0.560 ± 0.009*****	0.579 ± 0.007	0.574 ± 0.006	0.591 ± 0.009	0.579 ± 0.011	0.573 ± 0010	**0.568 ± 0.008***	**0.534 ± 0.012*****	**0.494 ± 0.010*****	**0.505 ± 0.011*****	**0.495 ± 0.012*****	**0.530 ± 0.014*****	**0.508 ± 0.013*****	**0.50 ± 0.012*****
Amide I/Amide II	1.38 ± 0.021	1.35 ± 0.041	1.40 ± 0.044	**1.45 ± 0.035****	**1.44 ± 0.022****	1.40 ± 0.043	**1.50 ± 0.038*****	**1.48 ± 0.038*****	**1.59 ± 0.061*****	**1.71 ± 0.070*****	**1.70 ± 0.087*****	**1.73 ± 0.070*****	**1.53 ± 0.073*****	**1.61 ± 0.048*****	**1.66 ± 0.096*****
1338/Amide II	0.154 ± 0.002	0.152 ± 0.003	**0.167 ± 0.002*****	**0.171 ± 0.001*****	**0.168 ± 0.005*****	**0.164 ± 0.005*****	**0.168 ± 0.003*****	**0.168 ± 0.003*****	**0.177 ± 0.003*****	**0.182 ± 0.006*****	**0.182 ± 0.008*****	**0.182 ± 0.003*****	**0.167 ± 0.005*****	**0.170 ± 0.003*****	**0.171 ± 0.006*****
1240/1454	1.02 ± 0.020	0.999 ± 0.019	**1.13 ± 0.031*****	**1.16 ± 0.036*****	**1.23 ± 0.081*****	**1.08 ± 0.030*****	**1.21 ± 0.046*****	**1.23 ± 0.036*****	1.05 ± 0.019	1.03 ± 0.011	1.03 ± 0.017	1.03 ± 0.016	1.02 ± 0.015	1.00 ± 0.022	1.00 ± 0.017

Table 12 - Mean and standard deviation values of spectral bands ratios of the native disc and the different decellularization procedures, considering the posterior zone of the disc. EtOH/Acet is ethanol/acetone, FT is freeze and thaw and Triton X-100 is Tri. Statistical significant differences are presented and calculated against the native disc using a Two-way ANOVA with Fisher's LSD *post-hoc* analysis and represented by * p<0.05, ** p<0.01 and *** p<0.001.

Ratios	Native	EtOH/Acet	0.1% SDS	0.5% SDS	1% SDS	FT 0.1% SDS	FT 0.5% SDS	FT 1% SDS	Accutase	0.1% Tri	0.5% Tri	1% Tri	FT 0.1% Tri	FT 0.5% Tri	FT 1% Tri
1033/1052	0.974 ± 0.032	**1.00 ± 0.021****	**1.05 ± 0.012*****	**1.05 ± 0.011*****	**1.02 ± 0.027*****	**1.04 ± 0.014*****	**1.00 ± 0.036****	0.966 ± 0.030	**1.04 ± 0.008*****	**1.05 ± 0.017*****	**1.05 ± 0.013*****	**1.05 ± 0.017*****	**1.04 ± 0.023*****	**1.00 ± 0.027****	**1.01 ± 0.024*****
1082/1052	1.10 ± 0.017	1.09 ± 0.010	**1.07 ± 0.018****	**1.05 ± 0.020*****	**0.977 ± 0.048*****	1.08 ± 0.028	**1.05 ± 0.031*****	**1.02 ± 0.039*****	1.12 ± 0.017	1.10 ± 0.012	1.10 ± 0.008	1.10 ± 0.016	1.09 ± 0.015	1.10 ± 0.023	**1.06 ± 0.021*****
1082/1240	0.828 ± 0.063	**0.777 ± 0.036****	**0.646 ± 0.023*****	**0.599 ± 0.025*****	**0.603 ± 0.038*****	**0.681 ± 0.030*****	**0.638 ± 0.028*****	**0.662 ± 0.029*****	**0.745 ± 0.024*****	**0.770 ± 0.050****	**0.774 ± 0.027****	**0.765 ± 0.049*****	**0.749 ± 0.049*****	0.810 ± 0.024	0.820 ± 0.053
1160/1082	0.772 ± 0.041	**0.802 ± 0.016***	**0.826 ± 0.016*****	**0.873 ± 0.022*****	**0.873 ± 0.056*****	**0.815 ± 0.012*****	**0.848 ± 0.063*****	**0.817 ± 0.039*****	0.791 ± 0.019	**0.826 ± 0.023*****	**0.829 ± 0.018*****	**0.813 ± 0.023*****	**0.824 ± 0.026*****	**0.796 ± 0.037***	0.791 ± 0.019
1203/1240	0.749 ± 0.015	**0.723 ± 0.009***	0.750 ± 0.012	0.768 ± 0.013	**0.803 ± 0.043*****	0.743 ± 0.017	**0.798 ± 0.033*****	**0.835 ± 0.039*****	0.735 ± 0.021	0.751 ± 0.018	0.752 ± 0.008	0.741 ± 0.020	0.729 ± 0.023	0.743 ± 0.011	0.772 ± 0.024
1283/1240	0.781 ± 0.022	0.790 ± 0.017	**0.691 ± 0.010*****	**0.675 ± 0.024*****	**0.637 ± 0.031*****	**0.712 ± 0.014*****	**0.661 ± 0.026*****	**0.640 ± 0.017*****	0.777 ± 0.019	**0.800 ± 0.017***	0.799 ± 0.009	0.790 ± 0.015	0.791 ± 0.028	0.798 ± 0.016	**0.835 ± 0.020*****
1317/1338	0.956 ± 0.027	0.948 ± 0.020	**0.902 ± 0.014*****	**0.879 ± 0.011*****	**0.905 ± 0.023*****	**0.919 ± 0.020*****	**0.887 ± 0.019*****	**0.914 ± 0.027*****	**0.895 ± 0.010*****	**0.910 ± 0.014*****	**0.917 ± 0.011*****	**0.912 ± 0.012*****	**0.934 ± 0.018****	**0.938 ± 0.009***	0.965 ± 0.012
1376/1338	1.03 ± 0.018	1.03 ± 0.017	**0.999 ± 0.008*****	**0.965 ± 0.010*****	**0.982 ± 0.018*****	**1.01 ± 0.013****	**0.981 ± 0.019*****	**0.996 ± 0.018*****	**0.978 ± 0.010*****	**0.983 ± 0.007*****	**0.86 ± 0.012*****	**0.986 ± 0.006*****	**1.01 ± 0.015*****	**1.01 ± 0.005*****	1.02 ± 0.012
1402/1454	0.938 ± 0.027	0.939 ± 0.024	**0.974 ± 0.013*****	**0.839 ± 0.014*****	**0.856 ± 0.013*****	**0.900 ± 0.025*****	**0.833 ± 0.028*****	**0.857 ± 0.016*****	**0.873 ± 0.012*****	**0.903 ± 0.017*****	**0.903 ± 0.017*****	**0.900 ± 0.015*****	0.931 ± 0.018	**0.919 ± 0.012***	**0.960 ± 0.023***
1534/1550	0.855 ± 0.029	0.885 ± 0.031*	**0.771 ± 0.012*****	**0.744 ± 0.014*****	**0.790 ± 0.040*****	**0.802 ± 0.021*****	**0.767 ± 0.027*****	**0.811 ± 0.050*****	**0.749 ± 0.007*****	**0.758 ± 0.014*****	**0.763 ± 0.011*****	**0.765 ± 0.015*****	**0.810 ± 0.028*****	**0.819 ± 0.025****	0.850 ± 0.025
1610/1630	0.671 ± 0.012	**0.681 ± 0.010***	**0.646 ± 0.008*****	**0.647 ± 0.017*****	0.665 ± 0.016	0.661 ± 0.011	**0.649 ± 0.016*****	0.666 ± 0.019	**0.646 ± 0.007*****	0.662 ± 0.010	**0.659 ± 0.006***	**0.659 ± 0.009***	0.633 ± 0.017	0.664 ± 0.007	0.675 ± 0.006
1749/1630	0.078 ± 0.005	0.073 ± 0.008	0.074 ± 0.005	0.079 ± 0.008	0.080 ± 0.008	**0.063 ± 0.010*****	0.087 ± 0.021	**0.088 ± 0.011***	0.084 ± 0.014	**0.090 ± 0.009***	**0.093 ± 0.009****	0.085 ± 0.007	0.071 ± 0.008	**0.090 ± 0.009***	0.077 ± 0.019
2875/2963	0.581 ± 0.013	**0.566 ± 0.010***	0.591 ± 0.009	0.579 ± 0.009	**0.612 ± 0.016*****	0.586 ± 0.013	**0.597 ± 0.011***	0.587 ± 0.012	**0.537 ± 0.021*****	**0.516 ± 0.009*****	**0.519 ± 0.013*****	**0.525 ± 0.010*****	**0.540 ± 0.014*****	**0.540 ± 0.014*****	**0.500 ± 0.037*****
Amide I/Amide II	1.40 ± 0.023	**1.34 ± 0.031***	1.38 ± 0.035	**1.46 ± 0.036***	1.44 ± 0.031	1.40 ± 0.038	**1.46 ± 0.049****	**1.48 ± 0.028*****	**1.51 ± 0.072*****	**1.58 ± 0.047*****	**1.58 ± 0.034*****	**1.55 ± 0.056*****	1.46 ± 0.095	**1.48 ± 0.057*****	**1.53 ± 0.083*****
1338/Amide II	0.161 ± 0.004	**0.153 ± 0.004*****	**0.167 ± 0.002****	**0.171 ± 0.001*****	**0.169 ± 0.005*****	**0.166 ± 0.003***	**0.171 ± 0.005*****	**0.168 ± 0.003*****	**0.172 ± 0.004*****	**0.177 ± 0.004*****	**0.176 ± 0.003*****	**0.175 ± 0.004*****	**0.165 ± 0.007***	0.164 ± 0.007	0.162 ± 0.007
1240/1454	1.02 ± 0.020	**0.981 ± 0.020***	**1.12 ± 0.024*****	**1.13 ± 0.051*****	**1.21 ± 0.072*****	**1.10 ± 0.017*****	**1.15 ± 0.062*****	**1.23 ± 0.055*****	1.01 ± 0.018	1.02 ± 0.010	1.03 ± 0.012	1.03 ± 0.014	1.01 ± 0.023	1.01 ± 0.030	0.99 ± 0.015

4.4.2 Second Derivative FTIR Spectra

Since through FTIR spectroscopy it is possible to visualize absorptions bands that are specific to certain molecules, it is possible to perform a quantitative analysis of the collagen and GAGs present in the TMJ discs (Saarakkala et al., 2010). Different methods have been applied to quantify these components. Collagen can be estimated by integrating the area under the amide I band (1720 cm^{-1} to 1590 cm^{-1}) and PG content can estimated by: *(i)* integrating the area under the carbohydrate band (1140 cm^{-1} to 985 cm^{-1}); or *(ii)* by the ratio of the carbohydrate region to the Amide I. Although this later ratio is performed to eliminate thickness variations of the sample, (Kim et al., 2005; Spalazzi et al., 2013; Zhou et al., 2018) the amide I region has also presented influence of the GAGs (Rieppo et al., 2012).

Different authors have proved the feasibility of the second derivative technique for the quantitative analysis of collagen and GAGs in articular cartilage of steers and humans compared to the analysis of the raw spectra (Rieppo et al., 2013, 2012). Considering this, the collagen content was estimated with 1338 cm^{-1} band, the sulfated GAGs content around 1052 cm^{-1} band and sulfated and non-sulfated GAGs around 1376 cm^{-1} band.

4.4.2.1 Native Disc Regionally Content

A quantitative analysis of the GAGs and collagen between the five morphological regions of the native disc was performed (Table 13 and Figure 16).

Different values are found in the literature for GAGs content, but it generally comprises 1-10% of its dry weight, where 5% is the most frequent reported value in the literature. Chondroitin sulfate and dermatan sulfate are believed to be the most abundant GAGs present in the disc, comprising 75-93% of the total GAGs content, followed by HA with 5-20%. In minor quantities, keratan sulfate and heparin sulfate are also present (Allen et al., 2006; Detamore et al., 2003). Detamore et al. (2005) investigated the biochemical content of the porcine TMJ disc and reported 5.3 ± 1.2% (dry weight) of GAGs content . Chondroitin sulfate was 75% of the total GAGs content (4.4 times more than dermatan sulfate, 8.2 times keratan sulfate and 164 times HA content).

Regionally, the GAGs content varies among species. In the porcine TMJ disc, GAGs are more predominant in the intermediary zone and less predominant in the posterior zone. It is also more predominant medially than laterally (Almarza et al., 2006). In bovine and human discs it is more concentrated in the central region than the periphery (Kopp et al., 1976; Nakano et al., 1996). However, in other separate study no differences were found in GAGs content in human discs (Kuo et al., 2010). More recently, Kalpakci et al. (2011) conducted a comparative study of the regional biochemical content in human, cow, goat, pig and rabbit TMJ discs, highlighting

a high variability among species. Generally, in all species, the central, medial, and lateral zone have more GAGs than the posterior and anterior zone. In the human disc, significantly lower content in the anterior zone is found compared to the remaining regions.

All studies mentioned above, only measured sulfated GAGs, except for the Nakano & Scott (1996) that also evaluated HA in bovine disc. For the human TMJ disc, sulfated GAGs were higher in the medial region, and statistically different from the central and lateral region (Kalpakci et al., 2011). This is in accordance with the results found in the current work, where the medial zone has a higher concentration of sulfated GAGs and statistical differences are found with the central and medial zone at a 0.1% significance and with the anterior and posterior at 5% significance. The central region was the one with the lowest sulfated GAGs content in the lamb disc, whereas in the human disc it was the anterior.

For sulfated and non-sulfated GAGs content in the lamb disc, it is not possible to compare with any study, but results point that the lateral and posterior region presents more concentrated GAGs. However no statistical differences are found with the central or lateral region. The regions that are significant different at 5% significance is the lateral-medial and posterior-medial zones.

Collagen comprises 37% of the wet weight, 50% of the wet volume or 69–85% of the dry weight of the disc. Collagen I is the most abundant biochemical component, but small quantities of collagen II, III and non-fibrillar collagens (VI, IX, XII) are also present (Detamore et al., 2003; Willard et al., 2011). As GAGs, the distribution of collagen varies among species. In the porcine disc, the highest content occurs in the intermediate zone (Almarza et al., 2006), whereas in the human disc no statistically differences were found (Kuo et al., 2010). Kalpakci et al. (2011) observed the same results for the human disc and for the goat, which is comparable with the present study due to the fact that the two are ruminants, where collagen are more concentrated in the posterior region. The lamb disc present higher collagen content in the central region. However, no statistical differences are found with the posterior region. The lateral region in the goat disc presents the lower content and no statistical differences are found with the central and medial region, whereas in the lamb disc is the medial region and is statistically different at 1% significance from the lateral and central region.

Table 13 - Statistically significant differences between the 5 regions of the native disc for GAGs and collagen content, concerning some bands at the derivative FTIR spectra, evaluated by One-way ANOVA with Fisher's LSD *post-hoc* analysis, and represented by * p<0.05, ** p<0.01 and *** p<0.001.

	Anterior	Central	Lateral	Medial	Posterior
1052 || 1376					
Anterior		ns	ns	ns	ns
Central	*		ns	ns	ns
Lateral	ns	ns		*	ns
Medial	*	***	***		*
Posterior	ns	*	ns	*	
1338					
Anterior					
Central	*				
Lateral	ns	ns			
Medial	ns	**	**		
Posterior	ns	ns	ns	**	

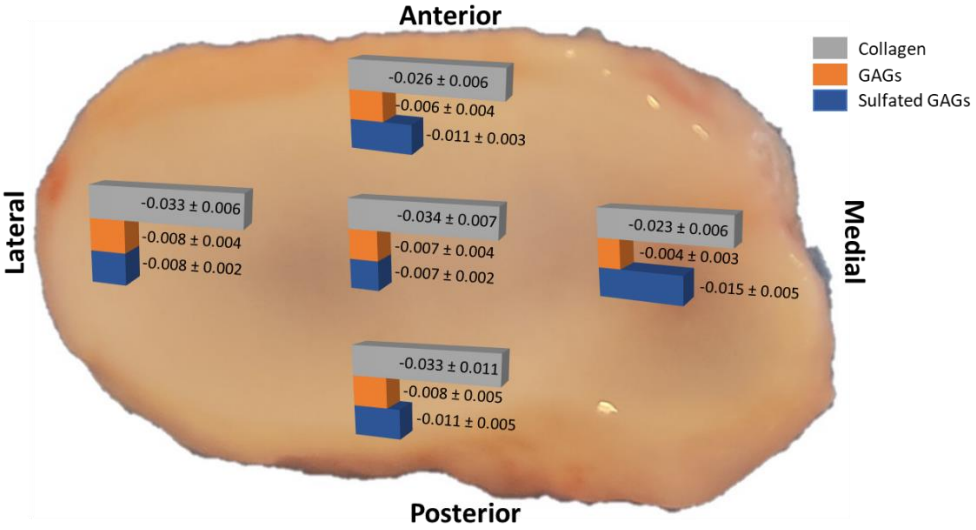

Figure 16 – Collagen and GAGs distribution along the lamb TMJ disc. Values presented as mean±SD.

It is worth to mention that the studies found in the literature differ from the present one, in which staining protocols are used. The spectral band associated with collagen is more pronounced than the GAGs band, which is in accordance with the native ECM disc components, having higher collagen content than GAGs. However, and as mentioned, the studies only analyse sulfated GAGs due to the complexity and difficulty of implementing a protocol that also detects HA, thus, the implementation of the quantification by FTIR spectroscopy may open the possibility to perform this study more effectively by analysing all types of GAGs present in the disc, and cartilage in general. Although with this type of evaluation, in which the second

derivative is used, the quantitatively exact value of the biochemical components is not obtained, with the use of more complex multivariate methods it may be possible.

4.4.2.2 Glycosaminoglycans content

GAGs are carbohydrate complexes that are divided into sulfate and non-sulfated. The first ones include chondroitin sulfate, dermatan sulfate, keratan sulfate, heparin and heparan sulfate. The latter includes HA (Gandhi et al., 2008).

The sulfated GAGs band is normally found at 1064 cm^{-1} in human and bovine articular cartilage, whereas in rat elastic cartilage, this band is not found (Vidal et al., 2016). In the native TMJ disc, a more prominent and consistent band between samples is found at 1052 cm^{-1} (Figure 17-A), which is in the range of the symmetric stretching of SO_3^- (1072–1040 cm^{-1}) (Mohamed et al., 2020).

For a quantitative analysis of the sulfated GAGs, the analysis of band for the decellularized discs was evaluated and a shift in bands of ± 2 cm^{-1} was accepted. In the ethanol/acetone treatment, this band was located in the 1052 cm^{-1} (Figure 17-B). However, for the remaining treatments, there was a shift of this band to higher wavelengths. For all SDS samples, this band was located at 1060 cm^{-1} (Figure 17-C, D, E, F, G, H), in accutase was located between 1052-1062 cm^{-1} (Figure 17-I) and for Triton X-100 samples between 1048-1064 cm^{-1} (Figure 17-J, K, L, M, N, O). It is known that lower infrared frequencies absorbed by a bond, means a larger mass of the bonded atoms, so the change in location of the bands found for sulfated GAGs is due to a change in the composition of the sample (Merlic et al., 2000). More specifically to decrease of mass in the SDS samples, since the band has changed to a higher wavenumber. Interestingly, for accutase and Triton X-100 samples, there was a wide variability between replicas, where bands have changed to higher and lower wavenumbers, meaning that there was both mass decrease and increase. The same phenomenon was found for the quantitative analysis of the GAGs, which include sulfated and non-sulfate, at a band 1376 cm^{-1}. For the native, ethanol/acetone and SDS samples treatments they were located at this band (Figure 17-A-H). However, for accutase, it was between 1375-1380 cm^{-1} (Figure 17-I) and for Triton X-100 samples between 1371-1380 cm^{-1} (Figure 17-J-O).

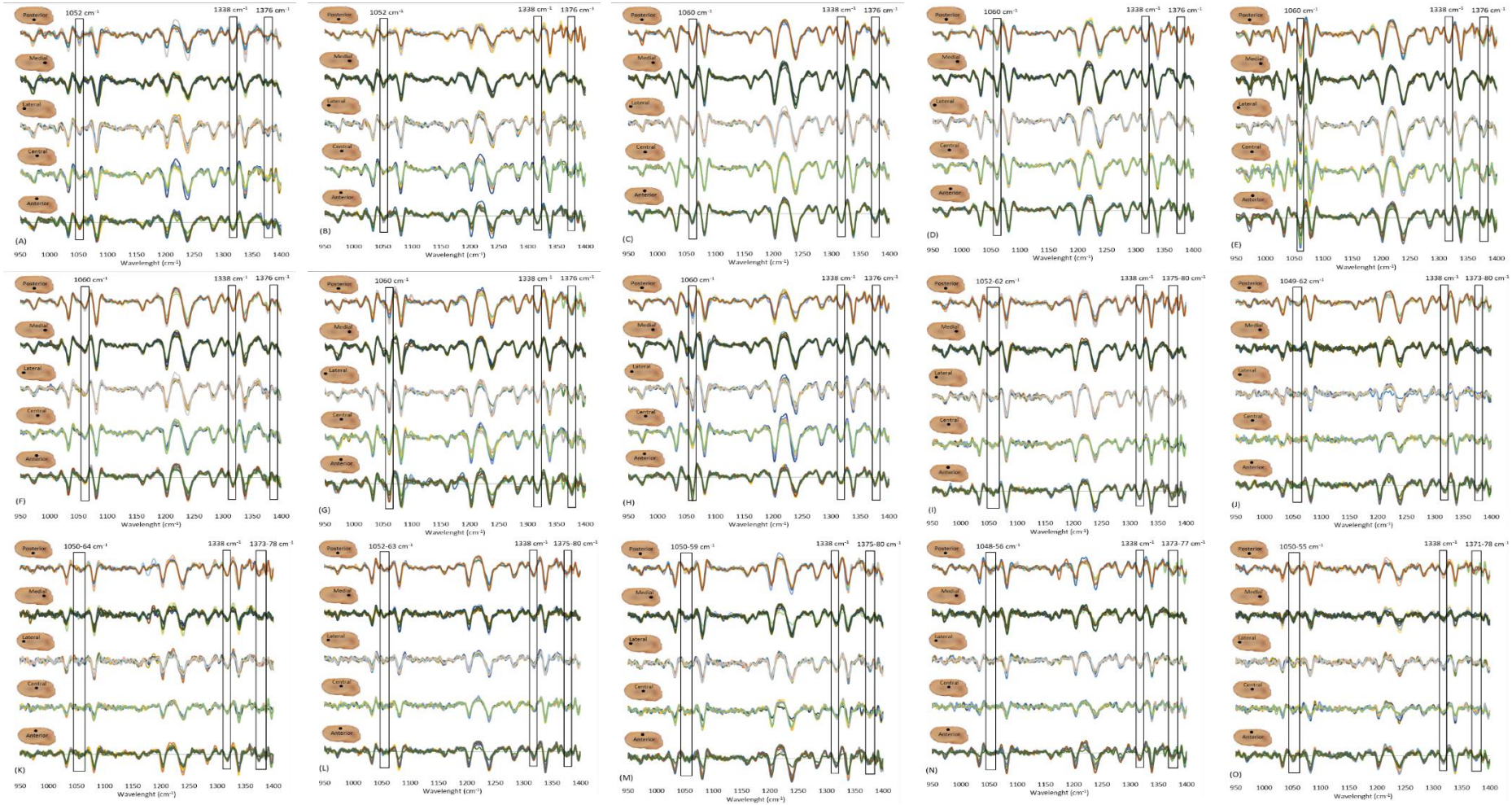

Figure 17 – Second derivative FTIR spectra of the native (A) and decellularized discs: ethanol/acetone (B), 0.1% SDS (C), 0.5% SDS (D) 1% SDS (E), freeze and thaw followed by 0.1% SDS (F), 0.5% SDS (G) 1% SDS (H), accutase (I), 0.1% Triton X-100 (J), 0.5% Triton X-100 (K) 1% Triton X-100 (L), freeze and thaw followed by 0.1% Triton X-100 (M), 0.5% Triton X-100 (N) and 1% Triton X-100 (O).

For sulfate GAGs quantitative analysis and comparing all treatments with the native (Figure 18, Table 1 of Appendix 2), ethanol/acetone treatment only leads to differences in the medial zone, where its content decreased by 38.8%. All SDS samples were largely affected ($p<0.001$) in all zones except for 0.1% SDS in the medial zone and freeze and thaw followed by 0.1% SDS in which no significant differences in content were found. Interestingly, it was expected a decrease in value, however, there was an increase. Accutase and all Triton X-100 samples maintained their sulfated GAGs content in the central and lateral region. For accutase, 0.1% Triton X-100, 0.5% Triton X-100 and freeze and thaw followed by 0.1% Triton X-100 similar results are present, where the anterior zone content decreased at 1% significance (decrease of 64.2%, 65.3%, 59.8% and 59.6%, respectively), the medial zone at 0.1% significance (decrease of 52.9%, 72.7%, 65.5%, and 67.7%, respectively) and the posterior zone at 5% significance (decrease of 54.9%, 53.6%, 51.1%, 44.8%, respectively). 1% Triton X-100 decreased 53.0% in the anterior region, 64.8% in the medial region and 53.9% in the posterior region. Freeze and thaw followed by 0.5% Triton X-100 present differences at 1% significance in the anterior (decrease of 57.9%) and medial regions (decrease of 46.5%), whereas freeze and thaw followed by 1% Triton X-100 is only affected in the medial region with a decrease of 43.9%.

Considering these results and arranging the treatments from the least to the most affected in sulfated GAGs, the following order can be established (Figure 1 of appendix 3): 1) freeze and thaw followed by 0.1% SDS; 2) ethanol/acetone; 3) freeze and thaw followed by 1% Triton X-100; 4) freeze and thaw followed by 0.5% Triton X-100; 5) 1% Triton X-100; 6) accutase, 0.1% Triton X-100, 0.5% Triton X-100 and freeze and thaw followed by 0.1% Triton X-100; 7) 0.1% SDS and 8) 0.5% and 1% SDS and freeze and thaw followed by either 0.5% or 1% SDS.

Regarding sulfated and non-sulfated GAGs at band 1376 cm^{-1} (Figure 19, Table 2 of Appendix 2), ethanol/acetone treatment only led to an increase in 44.6% in the central region. Once again, the SDS samples were largely affected ($p<0.001$), except for the freeze and thaw followed by 0.1% SDS, that although it was also affected in the central region at 1% significance (increased of 62%), in the lateral region no difference was found. There was also an increase of GAGs content in accutase samples at a 0.1% significance. For all triton X-100 samples, except for the freeze and thaw followed by 1% Triton X-100, only the central and lateral zone are unaffected, whereas in the remaining zones variations of the increase in the GAGs content was found. Interestingly, for freeze and thaw followed by 1% Triton X-100, GAGs content diminished 54.8% in the lateral zone.

Once again, considering these results and arranging the treatments from the least to the most affected in GAGs, the following order can be established (Figure 2 of appendix 3): 1) ethanol/acetone; 2) freeze and thaw followed by 1% Triton X-100; 3) freeze and thaw followed

by 0.5% Triton X-100; 4) 0.5% Triton X-100; 5) 0.1% Triton X-100; 6) 1% Triton X-100; 7) freeze and thaw followed by 0.1% Triton X-100; 8) freeze and thaw followed by 0.1% SDS and 9) remaining samples of SDS and accutase.

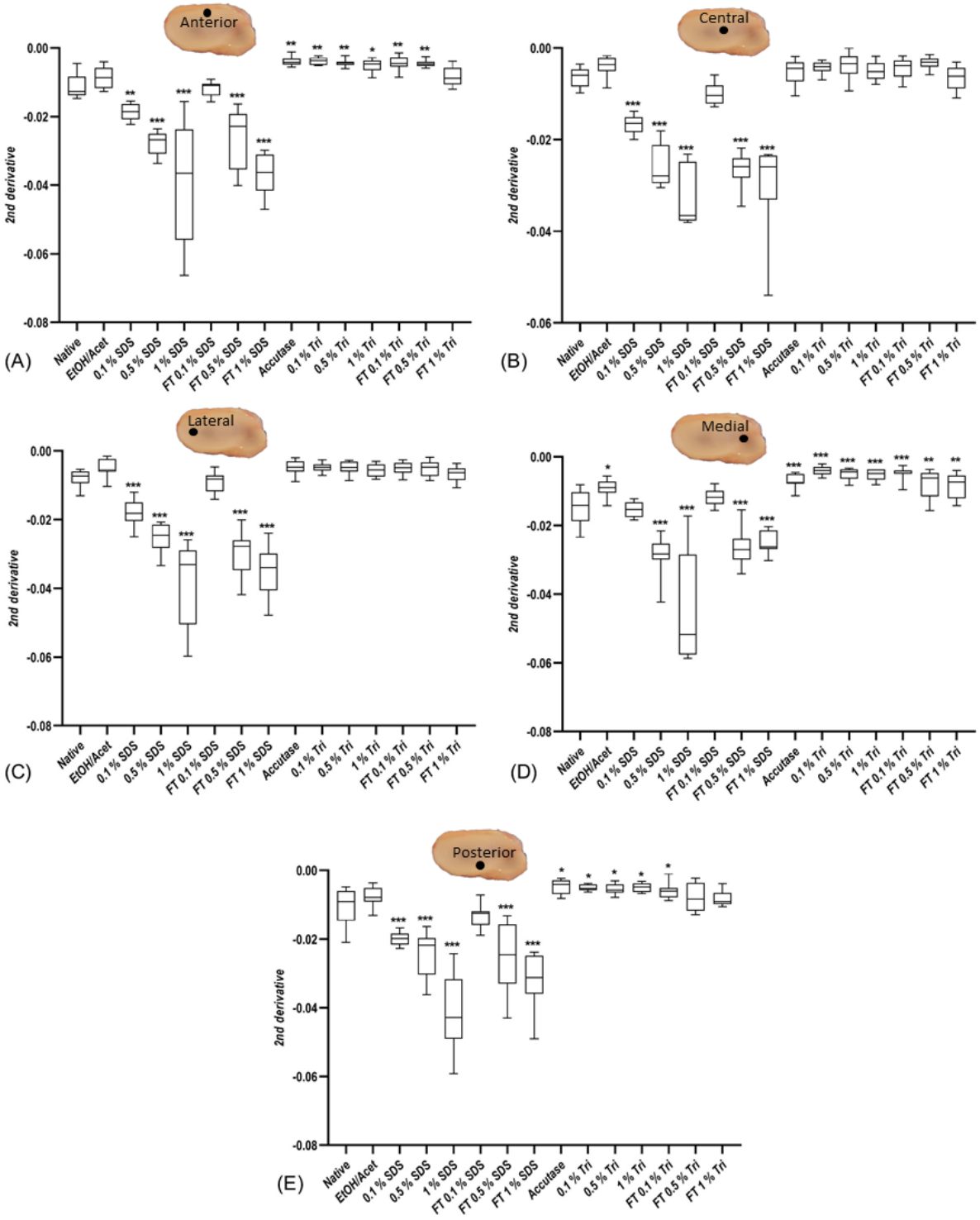

Figure 18 - Box-plot graphs of the sulfated GAGs bands at second derivative spectra from the disc with or without (i.e. native) decellularization procedures for the anterior (A), central (B), lateral (C), medial (D) and posterior (E) zone. EtOH/Acet is ethanol/acetone, FT is freeze and thaw and Triton X-100 is Tri. Statistically significant differences are presented and calculated against the native disc using a Two-way ANOVA with Fisher's LSD *post-hoc* analysis, and represented by * $p<0.05$, ** $p<0.01$ and *** $p<0.001$.

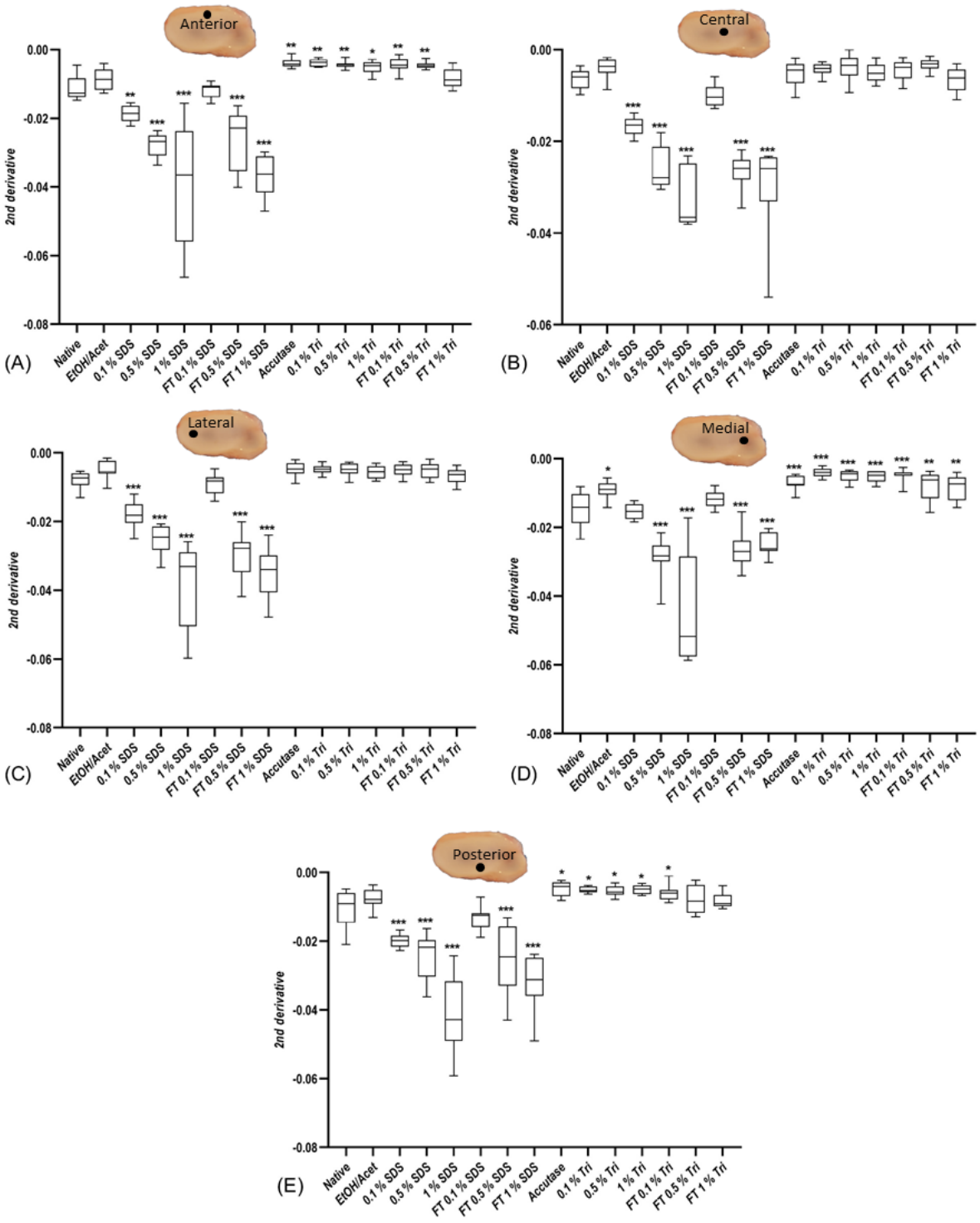

Figure 19 - Box-plot graphs of the sulfated and non sulfated GAGs bands at second derivative spectra from the disc with or without (i.e. native) decellularization procedures for the anterior (A), central (B), lateral (C), medial (D) and posterior (E) zone. EtOH/Acet is ethanol/acetone, FT is freeze and thaw and Triton X-100 is Tri. Statistically significant differences are presented and calculated against the native disc using a Two-way ANOVA with Fisher's LSD *post-hoc* analysis, and represented by * $p<0.05$, ** $p<0.01$ and *** $p<0.001$.

Although there is an increase in the content of both the sulfated and all the GAGs (sulfated and non sulfated), this is not due to a relative increase in content but rather to possible

degradation in GAGs, which, consequently, led to an increase in absorbance of infrared radiation. This was confirmed earlier where there was a shift of the bands to higher wavenumbers. Although the Triton X-100 samples were the least changed, it was possible to detect a great shift in the position of the bands between replicates, unlike the SDS that bands positions were consistent between replicates. For 1376 cm^{-1} band of the GAGs there was no shift in it, pointing that the Triton X-100 strongly interacts with the GAGs, destabilizing them in a randomized way.

As referred, although 1052 cm^{-1} band is used to estimate sulfated GAGs, this band is also associated with C-O vibrations, which helps to explain the differences in results between the two GAGs bands and that it is not only related to the fact that HA is not being accounted for. Considering this, the 1376 cm^{-1} band seems to be a more appropriate band to quantify GAGs content as attributed to the CH3 vibrations, which are present in all GAGs (Rieppo et al., 2012).

4.4.2.3 Collagen content

As referred 1338 cm^{-1} band is assigned o CH_2 side chains of collagen and it is used to analyse collagen content. In all decellularization procedures, this band was unaltered as it is possible to observe in Figure 17.

In Figure 20 and Table 3 of Appendix 2 the statistically significant differences are represented for the collagen content. Ethanol/acetone treatment led to an increase in the collagen content of 36.9% in the anterior region, 23.1% in the central region and 19.0% in the posterior region. From all SDS samples, the freeze and thaw followed by 0.1% SDS treated samples, were the less affected, where only the medial region increased 45.3%. The remaining SDS samples are affected at 0.1% significance, in particular upon 1% SDS treatment. The lateral region is the less impacted, where for the 0.5% SDS there is a difference at 5% significance (increase of 22.3%). Collagen content for accutase treated samples led to a difference at 0.1% significance in the anterior, medial and posterior zone (increase of 65.0%, 51.2% and 39.8%, respectively) and 5% significance in the lateral zone (increase of 20.2%).

For the Triton X-100 treated samples, some variations were found. In the anterior and posterior region, there was an increase in the collagen content, in the central and lateral regions there was a decrease and in the medial region, depending on the sample, both an increase and decrease derivative absorbances occurred. Despite these variations, not all of them are statistically significant. Samples treated by freeze and thaw followed by 0.1% SDS were the least affected ones, where only in the anterior region presented a 31.2% increase in the collagen. For samples not treated with freeze and thaw, only the medial region maintained unchanged, where the anterior region was the most affected.

Considering these observations, the decellularization treatments by increase impact on collagen to the most affected, are (Figure 3 of appendix 3): 1) freeze and thaw followed by 0.1% Triton X-100; 2) freeze and thaw followed by 0.1% SDS; 3) 1% Triton X-100; 4) ethanol/acetone; 5) 0.1% and 0.5% Triton X-100; 6) freeze and thaw followed by 0.5% Triton X-100; 7) freeze and thaw followed by 1% Triton X-100; 8) accutase; 9) freeze and thaw followed by 0.5% SDS; 10) 0.1% SDS and freeze and thaw followed by 1% SDS; 11) 0.5% SDS and 12) 1% SDS.

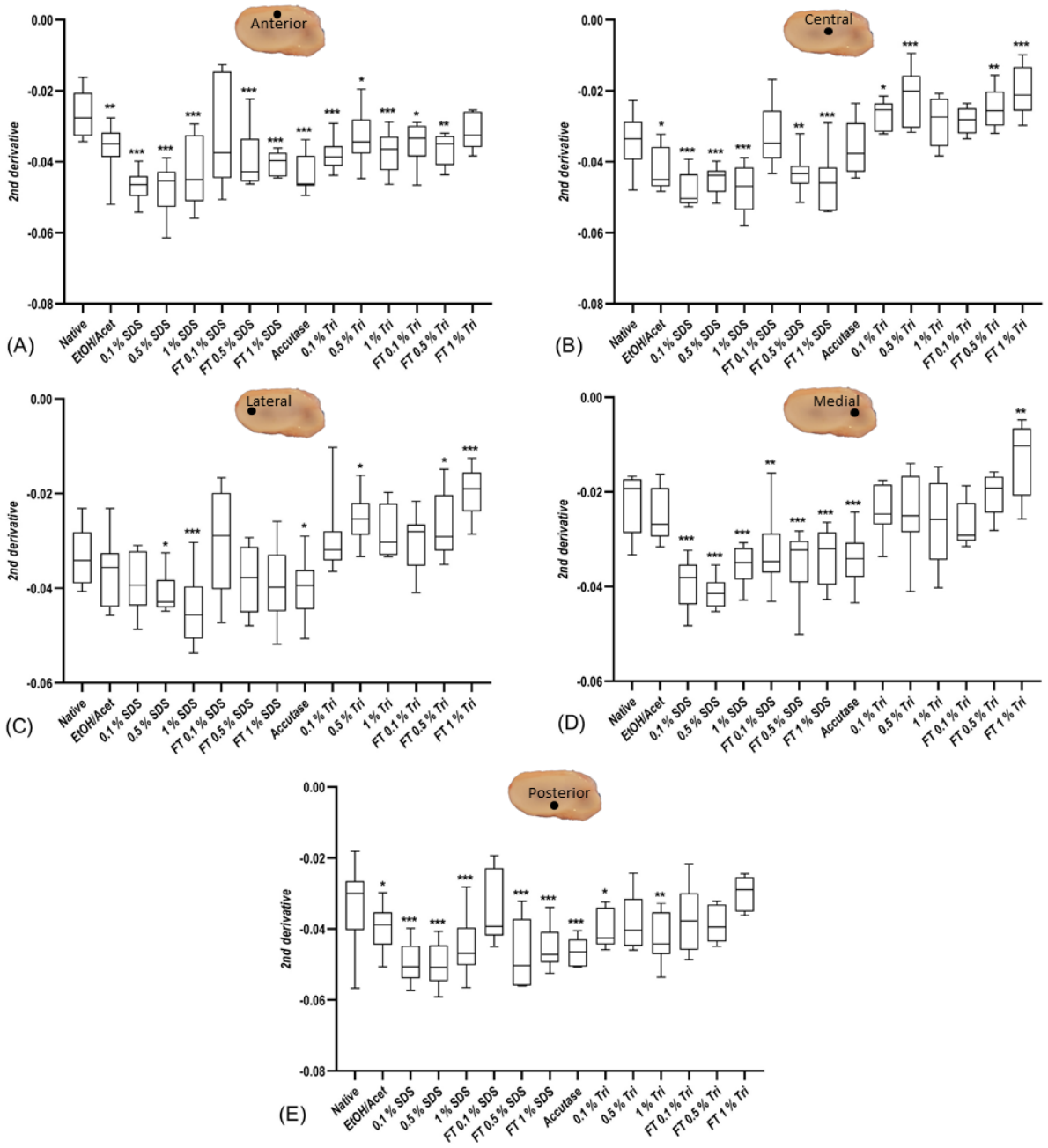

Figure 20 - Box-plot graphs of the collagen bands at second derivative spectra from the disc with or without (i.e. native) decellularization procedures for the anterior (A), central (B), lateral (C), medial (D) and posterior (E) zone. EtOH/Acet is ethanol/acetone, FT is freeze and thaw and Triton X-100 is Tri. Statistically significant differences are presented and calculated against the native disc using a Two-

way ANOVA with Fisher's LSD *post-hoc* analysis, and represented by * $p<0.05$, ** $p<0.01$ and *** $p<0.001$.

Once again there was an increase in the derivative absorbance values. However, without affecting the band position and according to the previous band ratios determination at 1338/amide II and 1240/1454 cm^{-1}, no collagen degradation was found. This points most probably to alteration of the collagen conformation, leading to more exposed amino acids residues and a consequent increase of infrared radiation absorption. Moreover, the increase was most pronounced on the SDS samples, as with the agitation method this detergent starts removing the surface cells of the disc and, only then, the ones present inside the ECM. With this, the first eliminated cells may release protease enzymes that are capable of destroying proteins present in the disc, in this case, collagen (Yusof et al., 2019). Interestingly, by quantifying the components by biochemical assays, an increase in collagen and a decrease in GAGs was also found in the decellularization of a porcine TMJ disc with a combination of freeze and thaw, 1% Triton X-100, hypotonic Tris–hydrochloric acid buffer and trypsin methods (Liang et al., 2020) and in the decellularization of a bovine meniscus with a combination of a sonication system and 0.1% SDS (Yusof et al., 2019).

4.4.3 Principal Component Analysis

Although different authors have performed a univariate analysis of the biochemical components of cartilage, a multivariate analysis helps to analyse spectrum characteristics and information more effectively. Principal component analysis (PCA) is a type of multivariate analysis that allows a qualitative interpretation, transforming the information extracted from correlated spectral variables into non-correlated variables, termed principal components (PC). The final information is converted into an orthogonal PC graph, where each spectrum is represented by a point, thus minimizing the data (Araújo et al., 2020; Mainreck et al., 2012). For this purpose, PCA was conducted with the second derivative spectra between 900-3800 cm^{-1}. The spectral limits were not considered, to minimise noise amplification, due to derivatives in the PCA.

To analyse the native disc regionally, PCA was performed. As seen in Figure 21 a great dispersion between the same region of the disc is found, demonstrating the high biological variability that exists between the discs.

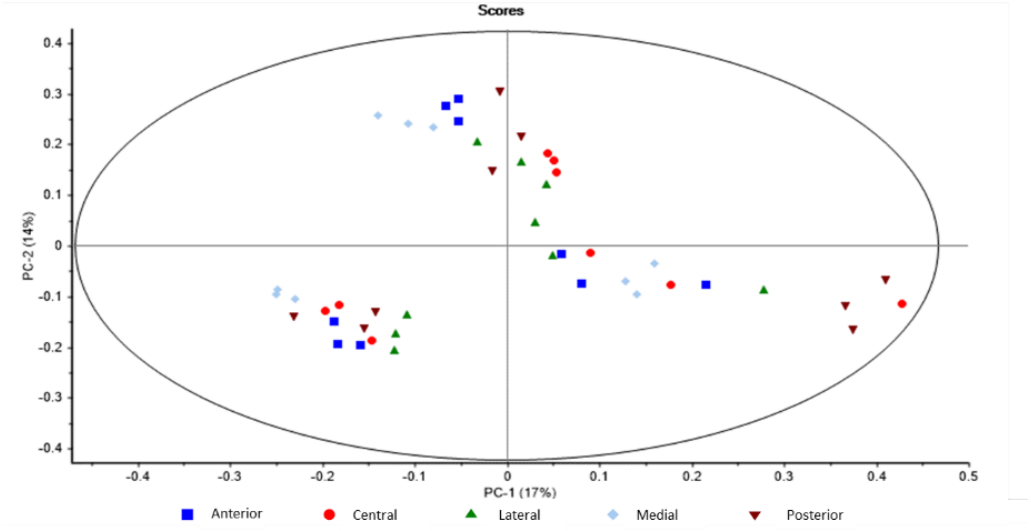

Figure 21 - Principal components analysis of the native disc in its five morphological regions

In Figure 22 it is possible to observe the spectral data of the decellularized and native TMJ disc, where all samples present a great variability due to the wide dispersion of the data. Ethanol and acetone decellularization have some overlap with the native disc, pointing to a whole molecular similarity between them, which is in concordance with the results so far, since this decellularization procedure presented a lower impact on collagen and GAGs content. SDS treated samples are localised in the first and second quadrant and no major differences are found within this sample, except for the freeze and thaw followed by 0.1% SDS that seem to be more separated from the remaining SDS samples and closer to the native disc. This sample in the quantitative analysis was the one that most closely resembled the native disc with a low significant impact on its biochemical components. Accutase presents a similar pattern to the native disc and although there were major alterations in the biochemical content, the analysis of the spectral ratios for evaluating spectral differences did not point to major alterations. Triton X-100 samples are localised in the third and fourth quadrant and no major differences are found within the samples, except for the freeze and thaw followed by 0.1 Triton X-100 samples that seem to be closer to the pattern of the TMJ disc. Interestingly, it can be observed that the SDS and Triton X-100 samples give rise to completely different molecular compositions as they are represented on opposite sides regions of the score-plot. Furthermore, it was observed that SDS treated samples, presented more similar molecular compositions between them in relation to samples treated with Triton X-100. This was in accordance with results from the previous sections, where: *i)* a sequence was found within the SDS samples, where the higher the concentration, the higher the impact of the ECM; and *ii)* with freezing and thawing, the impact was lower but also with a gradually increasing concentration. In the Triton X-100 treated samples, this pattern was more difficult to observe.

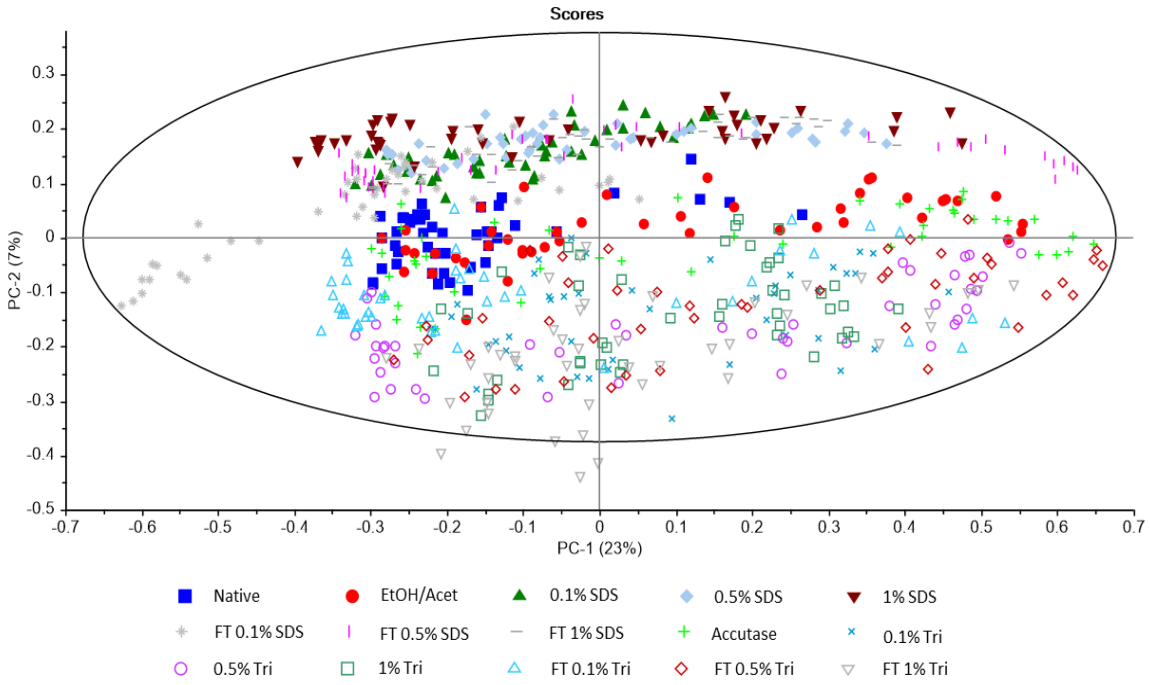

Figure 22 - Principal components analysis of the second derivative spectra of the decellularized and native discs. EtOH/Acet is ethanol/acetone, FT is freeze and thaw and Triton X-100 is Tri.

4.5 SEM Analysis

TMJ disc collagen fibres form bundles that exhibit a wavy shape (Detamore et al., 2003). The same pattern was observed by SEM on TMJ lamb discs. However, upon the first examination of the discs, a large number of bacteria was found (Figure 23-A), leading to the need to apply a sterilisation method that effectively eliminated these immunogenic components. To do so, three methods were tested on native discs: *(i)* 1% streptomycin and fungizone overnight; *(ii)* 1% streptomycin and fungizone combined with UV light overnight; and *(iii)* 2h of UV light while submerged in 70% ethanol, followed by UV light overnight. The latter was shown to be the most effective in removing the bacteria found in all samples (Figure 23-B).

Analysing cell content, for ethanol/acetone decellularization, it was not completely removed Figure 23-C). For SDS samples, cellular content removal varied between samples. Results obtained revealed that only with 1% SDS, all cellular content was completely removed (Figure 23-F). With the concentrations of 0.1% SDS, 0.5% SDS and freeze and thaw followed by 0.5% SDS some remanent debris was found (Figure 23-D, E, H). Interestingly, for freeze and thaw followed by 0.1% SDS and 1% SDS, cellular clusters were noted (Figure 23-G, I). For freeze and thaw followed by 0.1% SDS is important to highlight that some observations are not related to cells, but rather to collagen fibre ends. This same observation exists in the accutase (Figure 23-J) and Triton X-100 (Figure 23-K-P) samples, where all cellular content was removed.

Regarding collagen ultrastructure, for all decellularization procedures, no major changes were found. This is in accordance with the previous results, where no collagen degradation was found upon calculation of the ratios 1338/amide II cm^{-1} and 1240/1454 cm^{-1}. Despite this, as calculated with the second derivative 1338 cm^{-1} band, collagen content increases for almost all protocols. However, it does not lead to changes in their integrity. This was also found by Yusof et al. (2019) for decellularized bovine meniscus. Contradictorily, for rabbit tendon-to-bone insertion decellularization, collagen content decreased, but its integrity remained (Guo et al., 2015).

(A) Native without sterilization

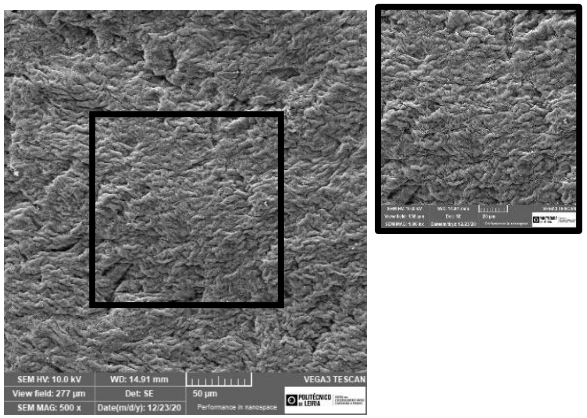

(B) Native with sterilization

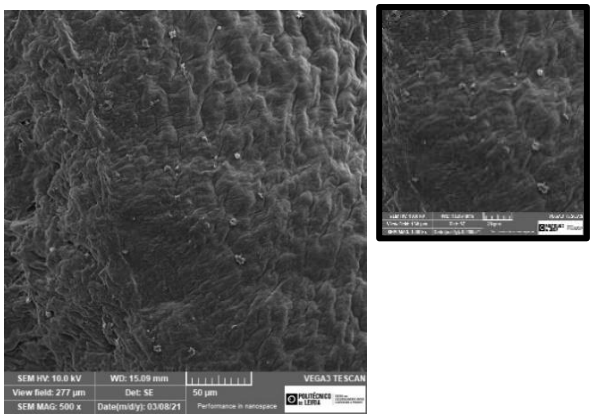

(C) EtOH/Acet

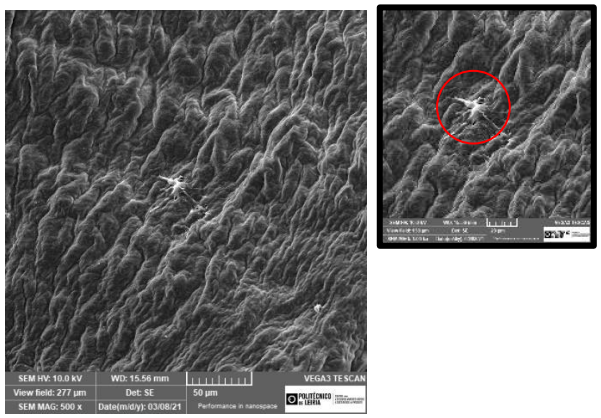

(D) 0.1% SDS

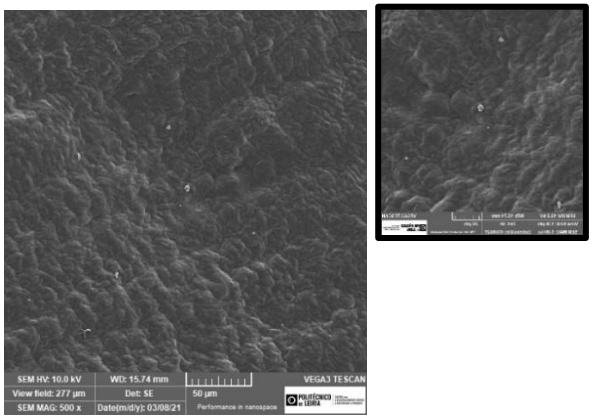

(E) 0.5% SDS

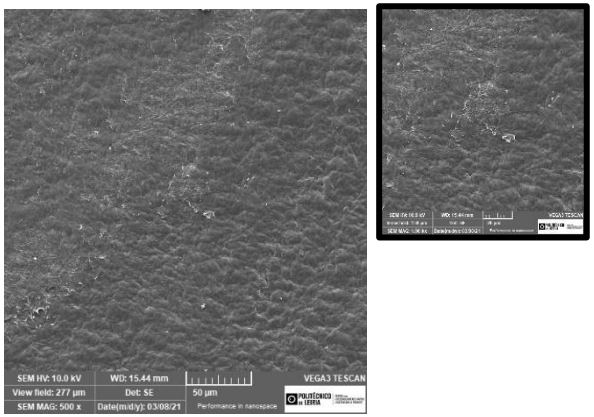

(F) 1% SDS

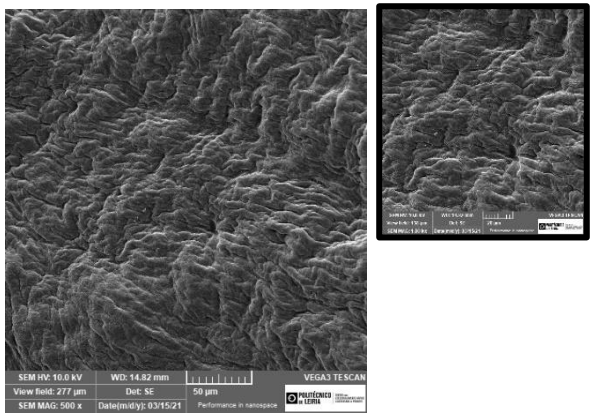

(G) FT 0.1% SDS

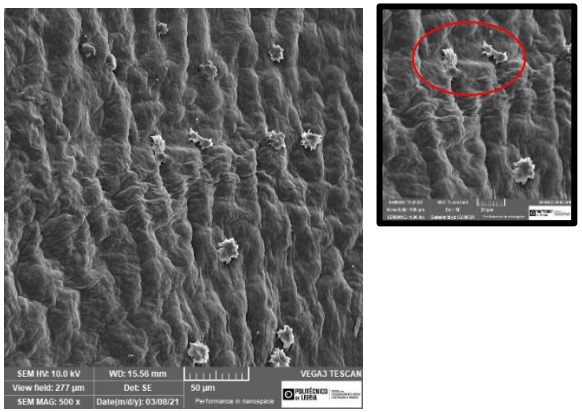

(H) FT 0.5% SDS

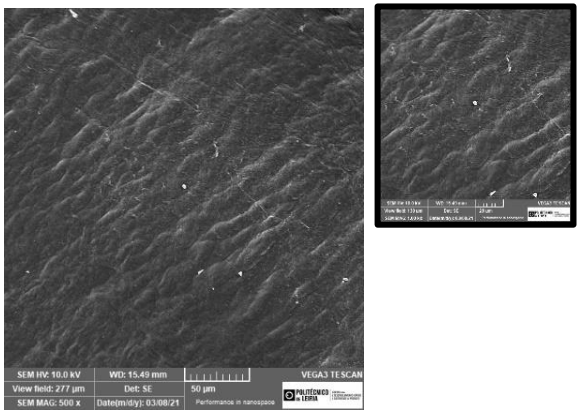

(I) FT 1% SDS

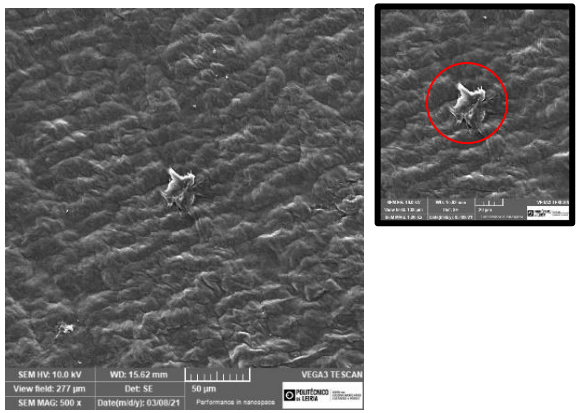

(J) Accutase

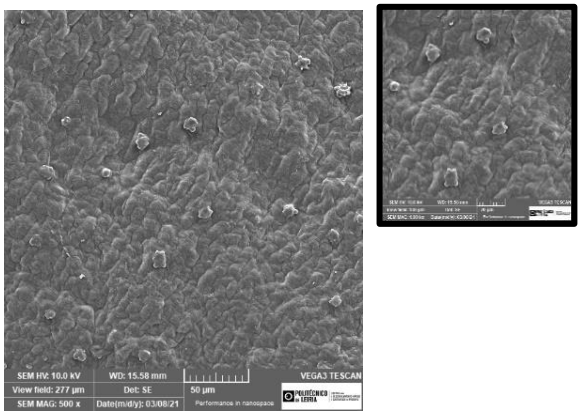

(K) 0.1% Tri

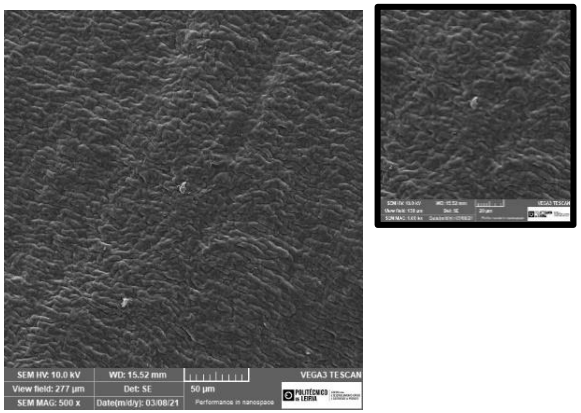

(L) 0.5% Tri

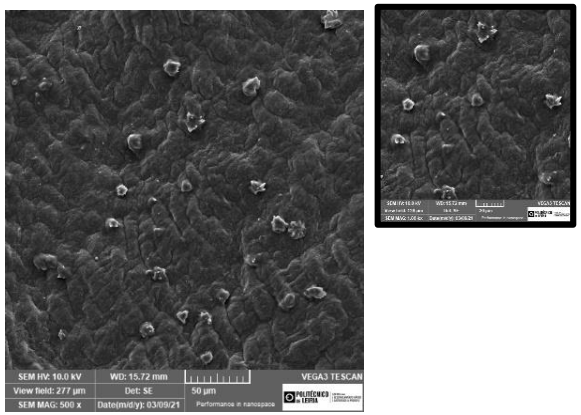

(M) 1% Tri

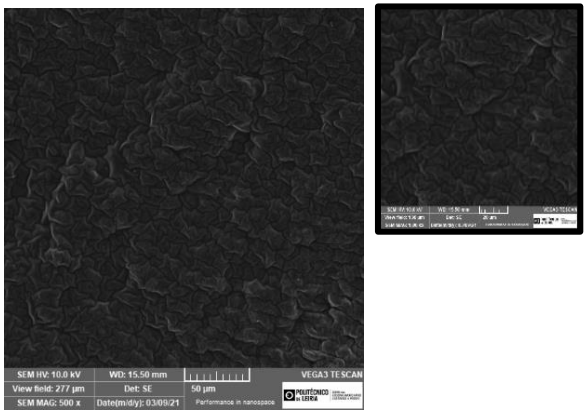

(N) FT 0.1% Tri

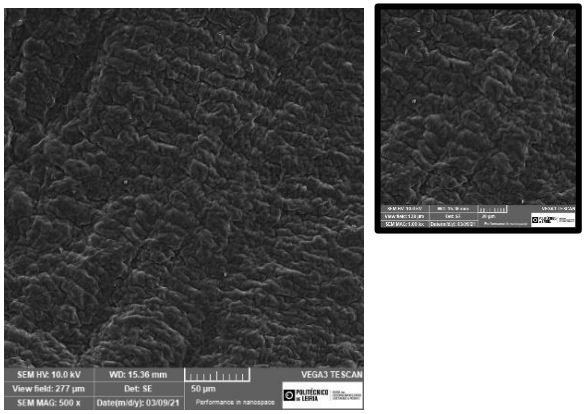

(O) FT 0.5% Tri

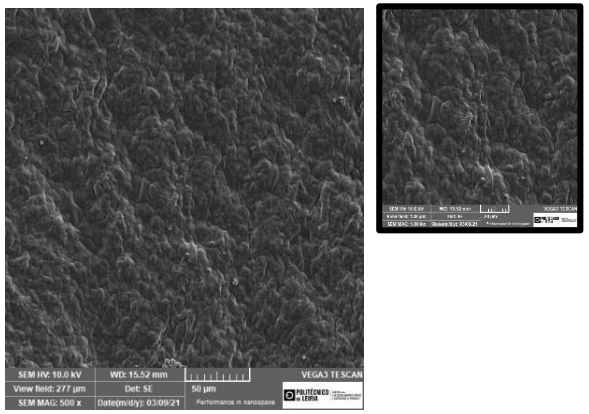

(P) FT 1% Tri

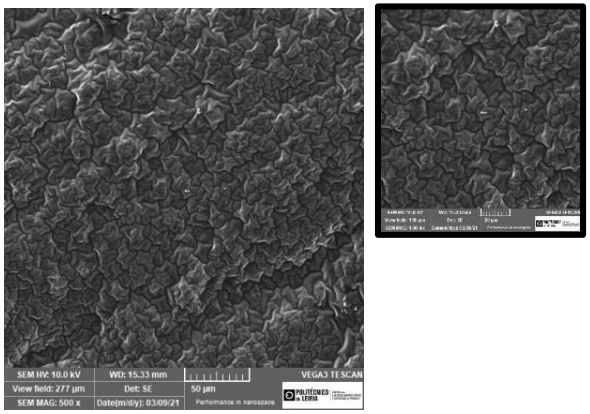

Figure 23 - Scanning electron microscopy analysis of the native without sterilization (A) and with sterilization (B) and decellularized discs: ethanol/acetone (C), 0.1% SDS (D), 0.5% SDS (E) 1% SDS (F), freeze and thaw followed by 0.1% SDS (G), 0.5% SDS (H) 1% SDS (I), accutase (J), 0.1% Triton X-100 (K), 0.5% Triton X-100 (L) 1% Triton X-100 (M), freeze and thaw followed by 0.1% Triton X-100 (N), 0.5% Triton X-100 (O) and 1% Triton X-100 (P). EtOH/Acet is ethanol/acetone, FT is freeze and thaw and Triton X-100 is Tri. Scale bar is 50 µm and 20 µm.

4.6 Micro-CT Analysis

As referred, TMJ disc is mainly composed of collagen and GAGs and histological analysis of the porcine TMJ disc stained with Masson's trichrome reports that the collagen fibres, which stains blue, are distributed along the periphery of the disc (Figure 24) (Tappert et al., 2020).

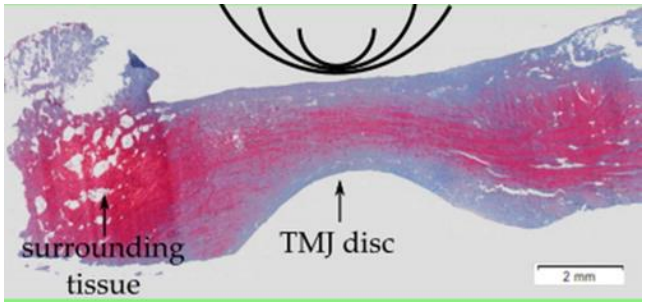

Figure 24 – Porcine TMJ disc histological staining with Masson's trichrome, where collagen is highlighted in blue. Retrieved from Tappert et al. (2020).

For visualisation of the internal structure of the native TMJ disc and the discs subjected to the different decellularization methods, Micro-CT analysis was performed to portions of the disc. Based on Figure 24 and the images obtained, a relation was established and it was possible to extract 3 parameters: percentage of *(i)* collagen, *(ii)* extracellular matrix (without collagen) and *(iii)* porosity of the discs (Table 14).

As expected, the native disc presents a higher collagen content (60.3%) than the remaining ECM components and a lower porosity (6.84%). When subjected to ethanol/acetone treatment this remained, but a higher porosity was found (41.4%). 0.1% SDS and freeze and thaw followed by 0.1% SDS have similar results (34.0% and 31.8%, respectively), where the collagen content was lower than the other components, and the porosity is also higher than the native disc. 1% SDS also presents lower collagen fibres (9.46%) and higher porosity (63.9%), whereas when treated with freeze and thaw, similar results to native disc were obtained. 0.5% SDS presents an impressive high collagen content (84.8%) and for the remaining ECM components, a lower value is found (8.85%). When freeze and thaw are applied, once again, similar results to the native disc were found.

Accutase presented high collagen content (84.6%) and low porosity (1.94%). For Triton X-100 samples, 0.1% with and without freeze and thaw similar results were obtained, where collagen fibres are low (12.5% and 28.6%, respectively) and porosity is higher (55.3% and 37.6%, respectively). 0.5% Triton X-100 presents high porosity (81.0%) and low collagen content (3.99%). 0.5% Triton X-100 and 1% Triton X-100 (with and without freeze and thaw) had similar results to the native disc.

The overall results highlight that freezing and thawing allow the disc structure to be maintained, as discussed in the previous sections where, for the quantification of collagen and GAGs, with this technique better results were shown. The differences found between the disc's ECM may be due to the removal of cellular content leading to possible pore opening or possible components degradation. Analysing these differences, it should be considered that only 1 portion of the disc was analysed, not considering its morphological regions and that there is great biological variability. Despite this, the internal structure was similar between the discs, making it possible to extract these different parameters.

Table 14 - Percentage of collagen, remaining ECM (without collagen) and porosity of the native and decellularized discs obtained by Micro-CT. EtOH/Acet is ethanol/acetone, FT is freeze and thaw and Triton X-100 is Tri.

Treatment	ECM (without collagen) (%)	Collagen (%)	Porosity (%)
Native	32.9	60.3	6.84
EtOH/Acet	17.8	40.7	41.4
0.1% SDS	45.7	20.2	34.0
0.5% SDS	8.85	84.8	6.38
1% SDS	26.6	9.46	63.9
FT 0.1% SDS	43.3	24.9	31.8
FT 0.5% SDS	31.9	62.0	6.05
FT 1% SDS	36.9	52.2	10.9
Accutase	13.4	84.6	1.94
0.1% Tri	32.2	12.5	55.3
0.5% Tri	14.9	3.99	81.0
1% Tri	24.6	66.5	8.94
FT 0.1% Tri	33.8	28.6	37.6
FT 0.5% Tri	34.8	61.2	4.06
FT 1% Tri	38.1	50.7	11.2

4.7 Compression Tests

The mechanical performance of the TMJ disc is defined by the cooperation of the different ECM components and it is characterised as a viscoelastic structure, as it helps to absorb stress and distribute loads on the disc, cartilage and bone components (David et al., 2016; Fazaeli et al., 2019). The different ECM components have the following functions: *(i)* elastin helps to restore the disc original shape, *(ii)* GAGs provide the compressive properties and *(iii)* collagen provides the tensile properties, and also helps in its compressive behaviour (Detamore et al., 2003; Fazaeli et al., 2016; Gutman et al., 2018).

Native lamb discs presented a compressive modulus of 2.36 ± 0.072 MPa. When subjected to the ethanol/acetone decellularization treatment the compressive modulus there was an increase of ~40% (3.31 ± 0.660 MPa) ($p<0.01$), whereas for accutase no statistical differences were found (2.72 ± 0.087 MPa) (Figure 25-A, D). Regarding SDS samples (Figure 25-B, D), 0.1% SDS was statistically significant at 5% significance, where there was an increase of more than 20% (2.92 ± 0.303 MPa), whereas when treated with freeze and thaw, the modulus was slightly lower, becoming closer to the native disc (2.73 ± 0.098 MPa). 0.5% SDS modulus was ~8% lower than the native (2.18 ± 0.328 MPa) and when treated with freeze and thaw presented a decrease to 1.88 ± 0.062 MPa, although both were not statistically different. On the contrary, 1% SDS presented a modulus of 2.68 ± 0.556 MPa and when treated with freeze and thaw the value increased at 1% significance to 3.19 ± 0.259 MPa.

For the Triton X-100 samples (Figure 25-C, D), the concentration 0.1% had a compressive modulus similar to the native disc (2.35 ± 0.108 MPa), and with increasing concentration, this module gradually increases, where 0.5% had a modulus of 2.51 ± 0.046 MPa and 1% had a modulus of 2.67 ± 0.261 MPa. With the application of freezing and thawing, there was also a successive increase of the modulus with increasing concentration, where 0.1% had a modulus of 2.72 ± 0.278 MPa, 0.5% a modulus of 2.84 ± 0.377 MPa and 1% a modulus of 3.06 ± 0.478 MPa, the latter being statistically different from the native ($p<0.05$).

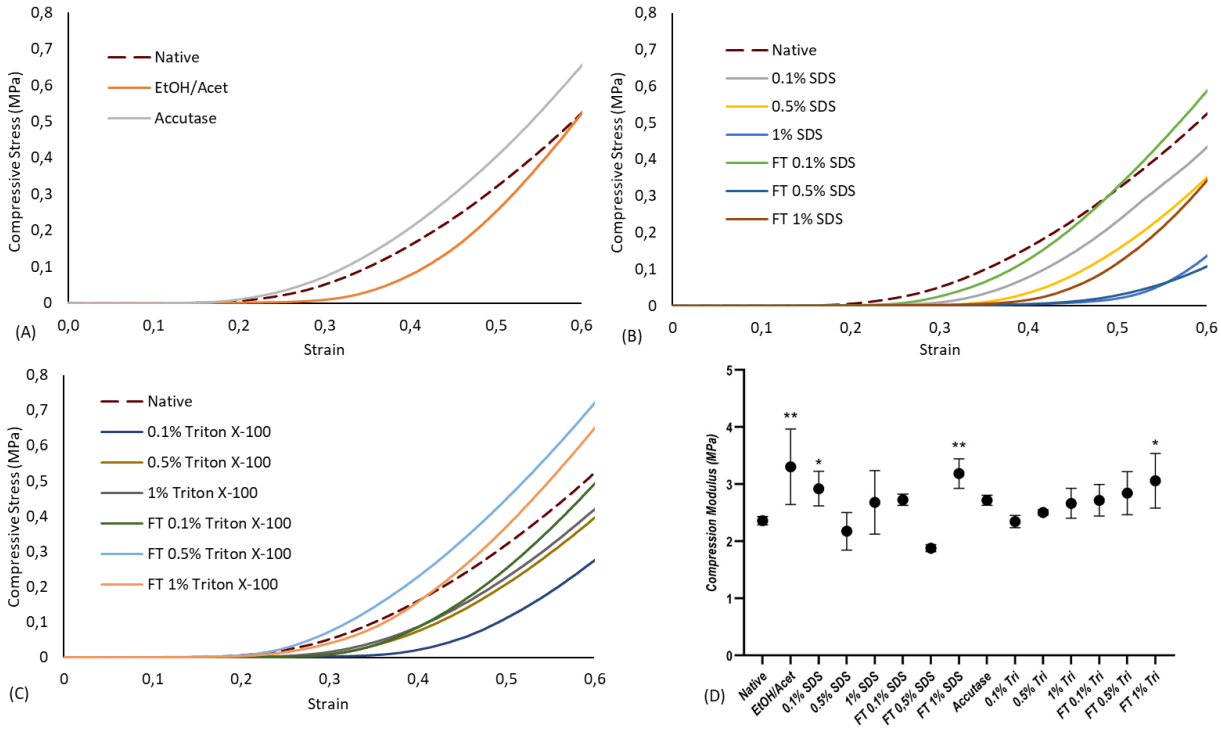

Figure 25 – Typical stress-strain graphs of the native discs (N=3) (A, B, C): ethanol/acetone and accutase (A), SDS samples (B), Triton X-100 samples (C) and correspondent compressive modulus (D). Statistically significant differences are represented by * $p<0.05$ and ** $p<0.01$.

The increase in the ethanol/acetone was excepted as the disc became stiffer. According to Lumpkins et al. (2008), a decellularization solution of 25%acetone/75%ethanol for 24h in porcine disc led to an increase in the instantaneous and steady-state modulus and peak stress, whereas, for the same solution used in the present work, but decellularization for 24h the tensile young's modulus was unchanged (Matuska et al., 2018). The concentration of 1% Triton X-100 for 24h in porcine discs led to a decrease in the instantaneous and steady-state modulus and peak stress due to a softer disc (Lumpkins et al., 2008), whereas in the present work, compression modulus increased 13%. For SDS samples in porcine discs, the concentration of 1% SDS for 24h led to no changes in the instantaneous and steady-state modulus and peak stress (Lumpkins et al., 2008), but for compression modulus there was an increase of more than 100% (from 1.65 ± 0.25 to 3.49 ± 1.01 MPa), corroborating with the present results (Juran et al., 2015).

No relationship was found between the compression modulus and the collagen and GAGs quantitative results. For ethanol/acetone, GAGs were mostly maintained, and collagen content increased. Since the compression behaviour increased due to a stiffer disc, it is possible that some interaction with the collagen fibres occurred. In contrast, for accutase, the GAGs and collagen content was altered, but its mechanical behaviour did not change. For the SDS samples, for both biochemical components, there was always a gradual increase with increasing concentration, and with the addition of the freeze-thaw treatment, the increase was

not pronounced. These samples when tested mechanically led to an increase in compressive modulus, except for the samples with 0.5% SDS (with and without freeze and thaw), where there was a decrease. Interestingly, freeze-thaw followed by 0.1% SDS was little affected biochemically, and biomechanically had a closer modulus to the native ones. In general, the Triton X-100 samples were little affected biochemically, and a relationship between the different concentrations was difficult to find. For GAGs content, the freeze and thaw followed by 1% Triton X-100 were little affected. On the other hand, for collagen content, the closest to native collagen content was the freeze and thaw followed by 0.1% Triton X-100, where there was no relationship with the mechanical behaviour where there was always a continuous increase.

As mentioned, although it was expected that the change in biochemical content would lead to a relationship with the mechanical tests, this did not occur. Furthermore, the literature states this. Reports found the loss of sulfated GAGs, but maintenance of the mechanical properties after decellularization of porcine (Stapleton et al., 2008) and bovine (Yusof et al., 2019) meniscus tissue.

Chapter 5: Conclusion and Future Work

The use of xenogeneic materials instead of synthetic ones could be an alternative for a TMJ engineered dis. However, the assessment of the decellularization procedure is crucial to understand its success/unsuccess and to effectively transpose this technique into clinical practice, as a suitable replacement for the TMJ disc needs to be accomplished.

In the present study, a preliminary study was developed by testing and characterising different decellularization agents/methods on TMJ lamb discs. A combination of 1:1 ethanol/acetone solution did not exhibit good results as a stiffer, dehydrated material with a higher anteroposterior dimension was obtained, and although no major changes were found in its biochemical content, the mechanical modulus increased. Accutase led to changes in the collagen and GAGs content. Nevertheless, cellular content was removed and mechanical behaviour and morphology remained unchanged. For SDS samples two overall outcomes can be extracted: the implementation of one freeze and thaw cycle and a lower concentration (0.1%) leads to better biochemical, biomechanical and morphological results. However, cellular content was found. For higher concentrations, its biochemical content is highly affected. For Triton X-100 samples, all cellular components were removed, and disc morphology was unaltered, except for 1% Triton X-100 whose anteroposterior dimension increased. The implementation of one freeze and thaw cycle also led to better results and when followed a higher concentration (1%) led to higher compression modulus, whereas the lower (0.1% and 0.5%) maintained its properties. Of the lower concentrations, 0.1% was the one which led to a few disrupt of the collagen content.

The work developed present promising results towards the optimal TMJ bioengineered substitute. Considering these results, freezing and thawing followed by 0.1% Triton X-100 seems to be the protocol to be used to effectively decellularize the lamb TMJ disc. However, more iterations should be tested and, thus, I propose as future work, to implement more cycles of freezing and thawing, as well as, to combine the accutase to this protocol, creating a further optimized protocol that combines a physical, chemical and enzymatic decellularization methods. Although freezing and thawing followed by 0.1% SDS did not effectively remove all cells, it seems logical that the same methodology is applied, comparing these two reagents.

In addition to assessing biochemical content regionally, the removal of cellular content can also be performed by this method. This may be relevant, as taking into consideration the organisation of the collagen it is likely that in certain regions cells are more trapped in the matrix, leading to different degrees of cellular content removal. Regarding the biochemical components evaluated by FTIR and to better understand the results, it is suggested to make collagen degradations with collagenase and HA degradations with hyaluronidase, separately,

to understand their effect on the fibrocartilaginous disc. Furthermore, correlation studies between the band values analysed and real quantification studies would be of interest to confirm the efficacy of the bands chosen.

Chapter 6: References

Acri, T. M., Shin, K., Seol, D., Laird, N. Z., Song, I., Geary, S. M., Chakka, J. L., Martin, J. A., & Salem, A. K. (2019). Tissue Engineering for the Temporomandibular Joint. *Advanced Healthcare Materials*, *8*(2), 1801236. https://doi.org/10.1002/adhm.201801236

Al-Moraissi, E. A. (2015). Open versus arthroscopic surgery for the management of internal derangement of the temporomandibular joint: a meta-analysis of the literature. *International Journal of Oral and Maxillofacial Surgery*, *44*(6), 763–770. https://doi.org/10.1016/j.ijom.2015.01.024

Allen, K.D., & Athanasiou, K. A. (2008). Scaffold and Growth Factor Selection in Temporomandibular Joint Disc Engineering. *Journal of Dental Research*, *87*(2), 180–185. https://doi.org/10.1177/154405910808700205

Allen, Kyle D., & Athanasiou, K. A. (2005). A Surface–Regional and Freeze–Thaw Characterization of the Porcine Temporomandibular Joint Disc. *Annals of Biomedical Engineering*, *33*(7), 951–962. https://doi.org/10.1007/s10439-005-3872-6

Allen, Kyle D., & Athanasiou, K. A. (2006). Tissue Engineering of the TMJ Disc: A Review. *Tissue Engineering*, *12*(5), 1183–1196. https://doi.org/10.1089/ten.2006.12.1183

Almarza, A.J., Bean, A. C., Baggett, L. S., & Athanasiou, K. A. (2006). Biochemical analysis of the porcine temporomandibular joint disc. *British Journal of Oral and Maxillofacial Surgery*, *44*(2), 124–128. https://doi.org/10.1016/j.bjoms.2005.05.002

Almarza, Alejandro J., & Athanasiou, K. A. (2004). Seeding Techniques and Scaffolding Choice for Tissue Engineering of the Temporomandibular Joint Disk. *Tissue Engineering*, *10*(11–12), 1787–1795. https://doi.org/10.1089/ten.2004.10.1787

Almarza, Alejandro J., Brown, B. N., Arzi, B., Ângelo, D. F., Chung, W., Badylak, S. F., & Detamore, M. (2018). Preclinical Animal Models for Temporomandibular Joint Tissue Engineering. *Tissue Engineering Part B: Reviews*, *24*(3), 171–178. https://doi.org/10.1089/ten.teb.2017.0341

Alpaslan, G. H., & Alpaslan, C. (2001). Efficacy of temporomandibular joint arthrocentesis with and without injection of sodium hyaluronate in treatment of internal derangements. *Journal of Oral and Maxillofacial Surgery*, *59*(6), 613–618. https://doi.org/10.1053/joms.2001.23368

Ângelo, D. F., Gil, F. M., González-García, R., Mónico, L., Sousa, R., Neto, L., Caldeira, I., Moura, C., Francisco, L. C., Sanz, D., Alves, N., Salvado, F., & Morouço, P. (2018). Effects of bilateral discectomy and bilateral discopexy on black Merino sheep rumination

kinematics: TEMPOJIMS – phase 1 – pilot blinded, randomized preclinical study. *Journal of Cranio-Maxillofacial Surgery*, *46*(2), 346–355. https://doi.org/10.1016/j.jcms.2017.11.022

Ângelo, D. F., Morouço, P., Monje Gil, F., Mónico, L., González-Gárcia, R., Sousa, R., Neto, L., Caldeira, I., Smith, M., Smith, S., Sanz, D., Abade dos Santos, F., Pinho, M., Carrapiço, B., Cavaco, S., Moura, C., Alves, N., Salvado, F., & Little, C. (2018). Preclinical randomized controlled trial of bilateral discectomy versus bilateral discopexy in Black Merino sheep temporomandibular joint: TEMPOJIMS – Phase 1- histologic, imaging and body weight results. *Journal of Cranio-Maxillofacial Surgery*, *46*(4), 688–696. https://doi.org/10.1016/j.jcms.2018.01.006

Araújo, R., Ramalhete, L., Da Paz, H., Ribeiro, E., & Calado, C. R. C. (2020). A Simple, Label-Free, and High-Throughput Method to Evaluate the Epigallocatechin-3-Gallate Impact in Plasma Molecular Profile. *High-Throughput*, *9*(2), 9. https://doi.org/10.3390/ht9020009

Armiento, A. R., Stoddart, M. J., Alini, M., & Eglin, D. (2018). Biomaterials for articular cartilage tissue engineering: Learning from biology. *Acta Biomaterialia*, *65*, 1–20. https://doi.org/10.1016/j.actbio.2017.11.021

Armijo-Olivo, S. L., & Gadotti, I. C. (2016). Temporomandibular Disorders. In *Pathology and intervention in musculoskeletal rehabilitation* (Vol. 3, pp. 119–156). Elsevier Health Sciences.

Aryaei, A., Vapniarsky, N., Hu, J. C., & Athanasiou, K. A. (2016). Recent Tissue Engineering Advances for the Treatment of Temporomandibular Joint Disorders. *Current Osteoporosis Reports*, *14*(6), 269–279. https://doi.org/10.1007/s11914-016-0327-y

Asadi, H., & Budenz, A. (2018). Anatomy of the Masticatory System. In H. A. Gremillion & G. D. Klasser (Eds.), *Temporomandibular Disorders* (pp. 17–33). Springer International Publishing. https://doi.org/10.1007/978-3-319-57247-5_2

Bae, W. C., Biswas, R., Statum, S., Sah, R. L., & Chung, C. B. (2014). Sensitivity of quantitative UTE MRI to the biomechanical property of the temporomandibular joint disc. *Skeletal Radiology*, *43*(9), 1217–1223. https://doi.org/10.1007/s00256-014-1901-y

Bae, Y., & Park, Y. (2013). The effect of relaxation exercises for the masticator muscles on temporomandibular joint dysfunction (TMD). *Journal of Physical Therapy Science*, *25*(5), 583–586.

Baker, M. J., Trevisan, J., Bassan, P., Bhargava, R., Butler, H. J., Dorling, K. M., Fielden, P. R., Fogarty, S. W., Fullwood, N. J., Heys, K. A., Hughes, C., Lasch, P., Martin-Hirsch, P. L., Obinaju, B., Sockalingum, G. D., Sulé-Suso, J., Strong, R. J., Walsh, M. J., Wood, B.

R., … Martin, F. L. (2014). Using Fourier transform IR spectroscopy to analyze biological materials. *Nature Protocols*, *9*(8), 1771–1791. https://doi.org/10.1038/nprot.2014.110

Balatgek, T. L., Demerjian, G. G., Sims, A. B., & Patel, M. (2018). CBCT and MRI of Temporomandibular Joint Disorders and Related Structures. In G. G. Demerjian, A. Barkhordarian, & F. Chiappelli (Eds.), *Temporomandibular Joint and Airway Disorders: A Translational Perspective* (pp. 201–218). Springer.

Bartley, E. J., Schmidt, J. E., Carlson, C. R., & Fillingim, R. B. (2018). Psychosocial Considerations in TMD. In Henry A Gremillion & G. D. Klasser (Eds.), *Temporomandibular Disorders* (pp. 193–217). Springer.

Basterzi, Y., Sari, A., Demirkan, F., Unal, S., & Arslan, E. (2009). Intraarticular Hyaluronic Acid Injection for the Treatment of Reducing and Nonreducing Disc Displacement of the Temporomandibular Joint. *Annals of Plastic Surgery*, *62*(3), 265–267. https://doi.org/10.1097/SAP.0b013e31817dadb1

Belbachir, K., Noreen, R., Gouspillou, G., & Petibois, C. (2009). Collagen types analysis and differentiation by FTIR spectroscopy. *Analytical and Bioanalytical Chemistry*, *395*(3), 829–837. https://doi.org/10.1007/s00216-009-3019-y

Benders, K. E. M., Weeren, P. R. van, Badylak, S. F., Saris, D. B. F., Dhert, W. J. A., & Malda, J. (2013). Extracellular matrix scaffolds for cartilage and bone regeneration. *Trends in Biotechnology*, *31*(3), 169–176. https://doi.org/10.1016/j.tibtech.2012.12.004

Bi, X., Li, G., Doty, S. B., & Camacho, N. P. (2005). A novel method for determination of collagen orientation in cartilage by Fourier transform infrared imaging spectroscopy (FT-IRIS). *Osteoarthritis and Cartilage*, *13*(12), 1050–1058. https://doi.org/10.1016/j.joca.2005.07.008

Bi, Xiaohong, Yang, X., Bostrom, M. P. G., & Camacho, N. P. (2006). Fourier transform infrared imaging spectroscopy investigations in the pathogenesis and repair of cartilage. *Biochimica et Biophysica Acta (BBA) - Biomembranes*, *1758*(7), 934–941. https://doi.org/10.1016/j.bbamem.2006.05.014

Bitiniene, D., Zamaliauskiene, R., Kubilius, R., Leketas, M., Gailius, T., & Smirnovaite, K. (2018). Quality of life in patients with temporomandibular disorders. A systematic review. *Stomatologija*, *20*(1), 3–9.

Bonotto, D., Machado, E., Cunali, R. S., & Cunali, P. A. (2014). Viscosupplementation as a treatment of internal derangements of the temporomandibular joint: retrospective study. *Revista Dor*, *15*(1), 2–5. https://doi.org/10.5935/1806-0013.20140001

Boskey, A., & Camacho, N. (2007). FT-IR imaging of native and tissue-engineered bone and

cartilage. *Biomaterials*, *28*(15), 2465–2478. https://doi.org/10.1016/j.biomaterials.2006.11.043

Bousnaki, M., Bakopoulou, A., Papadogianni, D., Barkoula, N.-M., Alpantaki, K., Kritis, A., Chatzinikolaidou, M., & Koidis, P. (2018). Fibro/chondrogenic differentiation of dental stem cells into chitosan/alginate scaffolds towards temporomandibular joint disc regeneration. *Journal of Materials Science: Materials in Medicine*, *29*(7), 97. https://doi.org/10.1007/s10856-018-6109-6

Brown, B. N., Chung, W. L., Almarza, A. J., Pavlick, M. D., Reppas, S. N., Ochs, M. W., Russell, A. J., & Badylak, S. F. (2012). Inductive, Scaffold-Based, Regenerative Medicine Approach to Reconstruction of the Temporomandibular Joint Disk. *Journal of Oral and Maxillofacial Surgery*, *70*(11), 2656–2668. https://doi.org/10.1016/j.joms.2011.12.030

Brown, B. N., Chung, W. L., Pavlick, M., Reppas, S., Ochs, M. W., Russell, A. J., & Badylak, S. F. (2011). Extracellular Matrix as an Inductive Template for Temporomandibular Joint Meniscus Reconstruction: A Pilot Study. *Journal of Oral and Maxillofacial Surgery*, *69*(12), e488–e505. https://doi.org/10.1016/j.joms.2011.02.130

Burk, J., Erbe, I., Berner, D., Kacza, J., Kasper, C., Pfeiffer, B., Winter, K., & Brehm, W. (2014). Freeze-Thaw Cycles Enhance Decellularization of Large Tendons. *Tissue Engineering Part C: Methods*, *20*(4), 276–284. https://doi.org/10.1089/ten.tec.2012.0760

Calvo-Gallego, J. L., Commisso, M. S., Domínguez, J., Tanaka, E., & Martínez-Reina, J. (2017). Effect of freezing storage time on the elastic and viscous properties of the porcine TMJ disc. *Journal of the Mechanical Behavior of Biomedical Materials*, *71*, 314–319. https://doi.org/10.1016/j.jmbbm.2017.03.035

Camacho, N. P., West, P., Torzilli, P. A., & Mendelsohn, R. (2001). FTIR microscopic imaging of collagen and proteoglycan in bovine cartilage. *Biopolymers*, *62*(1), 1–8. https://doi.org/10.1002/1097-0282(2001)62:1<1::AID-BIP10>3.0.CO;2-O

Cao, Z., Dou, C., & Dong, S. (2014). Scaffolding Biomaterials for Cartilage Regeneration. *Journal of Nanomaterials*, *2014*, 1–8. https://doi.org/10.1155/2014/489128

Chan, B. P., & Leong, K. W. (2008). Scaffolding in tissue engineering: general approaches and tissue-specific considerations. *European Spine Journal*, *17*(S4), 467–479. https://doi.org/10.1007/s00586-008-0745-3

Chandrashekhar, V. K. (2015). Arthrocentesis A Minimally Invasive Method for T MJ Disc Disorders - A Prospective Study. *JOURNAL OF CLINICAL AND DIAGNOSTIC RESEARCH*, *9*(10), 59–62. https://doi.org/10.7860/JCDR/2015/15045.6665

Chen, F.-M., & Liu, X. (2016). Advancing biomaterials of human origin for tissue engineering. *Progress in Polymer Science*, *53*, 86–168. https://doi.org/10.1016/j.progpolymsci.2015.02.004

Chisnoiu, A. M., Picos, A. M., Popa, S., Chisnoiu, P. D., Lascu, L., Picos, A., & Chisnoiu, R. (2015). Factors involved in the etiology of temporomandibular disorders-a literature review. *Clujul Medical*, *88*(4), 473–478.

Cobo, J., Cabrera-Freitag, M., Cobo, T., D. Muriel, J., M. Junquera, L., Cobo, J., & A. Vega, J. (2019). Nonsurgical Strategies for the Treatment of Temporomandibular Joint Disorders. In D. D. Nikolopoulos, G. K. Safos, & K. Dimitrios (Eds.), *Cartilage Tissue Engineering and Regeneration Techniques* (pp. 1–17). IntechOpen. https://doi.org/10.5772/intechopen.85186

Connor, R. C., Fawthrop, F., Salha, R., & Sidebottom, A. J. (2017). Management of the temporomandibular joint in inflammatory arthritis: Involvement of surgical procedures. *European Journal of Rheumatology*, *4*(2), 151–156. https://doi.org/10.5152/eurjrheum.2016.035

Craane, B., Dijkstra, P. U., Stappaerts, K., & De Laat, A. (2012). Randomized Controlled Trial on Physical Therapy for TMJ Closed Lock. *Journal of Dental Research*, *91*(4), 364–369. https://doi.org/10.1177/0022034512438275

Crapo, P. M., Gilbert, T. W., & Badylak, S. F. (2011). An overview of tissue and whole organ decellularization processes. *Biomaterials*, *32*(12), 3233–3243. https://doi.org/10.1016/j.biomaterials.2011.01.057

Dashnyam, K., Lee, J.-H., Mandakhbayar, N., Jin, G.-Z., Lee, H.-H., & Kim, H.-W. (2018). Intra-articular biomaterials-assisted delivery to treat temporomandibular joint disorders. *Journal of Tissue Engineering*, *9*, 204173141877651. https://doi.org/10.1177/2041731418776514

David, C. M., & Elavarasi, P. (2016). Functional anatomy and biomechanics of temporomandibular joint and the far-reaching effects of its disorders. *Journal of Advanced Clinical & Research Insights*, *3*(3), 101–106. https://doi.org/10.15713/ins.jcri.115

de Leeuw, R., & Klasser, G. D. (2018). Differential Diagnosis and Management of TMDs. In *Orofacial pain: guidelines for assessment, diagnosis, and management* (6th ed., pp. 143–207). Quintessence Publishing.

de Pontes, M. L. C., Melo, S. L. S., Bento, P. M., Campos, P. S. F., & de Melo, D. P. N. V.-5. (2019). Correlation between temporomandibular joint morphometric measurements and sex, disc position, and condylar position. *Oral Surgery, Oral Medicine, Oral Pathology and Oral Radiology*, *128*, 538–542.

Demerjian, G. G., Barkhordarian, A., & Chiappelli, F. (2018). Neuroanatomy of the Trigeminal Nerve and Proximal Innervation of the TMJ. In G. G. Demerjian, A. Barkhordarian, & F. Chiappelli (Eds.), *Temporomandibular Joint and Airway Disorders* (pp. 3–15). Springer International Publishing. https://doi.org/10.1007/978-3-319-76367-5_1

Deshpande, R. G., & Mhatre, S. (2010). TMJ disorders and occlusal splint therapy–a review. *International Journal of Dental Clinics*, *2*(2), 22–29.

Detamore, M. S., & Athanasiou, K. A. (2003). Structure and function of the temporomandibular joint disc: Implications for tissue engineering. *Journal of Oral and Maxillofacial Surgery*, *61*(4), 494–506. https://doi.org/10.1053/joms.2003.50096

Detamore, M. S., Orfanos, J. G., Almarza, A. J., French, M. M., Wong, M. E., & Athanasiou, K. A. (2005). Quantitative analysis and comparative regional investigation of the extracellular matrix of the porcine temporomandibular joint disc. *Matrix Biology*, *24*(1), 45–57. https://doi.org/10.1016/j.matbio.2004.11.006

Dimitroulis, G. (2004). The interpositional dermis-fat graft in the management of temporomandibular joint ankylosis. *International Journal of Oral and Maxillofacial Surgery*, *33*(8), 755–760. https://doi.org/10.1016/j.ijom.2004.01.012

Dimitroulis, G. (2011a). A critical review of interpositional grafts following temporomandibular joint discectomy with an overview of the dermis-fat graft. *International Journal of Oral and Maxillofacial Surgery*, *40*(6), 561–568. https://doi.org/10.1016/j.ijom.2010.11.020

Dimitroulis, G. (2011b). Temporomandibular joint surgery: what does it mean to the dental practitioner? *Australian Dental Journal*, *56*(3), 257–264. https://doi.org/10.1111/j.1834-7819.2011.01351.x

Dimitroulis, G., & Slavin, J. (2006). Histological Evaluation of Full Thickness Skin as an Interpositional Graft in the Rabbit Craniomandibular Joint. *Journal of Oral and Maxillofacial Surgery*, *64*(7), 1075–1080. https://doi.org/10.1016/j.joms.2006.03.011

Dolwick, M. F. (2001). Disc preservation surgery for the treatment of internal derangements of the temporomandibular joint. *Journal of Oral and Maxillofacial Surgery*, *59*(9), 1047–1050. https://doi.org/10.1053/joms.2001.26681

Dolwick, M. F., & Freburg-Hoffmeister, D. (2019). Disturbances of the Temporomandibular Joint Apparatus. In E. M. Ferneini & M. T. Goupil (Eds.), *Evidence-Based Oral Surgery* (pp. 399–421). Springer International Publishing. https://doi.org/10.1007/978-3-319-91361-2_19

Donahue, R. P., Gonzalez-Leon, E. A., Hu, J. C., & Athanasiou, K. A. (2019). Considerations

for Translation of Tissue Engineered Fibrocartilage From Bench to Bedside. *Journal of Biomechanical Engineering*, *141*(7), 070802. https://doi.org/10.1115/1.4042201

Donahue, R. P., Hu, J. C., & Athanasiou, K. A. (2019). Remaining Hurdles for Tissue-Engineering the Temporomandibular Joint Disc. *Trends in Molecular Medicine*, *25*(3), 241–256. https://doi.org/10.1016/j.molmed.2018.12.007

Edgar, L., Altamimi, A., García Sánchez, M., Tamburrinia, R., Asthana, A., Gazia, C., & Orlando, G. (2018). Utility of extracellular matrix powders in tissue engineering. *Organogenesis*, *14*(4), 172–186. https://doi.org/10.1080/15476278.2018.1503771

Embree, M. C., Iwaoka, G. M., Kong, D., Martin, B. N., Patel, R. K., Lee, A. H., Nathan, J. M., Eisig, S. B., Safarov, A., Koslovsky, D. A., Koch, A., Romanov, A., & Mao, J. J. (2015). Soft tissue ossification and condylar cartilage degeneration following TMJ disc perforation in a rabbit pilot study. *Osteoarthritis and Cartilage*, *23*(4), 629–639. https://doi.org/10.1016/j.joca.2014.12.015

Fazaeli, S., Ghazanfari, S., Everts, V., Smit, T. H., & Koolstra, J. H. (2016). The contribution of collagen fibers to the mechanical compressive properties of the temporomandibular joint disc. *Osteoarthritis and Cartilage*, *24*(7), 1292–1301. https://doi.org/10.1016/j.joca.2016.01.138

Fazaeli, Sepanta, Ghazanfari, S., Mirahmadi, F., Everts, V., Smit, T. H., & Koolstra, J. H. (2019). The dynamic mechanical viscoelastic properties of the temporomandibular joint disc: The role of collagen and elastin fibers from a perspective of polymer dynamics. *Journal of the Mechanical Behavior of Biomedical Materials*, 103406.

Fernandes, A. C. B. D. C. J., Moura, D. M. D., Da Silva, L. G. D., De Almeida, E. O., & Barbosa, G. A. S. (2017). Acupuncture in temporomandibular disorder myofascial pain treatment: a systematic review. *Journal of Oral & Facial Pain and Headache*, *31*(3), 225–232.

Fernández Sanromán, J., Fernández Ferro, M., Costas López, A., Arenaz Bua, J., & López, A. (2016). Does injection of plasma rich in growth factors after temporomandibular joint arthroscopy improve outcomes in patients with Wilkes stage IV internal derangement? A randomized prospective clinical study. *International Journal of Oral and Maxillofacial Surgery*, *45*(7), 828–835. https://doi.org/10.1016/j.ijom.2016.01.018

Gandhi, N. S., & Mancera, R. L. (2008). The Structure of Glycosaminoglycans and their Interactions with Proteins. *Chemical Biology & Drug Design*, *72*(6), 455–482. https://doi.org/10.1111/j.1747-0285.2008.00741.x

Garreta, E., Oria, R., Tarantino, C., Pla-Roca, M., Prado, P., Fernández-Avilés, F., Campistol, J. M., Samitier, J., & Montserrat, N. (2017). Tissue engineering by decellularization and

3D bioprinting. *Materials Today*, *20*(4), 166–178. https://doi.org/10.1016/j.mattod.2016.12.005

Gerbino, G., Zavattero, E., Bosco, G., Berrone, S., & Ramieri, G. (2017). Temporomandibular joint reconstruction with stock and custom-made devices: Indications and results of a 14-year experience. *Journal of Cranio-Maxillofacial Surgery*, *45*(10), 1710–1715. https://doi.org/10.1016/j.jcms.2017.07.011

Gil-Martínez, A., Paris-Alemany, A., López-de-Uralde-Villanueva, I., & La Touche, R. (2018). Management of pain in patients with temporomandibular disorder (TMD): challenges and solutions. *Journal of Pain Research*, *11*, 571–587.

Gilpin, A., & Yang, Y. (2017). Decellularization Strategies for Regenerative Medicine: From Processing Techniques to Applications. *BioMed Research International*, *2017*, 1–13. https://doi.org/10.1155/2017/9831534

Gopinath, A., Reddy, S. M. M., Madhan, B., Shanmguam, G., & Rao, J. R. (2014). Effect of aqueous ethanol on the triple helical structure of collagen. *European Biophysics Journal*, *43*(12), 643–652. https://doi.org/10.1007/s00249-014-0994-5

Gopinath, D., Ahmed, M. R., Gomathi, K., Chitra, K., Sehgal, P. ., & Jayakumar, R. (2004). Dermal wound healing processes with curcumin incorporated collagen films. *Biomaterials*, *25*(10), 1911–1917. https://doi.org/10.1016/S0142-9612(03)00625-2

Grigore, M. E. (2017). Biomaterials for Cartilage Tissue Engineering. *Journal of Tissue Science & Engineering*, *08*, 4–9. https://doi.org/10.4172/2157-7552.1000192

Grossmann, E., Poluha, R. L., Iwaki, L. C. V., Santana, R. G., & Iwaki Filho, L. (2019). The use of arthrocentesis in patients with temporomandibular joint disc displacement without reduction. *PLOS ONE*, *14*(2), e0212307. https://doi.org/10.1371/journal.pone.0212307

Guo, L., Qu, J., Zheng, C., Cao, Y., Zhang, T., Lu, H., & Hu, J. (2015). Preparation and Characterization of a Novel Decellularized Fibrocartilage “Book” Scaffold for Use in Tissue Engineering. *PLOS ONE*, *10*(12), e0144240. https://doi.org/10.1371/journal.pone.0144240

Gupta, S. K., Mishra, N. C., & Dhasmana, A. (2017). Decellularization Methods for Scaffold Fabrication. In K. Turksen (Ed.), *Decellularized Scaffolds and Organogenesis* (pp. 1–10). https://doi.org/10.1007/7651_2017_34

Gutman, S., Kim, D., Tarafder, S., Velez, S., Jeong, J., & Lee, C. H. (2018). Regionally variant collagen alignment correlates with viscoelastic properties of the disc of the human temporomandibular joint. *Archives of Oral Biology*, *86*, 1–6.

Guzzi Plepis, A. M. De, Goissis, G., & Das-Gupta, D. K. (1996). Dielectric and pyroelectric characterization of anionic and native collagen. *Polymer Engineering & Science*, *36*(24), 2932–2938. https://doi.org/10.1002/pen.10694

Hagandora, C. K., Gao, J., Wang, Y., & Almarza, A. J. (2013). Poly (Glycerol Sebacate): A Novel Scaffold Material for Temporomandibular Joint Disc Engineering. *Tissue Engineering Part A*, *19*(5–6), 729–737. https://doi.org/10.1089/ten.tea.2012.0304

Haketa, T., Kino, K., Sugisaki, M., Takaoka, M., & Ohta, T. (2010). Randomized Clinical Trial of Treatment for TMJ Disc Displacement. *Journal of Dental Research*, *89*(11), 1259–1263. https://doi.org/10.1177/0022034510378424

Han, M., Markiewicz, M., Miloro, M., Wolford, L., & Pogrel, M. A. (2019). Surgery of the Temporomandibular Joint: Discectomy and Arthroplasty. In S. T. Connelly, G. Tartaglia, & R. G. Silva (Eds.), *Contemporary Management of Temporomandibular Disorders* (pp. 107–127). Springer International Publishing. https://doi.org/10.1007/978-3-319-99909-8_6

Hancı, M., Karamese, M., Tosun, Z., Aktan, T. M., Duman, S., & Savaci, N. (2015). Intra-articular platelet-rich plasma injection for the treatment of temporomandibular disorders and a comparison with arthrocentesis. *Journal of Cranio-Maxillofacial Surgery*, *43*(1), 162–166. https://doi.org/10.1016/j.jcms.2014.11.002

Hargitai, I. A., Hawkins, J. M., & Ehrlich, A. D. (2018). The Temporomandibular Joint. In Henry A Gremillion & G. D. Klasse (Eds.), *Temporomandibular Disorders* (pp. 91–107). Springer.

Hasan, N. M. A., & Abdelrahman, T. E. F. (2014). MRI evaluation of TMJ internal derangement: Degree of anterior disc displacement correlated with other TMJ soft tissue and osseous abnormalities. *The Egyptian Journal of Radiology and Nuclear Medicine*, *45*(3), 735–744. https://doi.org/10.1016/j.ejrnm.2014.03.013

Heise, H. M. (1997). Medical Applications of Infrared Spectroscopy. In J. Mink, G. Keresztury, & R. Kellner (Eds.), *Progress in Fourier Transform Spectroscopy* (pp. 67–77). Springer Vienna. https://doi.org/10.1007/978-3-7091-6840-0_9

Hoshiba, T., Lu, H., Kawazoe, N., & Chen, G. (2010). Decellularized matrices for tissue engineering. *Expert Opinion on Biological Therapy*, *10*(12), 1717–1728. https://doi.org/10.1517/14712598.2010.534079

Hossameldin, R. H., & McCain, J. P. (2018). Outcomes of office-based temporomandibular joint arthroscopy: a 5-year retrospective study. *International Journal of Oral and Maxillofacial Surgery*, *47*(1), 90–97. https://doi.org/10.1016/j.ijom.2017.06.025

Hrebikova, H., Diaz, D., & Mokry, J. (2015). Chemical decellularization: a promising approach for preparation of extracellular matrix. *Biomedical Papers*, *159*(1), 12–17. https://doi.org/10.5507/bp.2013.076

Hussey, G. S., Dziki, J. L., & Badylak, S. F. (2018). Extracellular matrix-based materials for regenerative medicine. *Nature Reviews Materials*, *3*(7), 159–173. https://doi.org/10.1038/s41578-018-0023-x

Incesu, L., Taşkaya-Yılmaz, N., Öğütcen-Toller, M., & Uzun, E. (2004). Relationship of condylar position to disc position and morphology. *European Journal of Radiology*, *51*(3), 269–273. https://doi.org/10.1016/S0720-048X(03)00218-3

Ingawalé, S., & Goswami, T. (2009). Temporomandibular Joint: Disorders, Treatments, and Biomechanics. *Annals of Biomedical Engineering*, *37*(5), 976–996. https://doi.org/10.1007/s10439-009-9659-4

Israel, H. A. (2016). Internal Derangement of the Temporomandibular Joint: New Perspectives on an Old Problem. *Oral and Maxillofacial Surgery Clinics of North America*, *28*(3), 313–333. https://doi.org/10.1016/j.coms.2016.03.009

Ivkovic, N., & Racic, M. (2018). Structural and Functional Disorders of the Temporomandibular Joint (Internal Disorders). In *Oral and Maxillofacial Surgery-Practices and Updates*. IntechOpen. https://doi.org/10.5772/intechopen.81937

Juran, C. M., Dolwick, M. F., & McFetridge, P. S. (2015). Engineered Microporosity: Enhancing the Early Regenerative Potential of Decellularized Temporomandibular Joint Discs. *Tissue Engineering Part A*, *21*(3–4), 829–839. https://doi.org/10.1089/ten.tea.2014.0250

Kalpakci, K. N., Willard, V. P., Wong, M. E., & Athanasiou, K. A. (2011). An Interspecies Comparison of the Temporomandibular Joint Disc. *Journal of Dental Research*, *90*(2), 193–198. https://doi.org/10.1177/0022034510381501

Kaplan, P., Ruskin, J., Tu, H., & Knibbe, M. (1988). Erosive arthritis of the temporomandibular joint caused by Teflon-Proplast implants: plain film features. *American Journal of Roentgenology*, *151*(2), 337–339. https://doi.org/10.2214/ajr.151.2.337

Katzberg, R. W., & Tallents, R. H. (2005). Normal and Abnormal Temporomandibular Joint Disc and Posterior Attachment as Depicted by Magnetic Resonance Imaging in Symptomatic and Asymptomatic Subjects. *Journal of Oral and Maxillofacial Surgery*, *63*(8), 1155–1161. https://doi.org/10.1016/j.joms.2005.04.012

Keane, T. J., Saldin, L. T., & Badylak, S. F. (2016). Decellularization of mammalian tissues. In *Characterisation and Design of Tissue Scaffolds* (pp. 75–103). Elsevier.

https://doi.org/10.1016/B978-1-78242-087-3.00004-3

Keane, T. J., Swinehart, I. T., & Badylak, S. F. (2015). Methods of tissue decellularization used for preparation of biologic scaffolds and in vivo relevance. *Methods*, *84*, 25–34. https://doi.org/10.1016/j.ymeth.2015.03.005

Khan, M., Vijayalakshmi, K. R., & Gupta, N. (2013). Low Intensity Laser Therapy in Disc Derangement Disorders of Temporomandibular Joint: A Review Article. *International Journal of Odontostomatology*, *7*(2), 235–239. https://doi.org/10.4067/S0718-381X2013000200013

Kim, J.-Y., Jeon, K.-J., Kim, M.-G., Park, K.-H., & Huh, J.-K. (2018). A nomogram for classification of temporomandibular joint disk perforation based on magnetic resonance imaging. *Oral Surgery, Oral Medicine, Oral Pathology and Oral Radiology*, *125*(6), 682–692. https://doi.org/10.1016/j.oooo.2018.02.009

Kim, M., Bi, X., Horton, W. E., Spencer, R. G., & Camacho, N. P. (2005). Fourier transform infrared imaging spectroscopic analysis of tissue engineered cartilage: histologic and biochemical correlations. *Journal of Biomedical Optics*, *10*(3), 031105. https://doi.org/10.1117/1.1922329

Kim, Y. S., Majid, M., Melchiorri, A. J., & Mikos, A. G. (2019). Applications of decellularized extracellular matrix in bone and cartilage tissue engineering. *Bioengineering & Translational Medicine*, *4*(1), 83–95. https://doi.org/10.1002/btm2.10110

Kobayashi, E., Nakahara, T., Inoue, M., Shigeno, K., Tanaka, A., & Nakamura, T. (2015). Experimental Study on In Situ Tissue Engineering of the Temporomandibular Joint Disc using Autologous Bone Marrow and Collagen Sponge Scaffold. *Journal of Hard Tissue Biology*, *24*(2), 211–218. https://doi.org/10.2485/jhtb.24.211

Kondoh, T., Hamada, Y., Kamei, K., & Seto, K. (2003). Simple disc reshaping surgery for internal derangement of the temporomandibular joint: 5-year follow-up results. *Journal of Oral and Maxillofacial Surgery*, *61*(1), 41–48. https://doi.org/10.1053/joms.2003.50007

Kopp, S. (1976). Topographical distribution of sulphated glycosaminoglycans in human temporomandibular joint disks. A histochemical study of an autopsy material. *Journal of Oral Pathology and Medicine*, *5*(5), 265–276. https://doi.org/10.1111/j.1600-0714.1976.tb01775.x

Kramer, A., Lee, L., & Beirne, O. (2005). Meta-analysis of TMJ discectomy with or without autogenous/alloplastic interpositional materials: Comparative analysis of functional outcome. *International Journal of Oral and Maxillofacial Surgery*, *34*, 69–70. https://doi.org/10.1016/S0901-5027(05)81146-4

Kuo, J., Zhang, L., Bacro, T., & Yao, H. (2010). The region-dependent biphasic viscoelastic properties of human temporomandibular joint discs under confined compression. *Journal of Biomechanics*, *43*(7), 1316–1321. https://doi.org/10.1016/j.jbiomech.2010.01.020

Kurup, S. (2017). *Temporomandibular Joint Coronal Disc Position: Association with Clinical Signs and Symptoms: Vol. Master of*. State University of New York at Buffalo.

Lalue-Sanches, M., Gonzaga, A. R., Guimaraes, A. S., & Ribeiro, E. C. (2015). Disc Displacement with Reduction of the Temporomandibular Joint: The Real Need for Treatment. *Journal of Pain & Relief*, *04*(05), 2–5. https://doi.org/10.4172/2167-0846.1000200

Lee, H.-S., Baek, H.-S., Song, D.-S., Kim, H.-C., Kim, H.-G., Kim, B.-J., Kim, M.-S., Shin, S.-H., Jung, S.-H., & Kim, C.-H. (2013). Effect of simultaneous therapy of arthrocentesis and occlusal splints on temporomandibular disorders: anterior disc displacement without reduction. *Journal of the Korean Association of Oral and Maxillofacial Surgeons*, *39*(1), 14. https://doi.org/10.5125/jkaoms.2013.39.1.14

Legemate, K., Tarafder, S., Jun, Y., & Lee, C. H. (2016). Engineering Human TMJ Discs with Protein-Releasing 3D-Printed Scaffolds. *Journal of Dental Research*, *95*(7), 800–807. https://doi.org/10.1177/0022034516642404

Li, T., Li, C., Zhang, C.-Y., & Zhao, J. (2015). Effect of accutase or trypsin dissociation on the apoptosis of human striatum-derived neural stem cells. *Zhongguo Yi Xue Ke Xue Yuan Xue Bao*, *37*, 185–194. https://doi.org/10.3881/j.issn.1000-503X.2015.02.009

Liang, J., Yi, P., Wang, X., Huang, F., Luan, X., Zhao, Z., & Liu, C. (2020). Acellular matrix hydrogel for repair of the temporomandibular joint disc. *Journal of Biomedical Materials Research Part B: Applied Biomaterials*, *108*(7), 2995–3007. https://doi.org/10.1002/jbm.b.34629

List, T., & Axelsson, S. (2010). Management of TMD: evidence from systematic reviews and meta-analyses. *Journal of Oral Rehabilitation*, *37*(6), 430–451. https://doi.org/10.1111/j.1365-2842.2010.02089.x

Liu, F., & Steinkeler, A. (2013). Epidemiology, Diagnosis, and Treatment of Temporomandibular Disorders. *Dental Clinics of North America*, *57*(3), 465–479. https://doi.org/10.1016/j.cden.2013.04.006

Liu, M.-Q., Lei, J., Han, J.-H., Yap, A. U.-J., & Fu, K.-Y. (2017). Metrical analysis of disc-condyle relation with different splint treatment positions in patients with TMJ disc displacement. *Journal of Applied Oral Science*, *25*(5), 483–489. https://doi.org/10.1590/1678-7757-2016-0471

Liu, X. M., Zhang, S. Y., Yang, C., Chen, M. J., Y Cai, X., Haddad, M. S., Yun, B., & Chen, Z. Z. (2010). Correlation between disc displacements and locations of disc perforation in the temporomandibular joint. *Dentomaxillofacial Radiology*, *39*(3), 149–156. https://doi.org/10.1259/dmfr/72395946

Lumpkins, S. B., Pierre, N., & McFetridge, P. S. (2008). A mechanical evaluation of three decellularization methods in the design of a xenogeneic scaffold for tissue engineering the temporomandibular joint disc. *Acta Biomaterialia*, *4*(4), 808–816. https://doi.org/10.1016/j.actbio.2008.01.016

MacBarb, R. F., Murphy, M. K., & Athanasiou, K. A. (2011). Temporomandibular Joint: Structure, Function, and Current Perspectives. In B. A. Winkelstein (Ed.), *Orthopaedic Biomechanics* (pp. 153–177). Taylor & Francis.

Machado, E., Bonotto, D., & Cunali, P. A. (2013). Intra-articular injections with corticosteroids and sodium hyaluronate for treating temporomandibular joint disorders: a systematic review. *Dental Press Journal of Orthodontics*, *18*(5), 128–133. https://doi.org/10.1590/S2176-94512013000500021

Machon, V, Levorova, J., Hirjak, D., Drahos, M., & Foltan, R. (2017). Temporomandibular joint disc perforation: a retrospective study. *International Journal of Oral and Maxillofacial Surgery*, *46*(11), 1411–1416.

Machon, Vladimir, Sedy, J., Klima, K., Hirjak, D., & Foltán, R. (2012). Arthroscopic lysis and lavage in patients with temporomandibular anterior disc displacement without reduction. *International Journal of Oral and Maxillofacial Surgery*, *41*(1), 109–113. https://doi.org/10.1016/j.ijom.2011.07.907

Mäenpää, K., Ellä, V., Mauno, J., Kellomäki, M., Suuronen, R., Ylikomi, T., & Miettinen, S. (2010). Use of adipose stem cells and polylactide discs for tissue engineering of the temporomandibular joint disc. *Journal of The Royal Society Interface*, *7*(42), 177–188. https://doi.org/10.1098/rsif.2009.0117

Mainreck, N., Brézillon, S., Sockalingum, G. D., Maquart, F.-X., Manfait, M., & Wegrowski, Y. (2012). Characterization of Glycosaminoglycans by Tandem Vibrational Microspectroscopy and Multivariate Data Analysis. In Rédini F. (Ed.), *Proteoglycans. Methods in Molecular Biology (Methods and Protocols)* (pp. 117–130). Humana Press. https://doi.org/10.1007/978-1-61779-498-8_8

Malek, K., Wood, B. R., & Bambery, K. R. (2014). FTIR Imaging of Tissues: Techniques and Methods of Analysis. In M. Baranska (Ed.), *Optical Spectroscopy and Computational Methods in Biology and Medicine* (pp. 419–473). Springer Netherlands.

https://doi.org/10.1007/978-94-007-7832-0_15

Malik, A. H., & Shah, A. A. (2014). Efficacy of Temporomandibular Joint Arthrocentesis on Mouth Opening and Pain in the Treatment of Internal Derangement of TMJ—A Clinical Study. *Journal of Maxillofacial and Oral Surgery*, *13*(3), 244–248. https://doi.org/10.1007/s12663-013-0522-7

Manfredini, D., Guarda-Nardini, L., Winocur, E., Piccotti, F., Ahlberg, J., & Lobbezoo, F. (2011). Research diagnostic criteria for temporomandibular disorders: a systematic review of axis I epidemiologic findings. *Oral Surgery, Oral Medicine, Oral Pathology, Oral Radiology, and Endodontology*, *112*(4), 453–462.

Manoukian, O. S., Sardashti, N., Stedman, T., Gailiunas, K., Ojha, A., Penalosa, A., Mancuso, C., Hobert, M., & Kumbar, S. G. (2019). Biomaterials for Tissue Engineering and Regenerative Medicine. In R. Narayan (Ed.), *Encyclopedia of Biomedical Engineering* (pp. 462–482). Elsevier. https://doi.org/10.1016/B978-0-12-801238-3.64098-9

Marzook, H. A. M., Abdel Razek, A. A., Yousef, E. A., & Attia, A. A. M. M. (2020). Intra-articular injection of a mixture of hyaluronic acid and corticosteroid versus arthrocentesis in TMJ internal derangement. *Journal of Stomatology, Oral and Maxillofacial Surgery*, *121*(1), 30–34. https://doi.org/10.1016/j.jormas.2019.05.003

Matukas, V. J., & Lachner, J. (1990). The use of autologous auricular cartilage for temporomandibular joint disc replacement: A preliminary report. *Journal of Oral and Maxillofacial Surgery*, *48*(4), 348–353. https://doi.org/10.1016/0278-2391(90)90429-6

Matuska, A. M., Dolwick, M. F., & McFetridge, P. S. (2018). Approaches to improve integration and regeneration of an ex vivo derived temporomandibular joint disc scaffold with variable matrix composition. *Journal of Materials Science: Materials in Medicine*, *29*(10), 152. https://doi.org/10.1007/s10856-018-6164-z

Matuska, A. M., & McFetridge, P. S. (2015). The effect of terminal sterilization on structural and biophysical properties of a decellularized collagen-based scaffold; implications for stem cell adhesion. *Journal of Biomedical Materials Research Part B: Applied Biomaterials*, *103*(2), 397–406. https://doi.org/10.1002/jbm.b.33213

Matuska, A. M., & McFetridge, P. S. (2018). Laser micro-ablation of fibrocartilage tissue: Effects of tissue processing on porosity modification and mechanics. *Journal of Biomedical Materials Research Part B: Applied Biomaterials*, *106*(5), 1858–1868. https://doi.org/10.1002/jbm.b.33997

McCain, J. P., Hossameldin, R. H., Srouji, S., & Maher, A. (2015). Arthroscopic Discopexy Is Effective in Managing Temporomandibular Joint Internal Derangement in Patients With

Wilkes Stage II and III. *Journal of Oral and Maxillofacial Surgery*, *73*(3), 391–401. https://doi.org/10.1016/j.joms.2014.09.004

Merlic, C., & Strouse, J. (2000). *Introduction to IR spectra*. WebSpectra. https://webspectra.chem.ucla.edu/irintro.html

Mescher, A. L. (2018). Cartilage. In M. Weitz & B. Kearns (Eds.), *Junqueira's Basic Histology: Text and Atlas* (15th ed., pp. 129–137). McGraw-Hill Education.

Meyer, R. A. (1988). The autogenous dermal graft in temporomandibular joint disc surgery. *Journal of Oral and Maxillofacial Surgery*, *46*(11), 948–954. https://doi.org/10.1016/0278-2391(88)90332-1

Michelotti, A., Vollaro, S., & Cimino, R. (2019). Diagnosis of Temporomandibular Disorders Using DC/TMD Criteria. In S. T. Connelly, G. M. Tartaglia, & R. G. Silva (Eds.), *Contemporary Management of Temporomandibular Disorders* (pp. 205–227). Springer.

Miloro, M., & Henriksen, B. (2010). Discectomy as the Primary Surgical Option for Internal Derangement of the Temporomandibular Joint. *Journal of Oral and Maxillofacial Surgery*, *68*(4), 782–789. https://doi.org/10.1016/j.joms.2009.09.091

Mohamed, H. T., Untereiner, V., Cinque, G., Ibrahim, S. A., Götte, M., Nguyen, N. Q., Rivet, R., Sockalingum, G. D., & Brézillon, S. (2020). Infrared Microspectroscopy and Imaging Analysis of Inflammatory and Non-Inflammatory Breast Cancer Cells and Their GAG Secretome. *Molecules*, *25*(18), 4300. https://doi.org/10.3390/molecules25184300

Morales, H., & Cornelius, R. (2016). Imaging approach to temporomandibular joint disorders. *Clinical Neuroradiology*, *26*(1), 5–22.

Moura, C., Trindade, D., Vieira, M., Francisco, L., Ângelo, D. F., & Alves, N. (2020). Multi-Material Implants for Temporomandibular Joint Disc Repair: Tailored Additive Manufacturing Production. *Frontiers in Bioengineering and Biotechnology*, *8*, 342. https://doi.org/10.3389/fbioe.2020.00342

Movasaghi, Z., Rehman, S., & ur Rehman, D. I. (2008). Fourier Transform Infrared (FTIR) Spectroscopy of Biological Tissues. *Applied Spectroscopy Reviews*, *43*(2), 134–179. https://doi.org/10.1080/05704920701829043

Mujakperuo, H. R., Watson, M., Morrison, R., & Macfarlane, T. V. (2010). Pharmacological interventions for pain in patients with temporomandibular disorders. *Cochrane Database of Systematic Reviews*, *10*, CD004715. https://doi.org/10.1002/14651858.CD004715.pub2

Muñoz-Guerra, M. F., Rodríguez-Campo, F. J., Escorial Hernández, V., Sánchez-Acedo, C.,

& Gil-Díez Usandizaga, J. L. (2013). Temporomandibular Joint Disc Perforation: Long-Term Results After Operative Arthroscopy. *Journal of Oral and Maxillofacial Surgery*, *71*(4), 667–676. https://doi.org/10.1016/j.joms.2012.12.013

Murphy, M. K., Arzi, B., Hu, J. C., & Athanasiou, K. A. (2013). Tensile characterization of porcine temporomandibular joint disc attachments. *Journal of Dental Research*, *92*(8), 753–758.

Nakano, T., & Scott, P. G. (1996). Changes in the chemical composition of the bovine temporomandibular joint disc with age. *Archives of Oral Biology*, *41*(8–9), 845–853. https://doi.org/10.1016/S0003-9969(96)00040-4

Nascimento Falcão, I., Alonso, C., Carrazzone, M. B., da Silva, L. H., Lopes, S. L. P. de C., Comar, L. P., & Costa, A. L. F. (2017). 3D Morphology Analysis of TMJ Articular Eminence in Magnetic Resonance Imaging. *International Journal of Dentistry*, *2017*, 5130241.

Nasution, A. K., & Hermawan, H. (2016). Degradable Biomaterials for Temporary Medical Implants. In F. Mahyudin & H. Hermawan (Eds.), *Biomaterials and Medical Devices* (pp. 127–160). https://doi.org/10.1007/978-3-319-14845-8_6

Nitzan, D. W., & Naaman, H. L. (2018). Arthrocentesis: A Minimally Invasive Approach to the Temporomandibular Joint. In O. Nahlieli (Ed.), *Minimally Invasive Oral and Maxillofacial Surgery* (pp. 45–73). Springer.

Norton, N. S. (2016). Osteology. In E.-H. S. Division (Ed.), *Netter's Head and Neck Anatomy for Dentistry* (3nd ed., pp. 25–64). Elsevier Health Sciences.

Oinas, J., Rieppo, L., Finnilä, M. A. J., Valkealahti, M., Lehenkari, P., & Saarakkala, S. (2016). Imaging of Osteoarthritic Human Articular Cartilage using Fourier Transform Infrared Microspectroscopy Combined with Multivariate and Univariate Analysis. *Scientific Reports*, *6*(1), 30008. https://doi.org/10.1038/srep30008

Okeson, J. P. (2019). Functional Anatomy and Biomechanics of the Masticatory System. In E.-H. S. Division (Ed.), *Management of Temporomandibular Disorders and Occlusion* (pp. 2–20). Elsevier Health Sciences.

Okeson, J. P., Perez, C., & Fricton, J. R. (2017). Temporomandibular Joint Disorders. In J. N. A. R. Ferreira, J. Fricton, & N. Rhodus (Eds.), *Orofacial Disorders* (pp. 145–157). Springer.

Orhan, K., Nishiyama, H., Tadashi, S., Murakami, S., & Furukawa, S. (2006). Comparison of altered signal intensity, position, and morphology of the TMJ disc in MR images corrected for variations in surface coil sensitivity. *Oral Surgery, Oral Medicine, Oral Pathology, Oral*

Radiology, and Endodontology, *101*(4), 515–522. https://doi.org/10.1016/j.tripleo.2005.04.004

Patnaik, S. S., Wang, B., Weed, B., Wertheim, J. A., & Liao, J. (2014). Decellularized Scaffolds: Concepts, Methodologies, and Applications in Cardiac Tissue Engineering and Whole-Organ Regeneration. In Q. Liu (Ed.), *Tissue Regeneration: Where Nano-Structure Meets Biology* (pp. 77–124). World Scientific Company. https://doi.org/10.1142/9789814494847_0003

Pihut, M., Gorecka, M., Ceranowicz, P., & Wieckiewicz, M. (2018). The Efficiency of Anterior Repositioning Splints in the Management of Pain Related to Temporomandibular Joint Disc Displacement with Reduction. *Pain Research and Management*, *2018*, 1–6. https://doi.org/10.1155/2018/9089286

Qian, Z., Radke, D., Jia, W., Tahtinen, M., Wang, G., & Zhao, F. (2019). Bioengineering Scaffolds for Regenerative Engineering. In R. Narayan (Ed.), *Encyclopedia of Biomedical Engineering* (pp. 444–461). Elsevier. https://doi.org/10.1016/B978-0-12-801238-3.99891-X

Quinn, P., & Granquist, E. J. (2016). Stock Prostheses for Total Reconstruction of the Temporomandibular Joint. In L. G. Mercuri (Ed.), *Temporomandibular Joint Total Joint Replacement – TMJ TJR* (pp. 69–90). Springer International Publishing. https://doi.org/10.1007/978-3-319-21389-7_4

Rabelo, K. A., Melo, S. L. S., Torres, M. G. G., Campos, P. S. F., Bento, P. M., & de Melo, D. P. (2017). Condyle excursion angle, articular eminence inclination, and temporomandibular joint morphologic relations with disc displacement. *Journal of Oral and Maxillofacial Surgery*, *75*(5), 938-e1.

Rabelo, K. A., Melo, S. L. S., Torres, M. G. G., Peixoto, L. R., Campos, P. S. F., Rebello, I. M. C. R., & de Melo, D. P. (2017). Assessment of condyle position, fossa morphology, and disk displacement in symptomatic patients. *Oral Surgery, Oral Medicine, Oral Pathology and Oral Radiology*, *124*(2), 199–207.

Ramdan, R. D., Sunendar, B., & Hermawan, H. (2016). Naturally Derived Biomaterials and Its Processing. In F. Mahyudin & H. Hermawan (Eds.), *Biomaterials and Medical Devices* (pp. 23–39). https://doi.org/10.1007/978-3-319-14845-8_2

Ramdhan, R. C., & Iwanaga, J. (2019). Anatomy and Variations of the Temporomandibular Joint. In J. Iwanaga & R. S. Tubbs (Eds.), *Anatomical Variations in Clinical Dentistry* (pp. 187–202). Springer.

Renapurkar, S. K. (2018). Discectomy Versus Disc Preservation for Internal Derangement of

the Temporomandibular Joint. *Oral and Maxillofacial Surgery Clinics of North America*, *30*(3), 329–333. https://doi.org/10.1016/j.coms.2018.05.002

Rieppo, L., Närhi, T., Helminen, H. J., Jurvelin, J. S., Saarakkala, S., & Rieppo, J. (2013). Infrared spectroscopic analysis of human and bovine articular cartilage proteoglycans using carbohydrate peak or its second derivative. *Journal of Biomedical Optics*, *18*(9), 097006. https://doi.org/10.1117/1.JBO.18.9.097006

Rieppo, L., Rieppo, J., Jurvelin, J. S., & Saarakkala, S. (2012). Fourier Transform Infrared Spectroscopic Imaging and Multivariate Regression for Prediction of Proteoglycan Content of Articular Cartilage. *PLoS ONE*, *7*(2), e32344. https://doi.org/10.1371/journal.pone.0032344

Rieppo, L., Saarakkala, S., Närhi, T., Helminen, H. J., Jurvelin, J., & Rieppo, J. (2012). Application of second derivative spectroscopy for increasing molecular specificity of fourier transform infrared spectroscopic imaging of articular cartilage. *Osteoarthritis and Cartilage*, *20*(5), 451–459. https://doi.org/10.1016/j.joca.2012.01.010

Riera-Punet, N., Martinez-Gomis, J., Willaert, E., Povedano, M., & Peraire, M. (2018). Functional limitation of the masticatory system in patients with bulbar involvement in amyotrophic lateral sclerosis. *Journal of Oral Rehabilitation*, *45*(3), 204–210.

Roberts, W. E., & Stocum, D. L. (2018). Part II: Temporomandibular joint (TMJ)—Regeneration, degeneration, and adaptation. *Current Osteoporosis Reports*, *16*(4), 369–379.

Saarakkala, S., Rieppo, L., Rieppo, J., & Jurvelin, J. (2010). Fourier transform infrared (FTIR) microspectroscopy of immature, mature and degenerated articular cartilage. *Microscopy*, *1*, 403–414.

Sakul, B. U., Bilecenoglu, B., & Ocak, M. (2019). Anatomy of the Temporomandibular Joint. In I. Rozylo-Kalinowka & K. Orhan (Eds.), *Imaging of the Temporomandibular Joint* (pp. 9–41). Springer International Publishing. https://doi.org/10.1007/978-3-319-99468-0_2

Sanders, A. E., Akinkugbe, A. A., Fillingim, R. B., Ohrbach, R., Greenspan, J. D., Maixner, W., Bair, E., & Slade, G. D. (2017). Causal mediation in the development of painful temporomandibular disorder. *The Journal of Pain*, *18*(4), 428–436.

Sanromán, J. . (2004). Closed lock (MRI fixed disc): a comparison of arthrocentesis and arthroscopy. *International Journal of Oral and Maxillofacial Surgery*, *33*(4), 344–348. https://doi.org/10.1016/j.ijom.2003.10.005

Schilling, J., Gomes, L. C. R., Benavides, E., Nguyen, T., Paniagua, B., Styner, M., Boen, V.,

Gonçalves, J. R., & Cevidanes, L. H. S. (2013). Regional 3D superimposition to assess temporomandibular joint condylar morphology. *Dentomaxillofacial Radiology*, *43*(1), 20130273.

Schneider, C., Lehmann, J., van Osch, G. J. V. M., Hildner, F., Teuschl, A., Monforte, X., Miosga, D., Heimel, P., Priglinger, E., Redl, H., Wolbank, S., & Nürnberger, S. (2016). Systematic Comparison of Protocols for the Preparation of Human Articular Cartilage for Use as Scaffold Material in Cartilage Tissue Engineering. *Tissue Engineering Part C: Methods*, *22*(12), 1095–1107. https://doi.org/10.1089/ten.tec.2016.0380

Schwarz, S., Koerber, L., Elsaesser, A. F., Goldberg-Bockhorn, E., Seitz, A. M., Dürselen, L., Ignatius, A., Walther, P., Breiter, R., & Rotter, N. (2012). Decellularized Cartilage Matrix as a Novel Biomatrix for Cartilage Tissue-Engineering Applications. *Tissue Engineering Part A*, *18*(21–22), 2195–2209. https://doi.org/10.1089/ten.tea.2011.0705

Seddon, A. M., Curnow, P., & Booth, P. J. (2004). Membrane proteins, lipids and detergents: not just a soap opera. *Biochimica et Biophysica Acta (BBA) - Biomembranes*, *1666*(1–2), 105–117. https://doi.org/10.1016/j.bbamem.2004.04.011

Shoukri, B., Prieto, J. C., Ruellas, A., Yatabe, M., Sugai, J., Styner, M., Zhu, H., Huang, C., Paniagua, B., & Aronovich, S. (2019). Minimally Invasive Approach for Diagnosing TMJ Osteoarthritis. *Journal of Dental Research*, *98*(10), 1103–1111.

Slater, J. J. R. H., & de Leeuw, R. (2019). Internal Derangements of the Temporomandibular Joint. *Contemporary Oral Medicine: A Comprehensive Approach to Clinical Practice*, 1881–1918.

Smith, J. A., Sandler, N. A., Ozaki, W. H., & Braun, T. W. (1999). Subjective and objective assessment of the temporalis myofascial flap in previously operated temporomandibular joints. *Journal of Oral and Maxillofacial Surgery*, *57*(9), 1058–1065. https://doi.org/10.1016/S0278-2391(99)90325-7

Smolka, W., Yanai, C., Smolka, K., & Iizuka, T. (2008). Efficiency of arthroscopic lysis and lavage for internal derangement of the temporomandibular joint correlated with Wilkes classification. *Oral Surgery, Oral Medicine, Oral Pathology, Oral Radiology, and Endodontology*, *106*(3), 317–323. https://doi.org/10.1016/j.tripleo.2007.12.007

Spalazzi, J. P., Boskey, A. L., Pleshko, N., & Lu, H. H. (2013). Quantitative Mapping of Matrix Content and Distribution across the Ligament-to-Bone Insertion. *PLoS ONE*, *8*(9), e74349. https://doi.org/10.1371/journal.pone.0074349

Sperry, M. M., Kartha, S., Winkelstein, B. A., & Granquist, E. J. (2019). Experimental methods to inform diagnostic approaches for painful TMJ osteoarthritis. *Journal of Dental*

Research, *98*(4), 388–397.

Springer, I. N. G., Fleiner, B., Jepsen, S., & Açil, Y. (2001). Culture of cells gained from temporomandibular joint cartilage on non-absorbable scaffolds. *Biomaterials*, *22*(18), 2569–2577. https://doi.org/10.1016/S0142-9612(01)00148-X

Stanković, S., Vlajković, S., Bošković, M., Radenković, G., Antić, V., & Jevremović, D. (2013). Morphological and biomechanical features of the temporomandibular joint disc: an overview of recent findings. *Archives of Oral Biology*, *58*(10), 1475–1482.

Stapleton, T. W., Ingram, J., Katta, J., Knight, R., Korossis, S., Fisher, J., & Ingham, E. (2008). Development and Characterization of an Acellular Porcine Medial Meniscus for Use in Tissue Engineering. *Tissue Engineering Part A*, *14*(4), 505–518. https://doi.org/10.1089/tea.2007.0233

Stocum, D. L., & Roberts, W. E. (2018). Part I: Development and Physiology of the Temporomandibular Joint. *Current Osteoporosis Reports*, *16*(4), 360–368. https://doi.org/10.1007/s11914-018-0447-7

Sutherland, A. J., Converse, G. L., Hopkins, R. A., & Detamore, M. S. (2015). The Bioactivity of Cartilage Extracellular Matrix in Articular Cartilage Regeneration. *Advanced Healthcare Materials*, *4*(1), 29–39. https://doi.org/10.1002/adhm.201400165

Szarko, M., Muldrew, K., & Bertram, J. E. (2010). Freeze-thaw treatment effects on the dynamic mechanical properties of articular cartilage. *BMC Musculoskeletal Disorders*, *11*(1), 231. https://doi.org/10.1186/1471-2474-11-231

Talmaceanu, D., Lenghel, L. M., Bolog, N., Hedesiu, M., Buduru, S., Rotar, H., Baciut, M., & Baciut, G. (2018). Imaging modalities for temporomandibular joint disorders: an update. *Clujul Medical*, *91*(3), 280.

Tamimi, D., & Hatcher, D. C. (2016). TMJ Biomechanics and Structure of the Mandibular Condyle. In *Specialty Imaging: Temporomandibular Joint* (pp. 46–48). Elsevier Health Sciences.

Tanaka, E., Shibaguchi, T., Tanaka, M., & Tanne, K. (2000). Viscoelastic properties of the human temporomandibular joint disc in patients with internal derangement. *Journal of Oral and Maxillofacial Surgery*, *58*(9), 997–1002. https://doi.org/10.1053/joms.2000.8743

Tappert, L. K., Baldit, A., Guillaume, C., Velard, F., & Lipinski, P. (2020). Identification of macro-heterogenous mechanical behaviour of temporomandibular joint disc. *Computer Methods in Biomechanics and Biomedical Engineering*, *23*(sup1), S291–S293. https://doi.org/10.1080/10255842.2020.1816295

Taşkaya-Yılmaz, N., & Öğütcen-Toller, M. (2001). Magnetic resonance imaging evaluation of temporomandibular joint disc deformities in relation to type of disc displacement. *Journal of Oral and Maxillofacial Surgery*, *59*(8), 860–865. https://doi.org/10.1053/joms.2001.25015

Tint, D., Stabler, C. T., Hanifi, A., Yousefi, F., Linkov, G., Hy, K., Soliman, A. M. S., & Pleshko, N. (2019). Spectroscopic Analysis of Human Tracheal Tissue during Decellularization. *Otolaryngology–Head and Neck Surgery*, *160*(2), 302–309. https://doi.org/10.1177/0194599818806271

Ungor, C., Atasoy, K. T., Taskesen, F., Pirpir, C., & Yilmaz, O. (2015). Long-Term Outcome of Arthrocentesis Plus Hyaluronic Acid Injection in Patients With Wilkes Stage II and III Temporomandibular Joint Internal Derangement. *Journal of Craniofacial Surgery*, *26*(7), 2104–2108. https://doi.org/10.1097/SCS.0000000000002078

Urbani, G., Silva, C.-E. N., & deJesus, L. F. (2019). Temporomandibular joint dysfunction syndrome and police work stress: an integrative review. *Ciencia & Saude Coletiva*, *24*(5).

Urtane, I., Gardovska, K., Krisjane, Z., & Krumina, G. (2016). Assessment of Osseous Structure Disorders of TMJ in Class II and Class III Patients with Different Mandibular Rotation using CBCT. *Medicine & Pharmacy*.

Vapniarsky, N., Huwe, L. W., Arzi, B., Houghton, M. K., Wong, M. E., Wilson, J. W., Hatcher, D. C., Hu, J. C., & Athanasiou, K. A. (2018). Tissue engineering toward temporomandibular joint disc regeneration. *Science Translational Medicine*, *10*(446), eaaq1802. https://doi.org/10.1126/scitranslmed.aaq1802

Vidal, B. de C., & Mello, M. L. S. (2016). FT-IR Microspectroscopy of Rat Ear Cartilage. *PLOS ONE*, *11*(3), e0151989. https://doi.org/10.1371/journal.pone.0151989

Warmling, L. V., Dutra, M. E. P., Santos, K. C. P., & Oliveira, J. X. (2015). Evaluation of Retrodiskal Tissue Associated with Articular Eminence Morphology, Effusion Status and Disk Displacement in Symptomatic Patients. *Journal of International Dental and Medical Research*, *8*(1), 1.

West, P. A., Torzilli, P. A., Chen, C., Lin, P., & Camacho, N. P. (2005). Fourier transform infrared imaging spectroscopy analysis of collagenase-induced cartilage degradation. *Journal of Biomedical Optics*, *10*(1), 014015. https://doi.org/10.1117/1.1854131

Westesson, P.-L., Eriksson, L., & Lindström, C. (1987). Destructive lesions of the mandibular condyle following diskectomy with temporary silicone implant. *Oral Surgery, Oral Medicine, Oral Pathology*, *63*(2), 143–150. https://doi.org/10.1016/0030-4220(87)90302-1

Wiesinger, B., Malker, H., Englund, E., & Wänman, A. (2007). Back pain in relation to musculoskeletal disorders in the jaw-face: a matched case–control study. *Pain*, *131*(3), 311–319.

Willard, V. P., Arzi, B., & Athanasiou, K. A. (2012). The attachments of the temporomandibular joint disc: a biochemical and histological investigation. *Archives of Oral Biology*, *57*(6), 599–606.

Willard, V. P., Zhang, L., & Athanasiou, K. A. (2011). Tissue engineering of the temporomandibular joint. In P. Ducheyne (Ed.), *Comprehensive biomaterials* (pp. 221–235). Elsevier.

Wood, B. R. (2016). The importance of hydration and DNA conformation in interpreting infrared spectra of cells and tissues. *Chemical Society Reviews*, *45*(7), 1980–1998. https://doi.org/10.1039/C5CS00511F

Wu, Y, Cisewski, S. E., Wei, F., She, X., Gonzales, T. S., Iwasaki, L. R., Nickel, J. C., & Yao, H. (2017). Fluid pressurization and tractional forces during TMJ disc loading: A biphasic finite element analysis. *Orthodontics & Craniofacial Research*, *20*, 151–156.

Wu, Yang, Gong, Z., Li, J., Meng, Q., Fang, W., & Long, X. (2014). The Pilot Study of Fibrin with Temporomandibular Joint Derived Synovial Stem Cells in Repairing TMJ Disc Perforation. *BioMed Research International*, *2014*, 1–10. https://doi.org/10.1155/2014/454021

Yusof, F., Sha'ban, M., & Azhim, A. (2019). Development of decellularized meniscus using closed sonication treatment system: potential scaffolds for orthopedics tissue engineering applications. *International Journal of Nanomedicine*, *Volume 14*, 5491–5502. https://doi.org/10.2147/IJN.S207270

Zhang, S.-Y., Liu, X.-M., Yang, C., Cai, X.-Y., Chen, M.-J., Haddad, M. S., Yun, B., & Chen, Z.-Z. (2010). New Arthroscopic Disc Repositioning and Suturing Technique for Treating Internal Derangement of the Temporomandibular Joint: Part II—Magnetic Resonance Imaging Evaluation. *Journal of Oral and Maxillofacial Surgery*, *68*(8), 1813–1817. https://doi.org/10.1016/j.joms.2009.08.012

Zhou, Y., Chen, C., Guo, Z., Xie, S., Hu, J., & Lu, H. (2018). SR-FTIR as a tool for quantitative mapping of the content and distribution of extracellular matrix in decellularized book-shape bioscaffolds. *BMC Musculoskeletal Disorders*, *19*(1), 220. https://doi.org/10.1186/s12891-018-2149-9

Appendix

Appendix 1 – Spectral Band Ratios on the non-pre-processed FTIR spectra results.

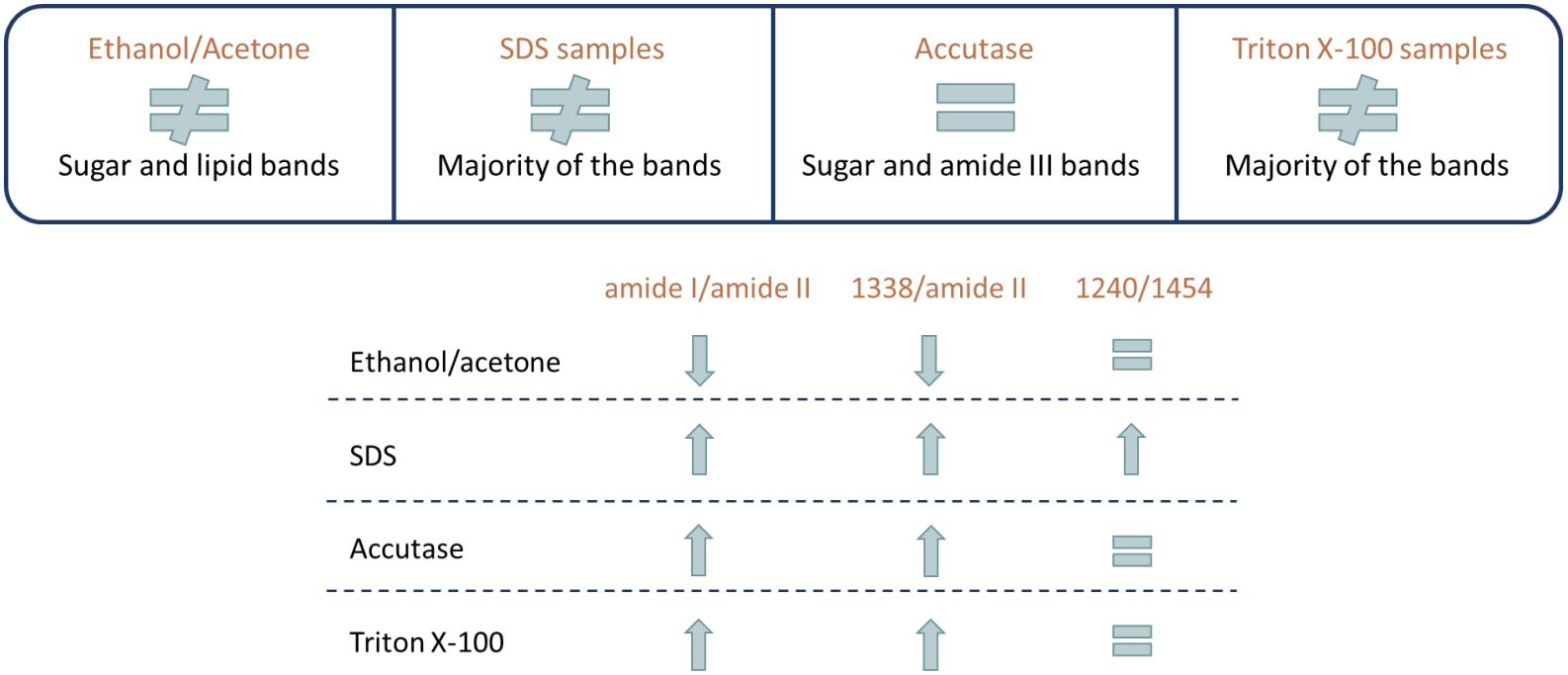

Figure 1 – Outline of the results obtained in respect of the spectral bands used in a general way for the five regions of the disc

Appendix 2 - Quantitative analysis of the GAGs and collagen content by second derivative spectra of the native and decellularized discs.

Table 1 - Mean and standard deviation values of the sulfated GAGs bands at second derivative spectra from the disc with or without (i.e. native) decellularization procedures. EtOH/Acet is ethanol/acetone, FT is freeze and thaw and Triton X-100 is Tri. Statistically significant differences are presented and calculated against the native disc using a Two-way ANOVA with Fisher's LSD *post-hoc* analysis and represented by * p<0.05, ** p<0.01 and *** p<0.001.

Region	Native (1052 cm^{-1})	EtOH/Acet (1052 cm^{-1})	0.1% SDS (1060 cm-1)	0.5% SDS (1060 cm-1)	1% SDS (1060 cm^{-1})	FT 0.1% SDS (1060 cm-1)	FT 0.5% SDS (1060 cm-1)	FT 1% SDS (1060 cm^{-1})	Accutase (1052-1062 cm^{-1})	0.1% Tri (1049-1062 cm-1)	0.5% Tri (1050-1064 cm-1)	1% Tri (1052-1063 cm^{-1})	FT 0.1% Tri (1050-1059 cm^{-1})	FT 0.5% Tri (1048-1056 cm^{-1})	FT 1% Tri (1050-1055 cm^{-1})
Anterior	-0.011 ± 0.003	-0.009 ± 0.003	-0.019 ± 0.003**	-0.028 ± 0.003***	-0.040 ± 0.017***	-0.012 ± 0.002	-0.026 ± 0.009***	-0.037 ± 0.006***	-0.004 ± 0.001**	-0.004 ± 0.001**	-0.004 ± 0.001**	-0.005 ± 0.002*	-0.004 ± 0.002**	-0.005 ± 0.001**	-0.008 ± 0.003
Central	-0.007 ± 0.002	-0.004 ± 0.002	-0.0017 ± 0.002***	-0.026 ± 0.005***	-0.033 ± 0.007***	-0.010 ± 0.002	-0.027 ± 0.004***	-0.030 ± 0.010***	-0.005 ± 0.003	-0.004 ± 0.001	-0.004 ± 0.003	-0.005 ± 0.002	-0.004 ± 0.002	-0.003 ± 0.001	-0.007 ± 0.003
Lateral	-0.008 ± 0.002	-0.005 ± 0.003	-0.018 ± 0.004***	-0.025 ± 0.004***	-0.039 ± 0.012***	-0.009 ± 0.003	-0.030 ± 0.006***	-0.035 ± 0.007***	-0.005 ± 0.002	-0.005 ± 0.001	-0.005± 0.002	-0.006 ± 0.002	-0.005 ± 0.002	-0.005 ± 0.002	-0.007 ± 0.002
Medial	-0.015 ± 0.005	-0.009 ± 0.002*	-0.015 ± 0.002	-0.029 ± 0.006***	-0.045 ± 0.016***	-0.012 ± 0.002	-0.026 ± 0.005***	-0.025 ± 0.003***	-0.007 ± 0.002***	-0.004 ± 0.001***	-0.005 ± 0.002***	-0.005 ± 0.002***	-0.005 ± 0.002***	-0.008 ± 0.004**	-0.008 ± 0.004**
Posterior	-0.011 ± 0.005	-0.008 ± 0.003	-0.020 ± 0.002***	-0.024 ± 0.006***	-0.041 ± 0.011***	-0.013 ± 0.004	-0.026 ± 0.010***	-0.032 ± 0.008***	-0.005 ± 0.002*	-0.005 ± 0.001*	-0.005 ± 0.002*	-0.005 ± 0.001*	-0.006 ± 0.002*	-0.008 ± 0.004	-0.008± 0.002

Table 2 - Mean and standard deviation values of sulfated and non sulfated GAGs bands at second derivative spectra from the disc with or without (i.e. native) decellularization. EtOH/Acet is ethanol/acetone, FT is freeze and thaw and Triton X-100 is Tri. Statistically significant differences are presented and calculated against the native disc using a Two-way ANOVA with Fisher's LSD *post-hoc* analysis *and* represented by * p<0.05, ** p<0.01 and *** p<0.001.

Region	Native (1376 cm^{-1})	EtOH/Acet (1376 cm^{-1})	0.1% SDS (1376 cm-1)	0.5% SDS (1376 cm-1)	1% SDS (1376 cm^{-1})	FT 0.1% SDS (1376 cm-1)	FT 0.5% SDS (1376 cm-1)	FT 1% SDS (1376 cm^{-1})	Accutase (1375-1380 cm^{-1})	0.1% Tri (1373-1380 cm-1)	0.5% Tri 1373-1378 cm-1)	1% Tri (1375-1380 cm^{-1})	FT 0.1% Tri (1375-1378 cm^{-1})	FT 0.5% Tri (1373-1377 cm^{-1})	FT 1% Tri (1371-1378 cm^{-1})
Anterior	-0.006 ± 0.004	-0.007 ± 0.005	-0.019 ± 0.003***	-0.018 ± 0.002***	-0.017 ± 0.003***	-0.013 ± 0.007***	-0.018 ± 0.003***	-0.018 ± 0.002***	-0.016 ± 0.003***	-0.010 ± 0.003**	-0.012 ± 0.004***	-0.010 ± 0.002**	-0.011 ± 0.001**	-0.011 ± 0.003***	-0.006 ± 0.006
Central	-0.007± 0.004	-0.011 ± 0.004*	-0.017 ± 0.002***	-0.016 ± 0.002***	-0.017 ± 0.003***	-0.012 ± 0.003**	-0.017 ± 0.002***	-0.017 ± 0.003***	-0.014 ± 0.004***	-0.007 ± 0.002	-0.008 ± 0.002	-0.008 ± 0.002	-0.010 ± 0.002	-0.008 ± 0.003	-0.006 ± 0.005
Lateral	-0.008± 0.004	-0.007 ± 0.003	-0.015 ± 0.002***	-0.014 ± 0.002***	-0.016 ± 0.002***	-0.010 ± 0.005	-0.016 ± 0.004***	-0.018 ± 0.003***	-0.015 ± 0.002***	-0.008 ± 0.004	-0.009 ± 0.002	-0.006 ± 0.003	-0.0010 ± 0.003	-0.006 ± 0.002	-0.004 ± 0.003**
Medial	-0.004 ± 0.003	-0.003 ± 0.003	-0.015 ± 0.003***	-0.016 ± 0.002***	-0.014 ± 0.001***	-0.013 ± 0.003	-0.016 ± 0.003***	-0.015 ± 0.003***	-0.014 ± 0.002***	-0.008 ± 0.002*	-0.007 ± 0.003	-0.008 ± 0.003**	-0.009 ± 0.004***	-0.004 ± 0.003	-0.003 ± 0.003
Posterior	-0.008 ± 0.005	-0.009 ± 0.005	-0.020 ± 0.002***	-0.018 ± 0.002***	-0.018 ± 0.002***	-0.014 ± 0.007***	-0.020 ± 0.003***	-0.021 ± 0.003***	-0.019 ± 0.003***	-0.012 ± 0.003**	-0.014 ± 0.003***	-0.013 ± 0.003**	-0.011 ± 0.002*	-0.012 ± 0.002**	-0.008 ± 0.003

Table 3 - Mean and standard deviation values of collagen bands at second derivative spectra from the disc with or without (i.e. native) decellularization procedures. EtOH/Acet is ethanol/acetone, FT is freeze and thaw and Triton X-100 is Tri. Statistically significant differences are presented and calculated against the native disc using a Two-way ANOVA with Fisher's LSD *post-hoc* analysis and represented by * p<0.05, ** p<0.01 and *** p<0.001.

Region	Native	EtOH/Acet	0.1% SDS	0.5% SDS	1% SDS	FT 0.1% SDS	FT 0.5% SDS	FT 1% SDS	Accutase	0.1% Tri	0.5% Tri	1% Tri	FT 0.1% Tri	FT 0.5% Tri	FT 1% Tri
Anterior	-0.026 ± 0.006	-0.036 ± 0.007**	-0.047 ± 0.004***	-0.047 ± 0.007***	-0.043 ± 0.010***	-0.032 ± 0.015	-0.040 ± 0.009***	-0.040 ± 0.003***	-0.044 ± 0.006***	-0.038 ± 0.004***	-0.033 ± 0.007*	-0.037 ± 0.006***	-0.035 ± 0.006*	-0.037 ± 0.004**	-0.031 ± 0.005
Central	-0.034 ± 0.007	-0.042 ± 0.006*	-0.048 ± 0.005***	-0.045 ± 0.004***	-0.047 ± 0.007***	-0.033 ± 0.009	-0.043 ± 0.005**	-0.046 ± 0.008***	-0.036 ± 0.007	-0.027 ± 0.004*	-0.022 ± 0.008***	-0.028 ± 0.007	-0.028 ± 0.004	-0.025 ± 0.006**	-0.020 ± 0.007***
Lateral	-0.033 ± 0.006	-0.037 ± 0.007	-0.039 ± 0.006	-0.041 ± 0.004*	-0.044 ± 0.007***	-0.031 ± 0.011	-0.039 ± 0.007	-0.039 ± 0.008	-0.040 ± 0.006*	-0.030 ± 0.008	-0.025 ± 0.005*	-0.028 ± 0.005	-0.030 ± 0.006	-0.027 ± 0.007*	-0.020 ± 0.005***
Medial	-0.023 ± 0.006	-0.025 ± 0.005	-0.039 ± 0.005***	-0.041 ± 0.003***	-0.035 ± 0.004***	-0.033 ± 0.008**	-0.035 ± 0.007***	-0.033 ± 0.006***	-0.034 ± 0.006***	-0.024 ± 0.005	-0.024 ± 0.008	-0.026 ± 0.009	-0.027 ± 0.005	-0.020 ± 0.005	-0.013 ± 0.008**
Posterior	-0.033 ± 0.011	-0.040 ± 0.006*	-0.049 ± 0.006***	-0.050 ± 0.006***	-0.045 ± 0.008***	-0.034 ± 0.010	-0.047 ± 0.009***	-0.045 ± 0.006***	-0.046 ± 0.004***	-0.040 ± 0.005*	-0.038 ± 0.008	-0.042 ± 0.007**	-0.037 ± 0.009	-0.039 ± 0.005	-0.030 ± 0.005

Appendix 3 – Results for the quantitative analysis of the GAGs and collagen content by second derivative spectra in a summarised form for the five regions of the disc.

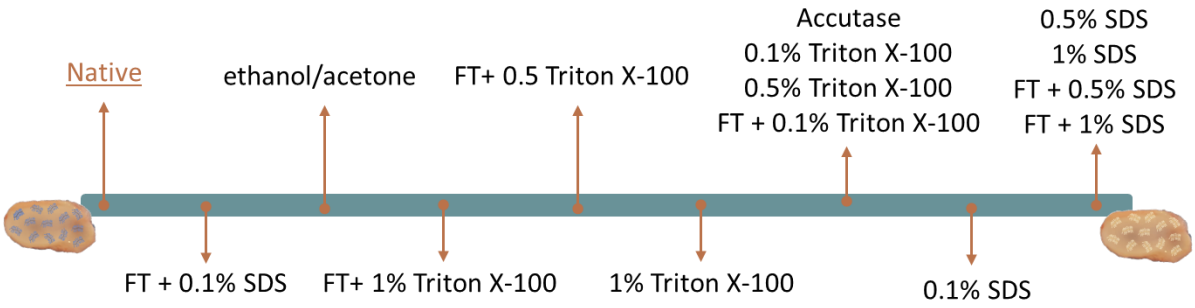

Figure 1 – Results of the second derivative for the sulfated GAGs considering the five regions of the disc and ordered from the least affected to the most.

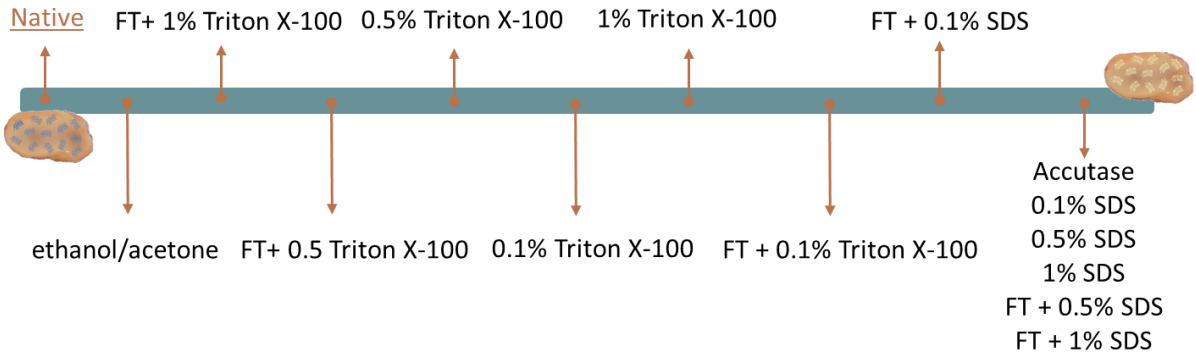

Figure 2 – Results of the second derivative for the sulfated and non-sulfated GAGs considering the five regions of the disc and ordered from the least affected to the most.

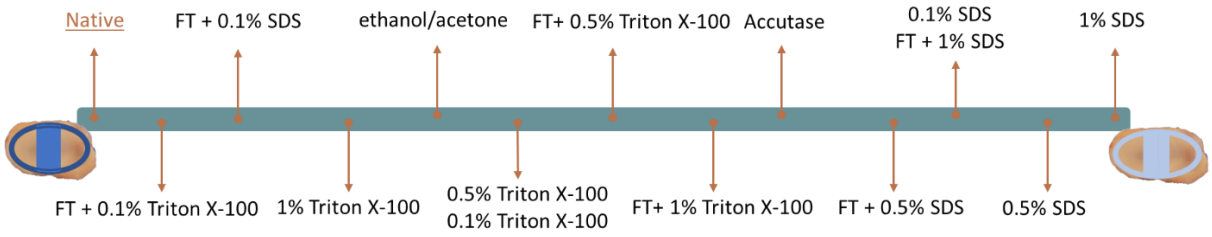

Figure 3 – Results of the second derivative for the collagen considering the five regions of the disc and ordered from the least affected to the most.